Recent developments of multiport DC/DC converter topologies, control strategies, and applications

A comparative review and analysis

Farajdadian, Shahriar; Hajizadeh, Amin; Soltani, Mohsen

Published in:
Energy Reports

DOI (link to publication from Publisher):
10.1016/j.egyr.2023.12.054

Publication date:
2024

Document Version
Publisher's PDF, also known as Version of record

Energy Reports 11 (2024) 1019–1052

Contents lists available at ScienceDirect

Energy Reports

journal homepage: www.elsevier.com/locate/egyr

Review article

Recent developments of multiport DC/DC converter topologies, control strategies, and applications: A comparative review and analysis

Shahriar Farajdadian *, Amin Hajizadeh, Mohsen Soltani

Department of Energy, Aalborg University, Denmark

ARTICLE INFO

Keywords:
DC/DC power converter
Multi-port DC/DC converter
Converter control
Non-isolated
Partially Isolated
Isolated

ABSTRACT

Recent developments in renewable energy-based power systems and smart grids have brought challenges to designing new power conversion systems. On account of the intermittent nature of the renewable sources and unpredictability of the load demand, a combination of two or more energy sources and auxiliary storage systems is usually mandatory to meet the load demand, improve dynamic and steady-state characteristics, and reliability and availability of the system. Conventionally, SISO (single-input-single-output) DC/DC converters are arranged in parallel at a common DC bus to exchange power. In this scheme, separate conversion stages are employed for respective renewable energy sources (RES) and energy storage systems (ESS), and the converters would be controlled independently. However, the multistage configuration generally leads to a large size due to the large number of conversion stages, relatively high cost, and low efficiency and power density. Also, the independent control of several converters and communication among the sources make the system complex. In order to overcome these disadvantages, multi-port DC/DC converters (MPDC) have been proposed. MPDCs are preferred against several independent converters in terms of efficiency, component count, size, cost, and performance point of view. In addition to RES, MPDCs can be utilized in other applications such as electric/hybrid vehicles, telecommunication and satellites, and UPSs. This paper aims to consider the recent advances in MPDC from a topology and control point of view and provide a helpful framework and point of reference for future converter design and applications.

1. Introduction

Recent advancements in RESs, electric/hybrid vehicles, telecommunication, and satellite applications have presented new challenges to designing DC/DC-power conversion systems. For instance, despite developments in the context of RES, they are not reliable enough for electric energy generation on their own. The major challenge with these resources is that they depend on weather and environmental conditions, and their generated energy is variable, making them uncertain. Therefore, a RES alone does not provide the characteristics of an efficient, stable, and reliable energy resource to supply the required demand (Zhang et al., 2016). To overcome this problem, the RESs and ESSs are combined as HRSs (Affam et al., 2021). Two major structures for power converters have been proposed in earlier works; In the typical structure to convert the power of each input source, a conventional SISO DC/DC converter is typically utilized. To provide the required load energy, the output of each of these individual converters is additionally coupled by a common DC-link. Each of the SISO DC/DC converters is regulated individually. Usually, a telecommunication bus is employed to exchange data between several input sources (Rehman et al., 2015). Using numerous different power converters and telecommunication equipment is inefficient, bulky, and raises the cost of this structure. Furthermore, the requirement to synchronize separate converters that are regulated individually adds to the complexity of such structures (Zhang et al., 2016; Affam et al., 2021). To avoid such issues, an integrated multi-port system has been suggested (Rehman et al., 2015; Khosrogorji

Abbreviations: DISO, Double-input-single-output; DAB, Dual active bridge; ESS, Energy storage system; EV, Electric vehicle; FC, Fuel cell; FB, Full bridge; HB, Half bridge; HRS, Hybrid renewable system; LLC, Inductor-inductor-capacitor; MIMO, Multi-input-multi-output; MPPT, Maximum power point tracking; MAB, Multiple active bridge; MPDC, Multi-port DC/DC converter; PFM, Phase frequency modulation; PS, Phase shift; PSM, Phase shift modulation; PV, Photovoltaic; RES, Renewable energy source; SIMO, Single-input-single-output; SISO, Single-input-single-output.; TAB, Triple active bridge; TISO, Three-input-single-output; ZCS, Zero current switching; ZVS, Zero voltage switching.

* Corresponding author.
E-mail address: shfa@et.aau.dk (S. Farajdadian).

https://doi.org/10.1016/j.egyr.2023.12.054
Received 30 August 2023; Received in revised form 18 November 2023; Accepted 22 December 2023
Available online 4 January 2024

et al., 2016). In integrated multi-port systems, the entire structure is regarded as a single converter capable of combining the energy of various input sources with varying specifications. The central unit controller is also in charge of adjusting the converter's output power. This type of MPDC is recommended for usage in applications such as hybrid power systems, electric/hybrid vehicles, satellites and telecommunication, and UPSs due to its simple structure, higher availability and reliability, higher power density, and lower cost (Affam et al., 2021; Bairabathina and Balamurugan, 2020).

MPDCs can be divided into three main categories: isolated, non-isolated, and partially insolated (Wang et al., 2020; Yi et al., 2022). Isolated converters provide high voltage gain and sustain good soft-switching conditions and are typically used in applications where galvanic isolation between high and low voltages is required. Electrical isolation is achieved using high-frequency transformers. However, the design of a high-frequency transformer for high-voltage applications is complex, costly, and makes the converter bulky. On the other hand, non-isolated converters are more straightforward in design, power density is high, the number of semiconductors is few, and are utilized in applications where the galvanic electrical separation between the source and the load is not required. However, soft switching cannot be realized easily, and voltage gain is relatively low. High-voltage gains can be obtained by utilizing coupled inductors in either isolated or non-isolated converters, although the complexity of the converter will rise. In applications where high voltage gain is required, but isolation between all ports is not essential, partially isolated converters can be opted (Zhang et al., 2016; Rehman et al., 2015; Bairabathina and Balamurugan, 2020; Wang et al., 2020; Bhattacharjee et al., 2019). In terms of modeling and control design, MPDCs have presented several challenges since to control the power flow of an n-port converter independently, (n-1) control variables are required and the cross-coupling between these control variables makes control system design complicated (Alhatlani and Batarseh, 2019; Zhao et al., 2008). Moreover, in conventional modeling and control approaches, non-linearities and uncertainties of converters, as well as disturbances in input sources, have not been taken into account (Damasceno et al., 2021; Bandyopadhyay et al., 2021; Rios et al., 2021).

Several review reports on MPDCs have recently been published (Zhang et al., 2016; Affam et al., 2021; Rehman et al., 2015; Khosrogorji et al., 2016). Nevertheless, many recently developed topologies, modulation and control strategies, and emerging applications are not reviewed in the aforementioned references, which is the aim of the present review paper. The rest of the article is organized as follows: Section 2 comprehensively discusses non-isolated MPDCs. In Section 3, partially isolated topologies will be analyzed, and in Section 4, isolated converters will be covered. Finally, Section 5 discusses the direction of future research and conclusion remarks. The comparison tables are shown in appendices A, B, C, and D.

2. Non-isolated MPDCs

2.1. Non-isolated MISO converter

Authors of (Dobbs and Chapman, 2003) have described a topology for buck-boost converters that can combine the energy of multiple input sources with varying voltage-current characteristics and use it to supply the load. The power flow is unidirectional, and the output always equals the inverse value of the input sources. A separate converter between output and input sources is required to provide bidirectional power transfer capabilities, which increases the number of components, size, and weight of the converter. Only one input source can send energy to the load at any moment. Another flaw of this structure is the high ripple and discontinuous character of the input source current. The time-sharing switching technique for (Dobbs and Chapman, 2003) is discussed in (Onwuchekwa and Kwasinski, 2012). The topology is shown in Fig. 1. A DISO PWM converter for high/low voltage

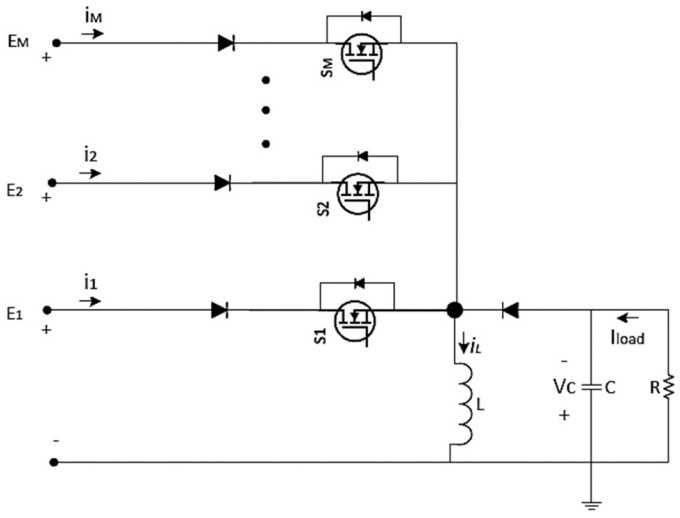

Fig. 1. MISO buck-boost converter (Onwuchekwa and Kwasinski, 2012).

application has been presented in (Chen et al., 2006), and further investigated in (Gavris et al., 2011a; Veerachary, 2008). The suggested converter, shown in Fig. 2, comprises buck and buck-boost converters that share a common inductor and capacitor as filters. As a result, this structure can work in step-down or step-down/up modes. Using a common inductor and capacitor as a filter reduced the number of components, size, and cost of the converter. However, the energy from input sources cannot be transferred to the load and inductor simultaneously. As a result, many operation modes are generated, and the time interval between the converter's operation modes reduces. This causes an increase in the ripple and discontinuity of the input source current, output voltage drops, and a reduction in the power delivered to the load. The topology of (Chen et al., 2006) has been studied for PV-wind-water pump hybrid system in (Ferreira et al., 2020), and for the controller's design, the linear quadratic gaussian (LQG) with loop transfer recover (LTR) regulator and the loop shaping approach were applied.

Authors of (Zhu et al., 2020a) have proposed an expandable bidirectional MISO topology for ESS in DC microgrid application. Despite component count, voltage gain is not high; in DISO structure, it is twice the boost topology. A modular boost topology is discussed in (Colalongo et al., 2017) for low-voltage applications. Two DISO configurations have been proposed in (Yalamanchili et al., 2006) for automotive applications. The first topology comprises two buck converters with a common inductor and capacitor. The power of the input sources can be transferred to load simultaneously or individually. The number of current sensors is reduced using the same inductor for both input sources. The power flow in the given converter is unidirectional; however, the kind of switches can be changed to enable bidirectional power flow. This structure suffers from low voltage gain, high ripple, and discontinuous

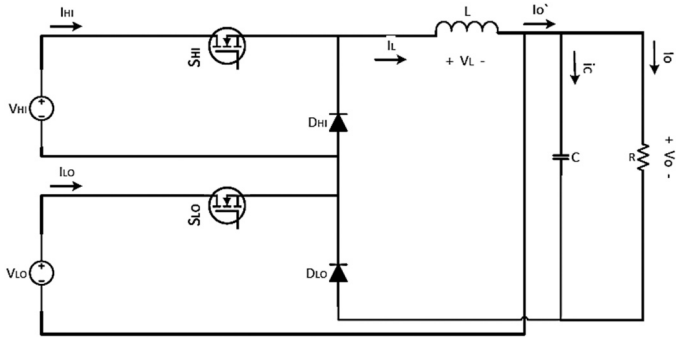

Fig. 2. DISO buck/buck-boost converter (Chen et al., 2006).

input current. The second structure is a DISO structure made up of a combination of two buck-boost converters. Using the same inductor for both input sources reduces the number of converter current sensors. Furthermore, the proposed structure can function as a step-down or step-up. The shortcomings of the suggested converter are the inability to simultaneously transfer the energy of input sources, the inability to bidirectional power flow, low voltage gain, the large current ripple of sources, and the discontinuous nature of input sources' current. A similar topology with two switches, two diodes, and two inductors is presented in (Veerachary et al., 2013). The robust control design of (Veerachary et al., 2013) is discussed in (Reddy and Veerachary, 2016; Mummadi and Bhimavarapu, 2020). To reduce inductor current ripple, (Li et al., 2008) proposed interleaved dual-edge modulation for a DISO buck converter. The general structure for MISO converters is provided in (Khaligh et al., 2009; Khaligh, 2008; Onar et al., 2010). While using a small number of switches and diodes, this structure can perform any of the buck/boost actions. It can either have a unidirectional or bidirectional power flow. Because all inputs share a single inductor and power is transferred by only one input source at a time, a current sensor may be used to monitor the command signals of the switches, and the current of each input source at all times. The inability of this structure to simultaneously transmit the energy of the input sources to the load, as well as the large current ripple, the discontinuous character of the input current, and low efficiency are the converter's most significant flaws.

Another MISO converter for hybrid energy systems is provided in (Kumar and Jain, 2013a, 2013b). The proposed MPDC, which is shown in Fig. 3, has several advantages, including a simple and compact structure, buck, boost, or buck-boost operation mode, unidirectional and bidirectional power flow, the possibility of simultaneous or independent transmission of energy of input sources, using only one inductor and thus only one current sensor. However, the discontinuous and high ripple character of the input sources, low voltage gain, as well as a large number of active elements in the conduction path are the main shortcomings of the suggested structure, which increase losses and hence affect the converter's efficiency. Furthermore, in bidirectional power flow, all input cell diodes (excluding the energy storage diode) must be replaced with a switch, which increases the number of power switches, the number of driver circuits, and the size, cost, and complexity. The same authors discuss the power management strategy for the proposed converter in (Agrawal et al., 2016). For the same topology, the authors of (Hema Rani et al., 2019) suggested a fuzzy logic supervisory controller for power management.

A MISO converter has been provided in (Di Napoli et al., n.d.), where each input source is connected to a DC-link by a bidirectional buck/-boost converter. When power flows from each input source to the DC-link, the cell operates as a step-up converter, whereas the return of energy from the output to each input source provides a step-down operation. Bidirectionality, low ripple, and continuous nature of the input current are advantages of this MPDC. However, the requirement to utilize an individual inductor for each input source increases the converter's cost, weight, and volume. As input sources for hybrid/-electric vehicles, (Thounthong et al., 2010) provides a DISO converter with FC and supercapacitor. Because of the FC's sluggish nature, it is utilized to keep the supercapacitor charge at the desired level, while the supercapacitor regulates the DC link energy. Two boost converters connect each source to a common link. The output current ripple of the FC can be decreased to a great extent by introducing an interleaving switching technique. Also, flatness control is presented and compared to the classical linear PI controller. The large number of switches, diodes, and inductors employed in the converter, on the other hand, increases the size, weight, and expense of the MPDC (particularly for a large number of inputs).

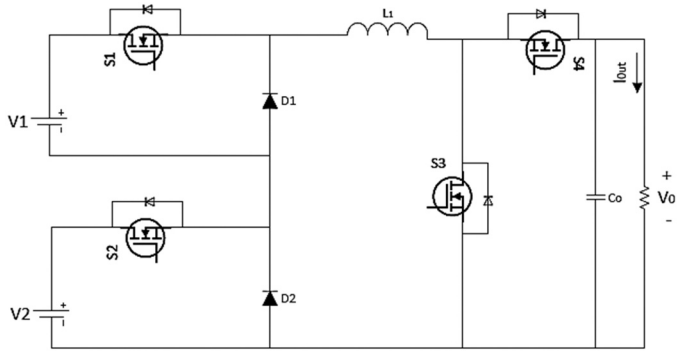

Fig. 3. DISO converter proposed in (Kumar and Jain, 2013a).

Authors of (Fan et al., 2010) have proposed an MISO converter for a hybrid thermoelectric-PV system in hybrid electric vehicles. The suggested hybrid system is composed of a TISO Cuk-Cuk-Cuk converter. It is possible to supply energy from the input sources simultaneously. MPPT algorithm is also presented for solar cells. However, at high power levels, the converter's cost, volume, and weight rise due to the necessity of a separate inductor for each input and the requirement to utilize a filter to reduce output voltage ripple. In (Smith and McCann, 2012), a similar Cuk-based topology has been proposed for grid-connected hybrid thermoelectric-PV systems. The structure allows independent or simultaneous energy transmission from input sources to the load. Also, the P&O algorithm is implemented for MPPT. A bidirectional DISO structure has been presented in (Hintz et al., 2015). This MPDC is recommended for use in FC-based hybrid vehicles since such applications require the capacity to transfer power in both directions as well as the ability to combine input sources with different voltage levels. The proposed converter can perform both step-down and step-up functions. It is possible to transmit energy individually or simultaneously from many input sources. This topology is expandable and has a simple control system. However, the requirement to utilize a separate inductor for each input source raises the volume, cost, and weight of the converter for a high number of inputs.

The authors of (Gavris et al., 2012, 2011b) have described a DISO hybrid buck LC converter for HRS applications, hybrid/electric automobiles, and communication power systems. The converter's advantages include the ability to utilize input energy simultaneously or individually and a wide voltage conversion ratio. The converter's size and weight have increased due to a large number of components. Furthermore, a large number of diodes in the conduction path increase losses and reduce efficiency. In (Zahedi Saadabad et al., 2020), a DISO three-winding coupled inductors-based topology proper in use in a PV-battery application is suggested. Based on the quadratic boost converter, a DISO structure is proposed for stand-alone PV-battery systems (Rostami et al., 2020). In (Chen et al., 2013), a DISO structure for a stand-alone PV-battery system is suggested, which employs two coupled inductors to enhance voltage gain. In this topology, two buck-boost type active-clamp circuits recycle the leakage-inductance energy and provide soft-switching conditions. However, utilizing two coupled inductors, two inductors, five switches, and five capacitors makes the converter bulky and expensive.

A MISO converter recommended for EVs has been proposed in (Akar et al., 2016) and is shown in Fig. 4. The two-input converter has four power switches with anti-parallel diodes, two inductors, and two power diodes. This converter's two-input operation consists of four operating modes:

- The switches S_1, S_2, and Q are in conduction mode during the interval $[0 < t < (1 - d_{To})T_s]$. As a result, using the Q switch, the energy from both input sources, as well as the energy stored in inductors L_1 and L_2, is transferred to the output load and capacitor.
- In the second operating mode, the time interval $[(1 - d_{To})T_s < t < (d_{s2})T_s]$, the Q switch is deactivated, and the T switch is activated. The energy from each input source is stored in the matching inductor. As a result, the inductors' current and energy

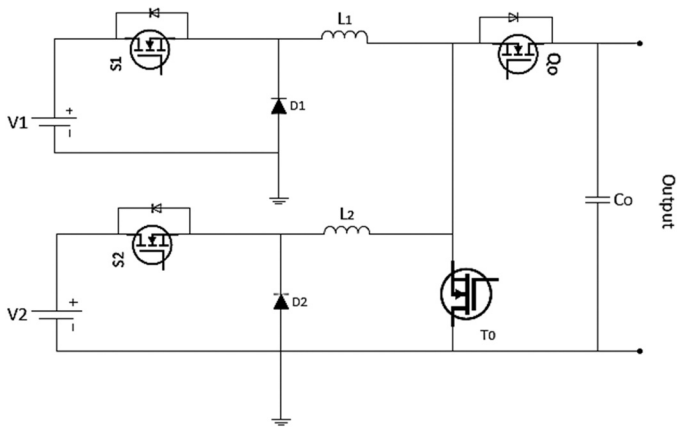

Fig. 4. Bidirectional DISO converter proposed in (Akar et al., 2016).

stored in them rise. The output capacitor is discharged and supplies the required load energy in this time interval.

- Switch S_2 is OFF, switches S_1 and T are ON, and diode D_2 begins to conduct in the third operating mode, the time interval $[(d_{s2})T_s < t < (d_{s1})T_s]$.In this operating mode, the inductor L_1 continues to be charged, and the L_2 current starts to be decreased due to the body resistance of the T switch. The output capacitor supplies the required load energy.
- In the fourth operating mode, the time interval $[(d_{s1})T_s < t < T_s]$, S_1 and S_2 are turned OFF, and the diodes D_1 and D_2 are turned ON. In this time interval, the energy is stored in inductors L_1 and L_2. In this fourth operating mode, the output capacitor current is negative.

The input sources in this converter can transmit power to the load or inductor simultaneously or individually. However, input sources current are discontinuous and have a high ripple. Moreover, because each input cell has its own inductor, the number of inductors increases with the number of inputs, increasing the size, weight, and expense of the converter. In (Akar et al., 2017), the same authors proposed a fuzzy logic-based energy management system for the topology of (Akar et al., 2016), which employs a supercapacitor and a battery as input. The structure is shown in Fig. 5. In the first operating mode, both input sources are discharged to provide the load demand simultaneously. Energy goes from the output to the input sources and is stored in the second operating mode. If the battery energy alone is sufficient to supply the load in the third operating mode, the battery is discharged to supply the load. Excess energy from the battery is kept in the supercapacitor, increasing its charge.

A TISO boost converter for hybrid energy systems has been provided in (Nejabatkhah et al., 2012). It is shown in Fig. 6. Two of the input ports are unidirectional, and one is bidirectional and suitable for ESS. Each input source can provide the required energy to the load individually or simultaneously and assist the battery charge/discharge process. Four power switches are utilized in this MPDC, each separately controlled by four duty cycles (corresponding to each switch). In addition to the MPPT of the PV, the power of the FC, the amount of charge and discharge of the battery, and the voltage of the output load may all be controlled by regulating the duty cycle of each of these four switches. Also, two types of decoupling networks are developed to design closed-loop control systems. However, power flow from load to ESS is not provided in this topology. Moreover, many active switches/diodes in the conduction path increase losses and affect the converter efficiency. Another TISO topology for PV/FC/Battery hybrid application with one bidirectional port and two unidirectional ports is discussed in (Kardan et al., 2017). In this structure, the battery can be charged individually or simultaneously with energy sources.

A family of DISO H-bridge-based topologies has been discussed in (Ahmadi and Ferdowsi, 2012), as is shown in Fig. 7. The structure in Fig. 8.a allows for the independent or simultaneous transmission of energy from input sources to the load. Because only one inductor is used for both input sources, the number of elements, cost, and weight of the converter is reduced. This converter does not support bidirectional power flow (to offer bidirectional power transmission, bidirectional switches must be used). The configurations depicted in Fig. 8. b, Fig. 8. c, and Fig. 8. d allow for independent or simultaneous transfer of input energy to the inductor. Because the converter uses just one inductor, the current of each input source at any point in time may be measured with a single current sensor. The power flow in these converters, however, is unidirectional. The energy from the second input source cannot be transferred directly to the load in the configurations depicted in Fig. 8. b, Fig. 8. c. To do this, the energy from the second source must first be stored in the inductor before being transmitted to the output load at a different switching time. The current of input sources is discontinuous, and the ripple is considerable in all structures depicted in Fig. 8.

A general approach for achieving MISO converters has been provided in (Liu and Chen, 2009) by introducing the pulsating voltage source cell and pulsating current source cell. All input sources can transfer energy individually or simultaneously. The number of inductors and capacitors used in the proposed structures are fewer than in the case of parallel connection of many basic independent converters. These MPDCs are indicated for use in HRS. However, energy cannot transfer from one of

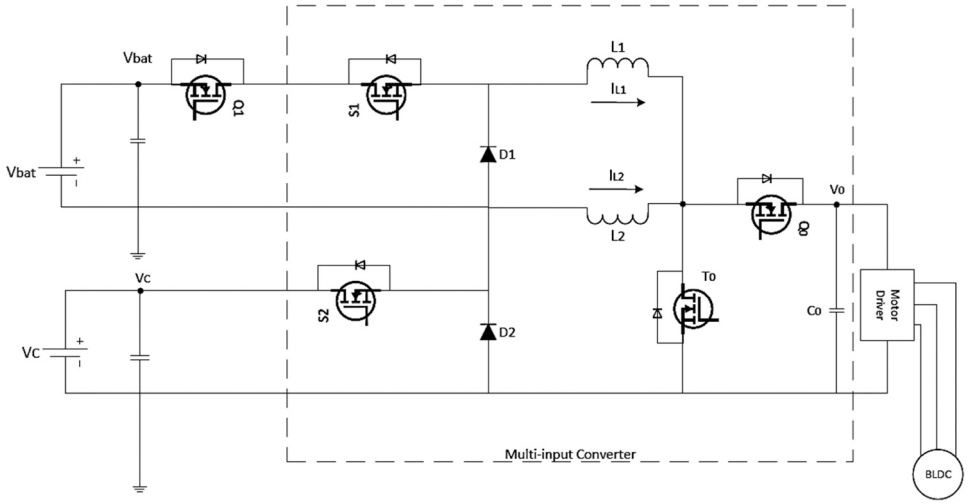

Fig. 5. DISO converter for battery/FC HESs (Akar et al., 2017).

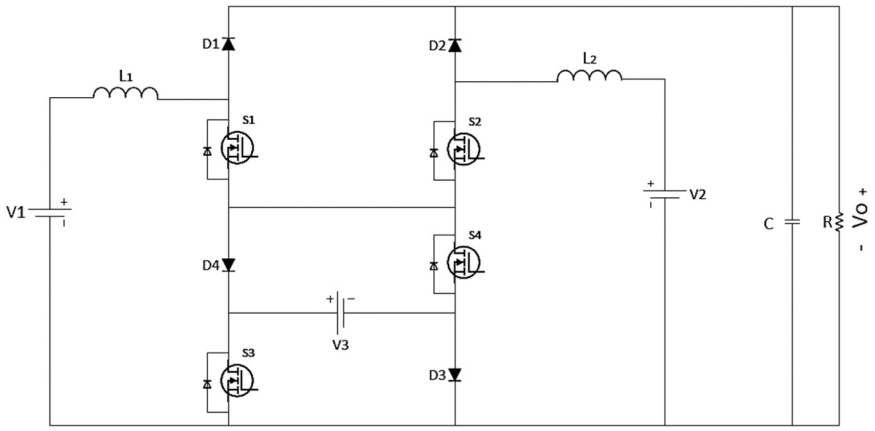

Fig. 6. TISO boost converter (Nejabatkhah et al., 2012).

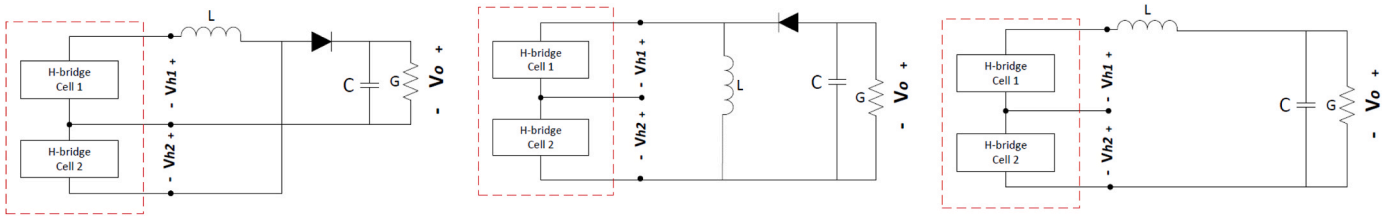

Fig. 7. Cascaded H-bridge cell to synthesis DISO topologies (Ahmadi and Ferdowsi, 2012).

the inputs to another. Moreover, the converters require several high-current sensors.

Authors of (Xian et al., 2012) have described a DISO buck structure as well as a new control strategy. This MPDC is recommended for usage in FC-based applications. Due to the inherent time delay in the electrical properties of FCs, it is frequently required to use another energy source with a faster and better dynamic response in hybrid energy systems containing FCs. The proposed structure has several advantages, including relatively high efficiency, fewer elements employed, low cost, simple construction, and a control system. The main disadvantages of this structure are the high ripple and discontinuous nature of the input current.

In (Ahrabi et al., 2017), a TISO converter developed from structures (Nejabatkhah et al., 2012; Khadem Haghighian and Hosseini, 2015) is offered for use in hybrid/electric vehicles. The topology is shown in Fig. 9. The suggested structure's input sources include FC, solar cell, and battery. Although this structure has a more significant voltage gain than (Nejabatkhah et al., 2012; Khadem Haghighian and Hosseini, 2015), the output voltage gain is not considerable compared to other MISO topologies. Moreover, the load can be supplied even when only one source is available, resulting in high reliability. This structure is intended for use in hybrid/electric vehicles that do not have the capability of bidirectional power flow. Furthermore, this structure cannot be generalized to the arbitrary number of input/output ports. In (Shayeghi et al., 2021), a three-port switched-capacitor-based converter with low input current ripple, and low component count is proposed, which can be operated in both step-up/ step-down modes. This MPDC is recommended for usage in EV applications. In (Farakhor et al., 2019), a bidirectional DISO topology has been suggested, in which the continuous input current makes it proper for HRS. Authors of (Xu et al., 2021) proposed a DISO structure comprising a switching capacitor converter, a series resonant converter, and a bidirectional buck-boost converter for PV-battery application. Hybrid PWM and PFM methods are applied to minimize cross regulation effect and realize power balancing among ports. However, the converter suffers from a high number of components.

In (Prabhala et al., 2016), a unidirectional DISO converter with diode-capacitor voltage multiplier cells and two boost stages at the input has been proposed to obtain high voltage gain. Fig. 10 depicts the proposed structure with four diode-capacitor multiplier cells. The operation modes of the converter are as follows:

- Both S_1 and S_2 switches are ON in the first operating mode, and diodes D_1, D_2, D_3, D_4, and D_{out} are turned OFF. As a result, the relevant input source charges each inductor. The output capacitor also provides load energy.
- S_1 is turned off, and S_2 is ON in the second operating mode, and D_1, D_3, and D_{out} begin to conduct. As a result, the first source and the inductor L_1 charge capacitors C_1 and C_3 and discharge C_2 and C_4. D_{out} is forward-biased, and energy is transferred to the load and output capacitor C_o.
- S_2, D_1, D_3, and D_{out} are turned OFF in the third operating mode, and the S_1, D_2, and D_4 begin to conduct. Energy from the first source is stored in the L_1 just as in the first operating mode. Therefore, the second source and L_2 charge capacitors C_2 and C_4 and discharge C_1 and C_3, and the load is supplied by C_{out}.

The advantages of this MPDC include input sources that can be controlled simultaneously or independently of one another, continuous current flow and small current ripples, and the voltage across the switches and diodes is less than V_{out}. Another advantage of this structure is the ability to conduct power control amongst input sources. However, getting significant voltage gains necessitates using more diode-capacitor multiplier cells, which increases the number of components utilized, the cost, size, and converter losses, and reduces the efficiency.

Ref (Banaei et al., 2014). describes a unidirectional MISO topology for hybrid energy generation systems. This structure consists of several buck and buck-boost converters. Among the advantages are the ability to transfer input source power simultaneously or individually, continuous source current, minimal current stress on switches, a wide range of switching duty cycles, and high voltage gain. However, to achieve significant voltage gains, the number of inputs must be increased, which increases voltage stress on the switches and diodes. As a result, while

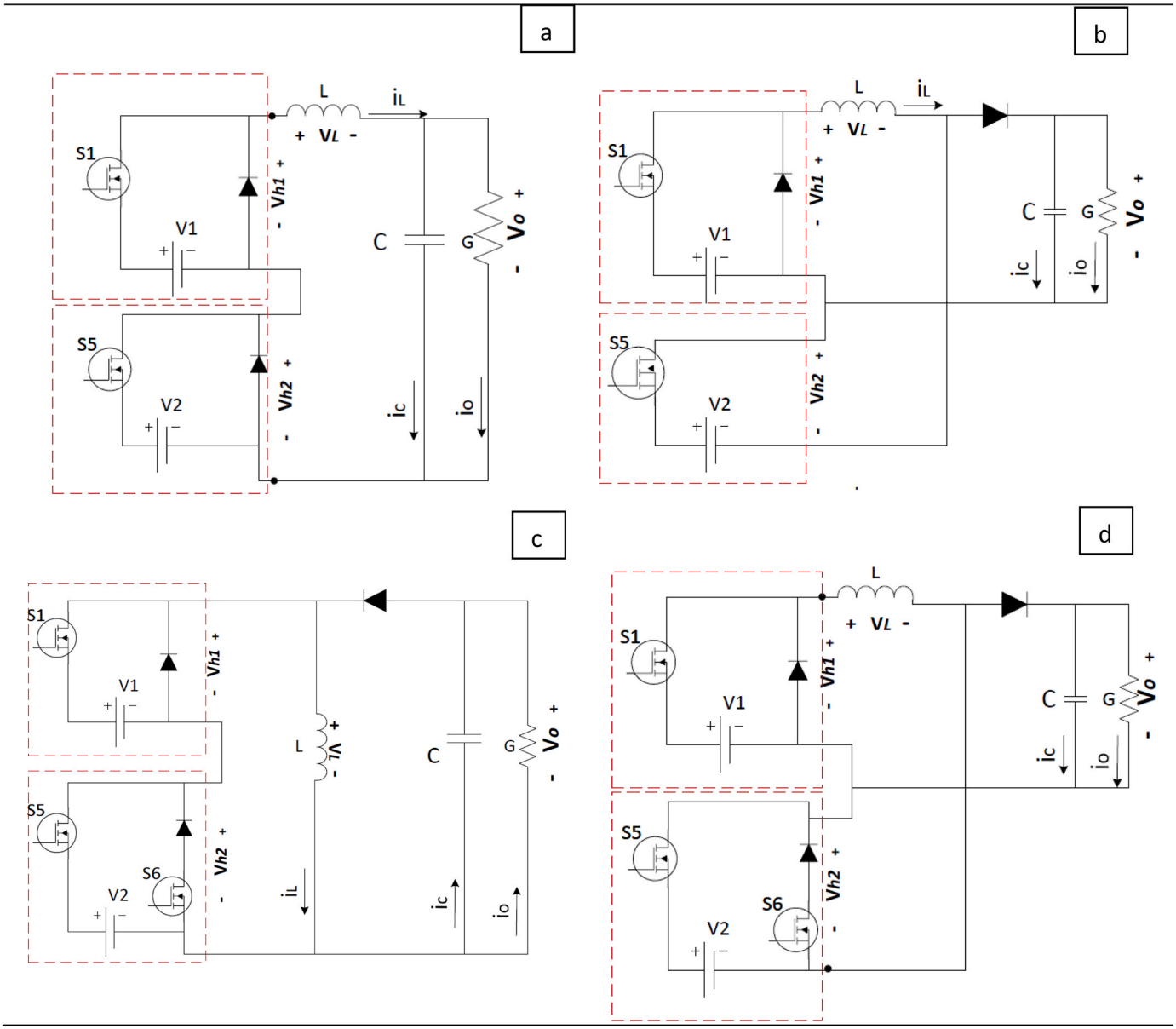

Fig. 8. The topologies proposed in (Ahmadi and Ferdowsi, 2012). (a) Buck-buck converter. (b) Buck-buck boost converter. (c) Buck boost-buck boost converter. (d) Boost-buck boost converter.

determining the number of inputs, a compromise must be struck between the voltage gain and the voltage across the switches/diodes. For the mentioned converter, the authors of (Mahmoudi and Safari, 2019) discussed an LMI-based robust control. A series-parallel switched-capacitor structure that can operate in a buck or boost mode is discussed in (Abraham et al., 2017). However, the converter suffers from discontinuous input current and limited voltage gain.

In (Yuan-mao and Cheng, 2013), a unidirectional MISO structure based on switched capacitors is proposed that does not incorporate any inductors. The proposed structure is made up of $(n + 1)$ capacitors, $(n + 1)$ switches, and $(2\,n + 1)$ diodes. This structure's performance can be evaluated in two modes of operation. The Q_0 switch and all diodes except D_o are conducting in the first operating mode. Capacitors C_i are therefore charged from sources V_i. All switches except the Q_0 and the diode D_o begin to conduct in the second operating mode. The converter's maximum output voltage equals the total voltage of the input sources. To enhance the output voltage, the number of switched capacitor cells must be increased. Because each cell contains a switch, a capacitor, and two diodes, the number of components required and the cost, size, and losses of the converter grow as the output voltage increases. Also, the input current is discontinuous, and to realize soft switching conditions, resonant inductor is to be used.

In (Deihimi et al., 2017), a structure for a MISO converter has been presented, as shown in Fig. 11, which combines typical boost converters. The proposed converter has (n) inductors, (2 n) capacitors, (n) switches, and (2n-1) diodes. Consider the type of the suggested structure's two inputs for a better explanation. The converter's performance can be evaluated in four different operating modes, as follows:

- Switches S_1 and S_2, as well as diode D_2, are turned ON in the first operating mode, while all other switches and diodes are turned OFF. Thus, input sources V_1 and V_2 charge inductors L_1 and L_2, respectively. Capacitors C_o and C_1 are discharged to charge capacitors C_2 and C_3. The output capacitor C_o supplies the appropriate power to the load.
- The S_1 and S_2 continue to conduct in the second operating mode, but D_2 is turned OFF. In this operating mode, charging L_1 and L_2 is continued through V_1 and V_2, respectively.

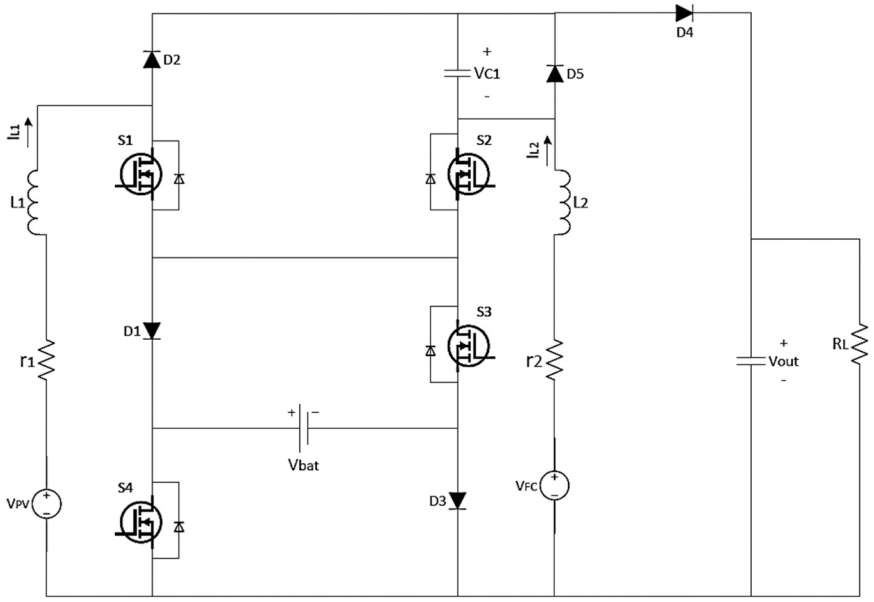

Fig. 9. TISO converter for hybrid/electric vehicles (Ahrabi et al., 2017).

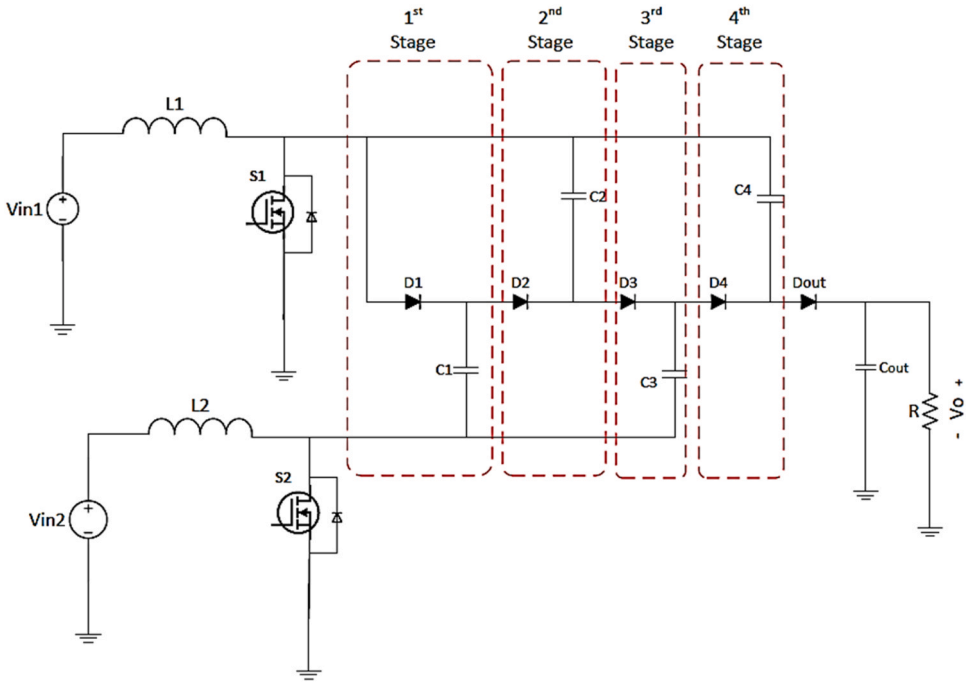

Fig. 10. DISO converter with diode-capacitor voltage multiplier (Prabhala et al., 2016).

- The S_2 is turned OFF in the third operating mode, and D_3 begins to conduct. In this situation, the L_1 keeps charging from the V_1. When the S_2 is turned OFF, and the D_3 is turned ON, the energy from V_2, L_2, and C_3 is transferred to the load, output capacitor C_o, C_1, and C_2.
- The S_1 is turned OFF in the fourth operating mode. As a result, the energy from sources V_1 and V_2, the energy from L_1 and L_2, and the energy stored in C_3 are transmitted to the load, the output capacitor C_o, and C_1 and C_2.

As is observed, the proposed converter's output voltage equals the entire output voltage of the conventional boost converters utilized in its structure. The advantages of the discussed structure are continuous current of input sources, low voltage stress on diodes/switches, and the possibility of simultaneous or individual energy transmission by input sources. The power flow in this system, on the other hand, is unidirectional and from the input sources to the load. Furthermore, if ESSs are used, they cannot be charged from different input sources. As a result, power control between input sources is not possible in this topology.

An expandable unidirectional DISO converter is proposed for grid-connected PV systems (Zhou et al., 2012), allowing it to work as a boost converter and provide high voltage gain. This converter's performance can be evaluated in four different operating modes as follows:

- Switches S_1 and S_2 are turned ON, and diodes D_1 and D_2 are turned OFF in the first operating mode. As a result, the energy of each input source V_1 and V_2 is stored in the corresponding inductors L_1 and L_2.

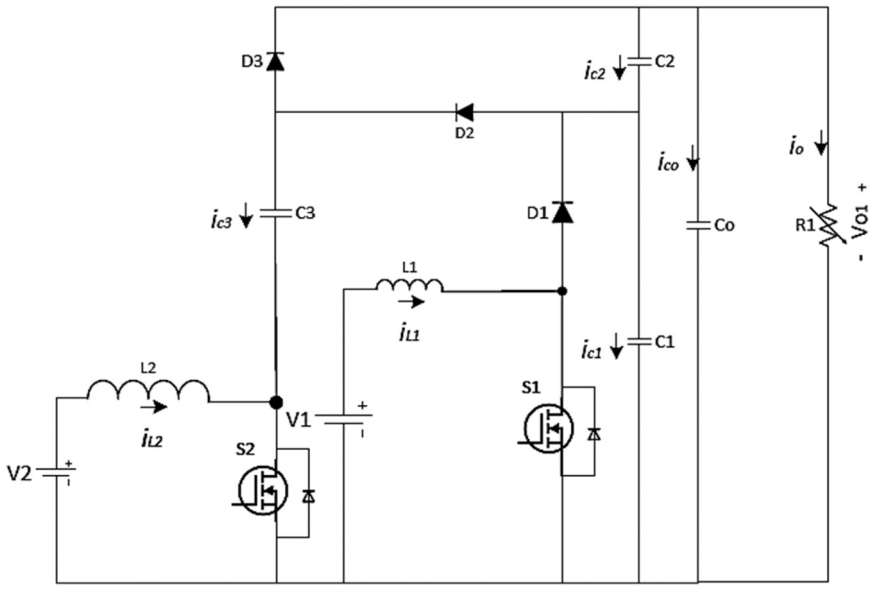

Fig. 11. Expandable DISO converter (Deihimi et al., 2017).

Because D_1 and D_2 are turned OFF, and no current flows through them, the capacitor voltage C_1 remains constant.

- The S_2 and D_1 are turned OFF in the second operating mode, and S_1 and D_2 begin to conduct. As a result, L_1 current increases, and L_2 current decreases. The energy stored in the L_1 is also transferred to C_1 and increases C_1 voltage.
- The third operating mode is similar to the first, in which the energy from both input sources is stored in the L_1 and L_2 inductors via S_1 and S_2.
- In the fourth operating mode, S_1 is OFF, and S_2 is ON, while D_1 is ON and D_2 is OFF. As a result, the energy from the V_2 is transmitted to and stored in the L_2. Furthermore, C_1 is discharged, and its voltage decreases.

The proposed framework includes a straightforward control structure and system. The converter's advantages are the continuity of the input source current, the minimal ripple of the source current, and the possibility of simultaneous or individual transfer of source energy. The proposed structure's output voltage is equivalent to the total output voltage of the conventional boost converters used. In addition, the structure with MISO requires n-inductors and n-switches, which increases the number of gate driver circuits, size, cost, and converter complexity.

A MISO step-up non-coupled inductor-based converter has been provided in (Varesi et al., 2017). The proposed structure's n-input version, which is a combination of typical boost converters, has $(n + 1)$ inductors, $(n + 1)$ capacitors, $(n + 1)$ switches, and $(n + 1)$ diodes. Three inputs structure is shown in Fig. 12 and is explored to provide better knowledge of how the proposed converter operates. Four operating modes for the structure's performance can be imagined based on the employed switches.

- The switches S_1, S_2, S_3, and Q are in conduction mode in the first operating mode, and all diodes are turned OFF. Inductors L_{1a}, L_2, and L_3 are thus charged by sources V_1, V_2, and V_3, respectively. Capacitor C_1 is also discharged, and the energy it contains is transferred to inductor L_{1b}. The output capacitor C_o provides the appropriate power to the load.
- The S_3 switch is turned OFF in the second operating mode, and diode D_3 begins to conduct. As a result, the energy from the third source and inductor L_3 is transferred to capacitor C_2 through D_3 and S_2. The output capacitor C_o provides the load demand.
- The switch S_2 and diode D_3 are switched OFF in the third operating mode, and the switch S_3 and diode D_2 begin to conduct. The energy from the V_2, inductor L_2, and capacitor C_3, is transferred to capacitor C_2 via diode D_2 and switches S_1 and Q. Also, L_{1a} and L_{1b} are charged by V_1 and C_1, respectively.
- Finally, in the fourth operating mode, the switches S_1, Q, and diode D_2 are deactivated, and the switches S_2, S_3, and diode D_o begin to conduct. As a result, the energy from V_1, inductors L_{1a} and L_{1b}, and

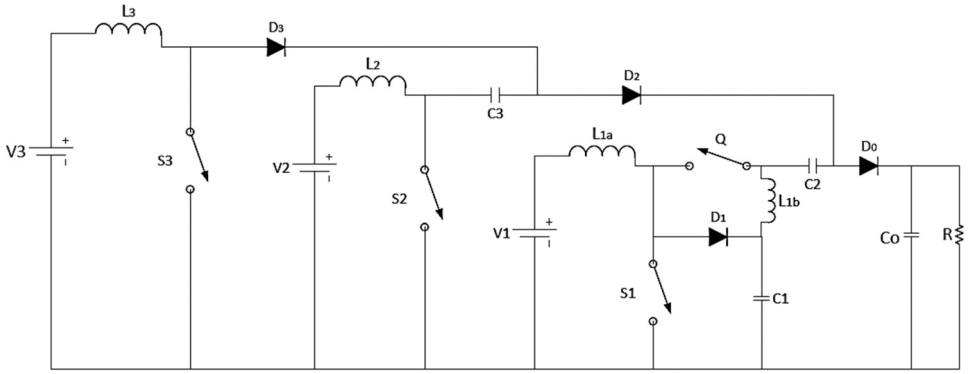

Fig. 12. MISO step-up non-coupled inductor-based converter (Varesi et al., 2017).

capacitor C_2 is transferred to the load through D_1 and D_o. The V_1 and the inductor L_{1a} both charge C_1.

The voltage across the switches/diodes is modest despite the significant voltage gain. The voltage stress of all switches/diodes, including the Q switch and the D_o diode, is less than V_o, which decreases the converter's cost and losses and helps to increase the converter's efficiency. The structure's main advantages are continuous and low input sources current ripple, simultaneous or individual power transfer of input sources, the ability to increase the number of inputs, and low voltage stress on switches and diodes. Power flow in this topology is unidirectional, and power management between input sources is not possible. Improved noncoupled-inductor-based topologies are discussed in (Varesi et al., 2018, 2019). In (Varesi et al., 2019), besides the hard switching, this configuration employs high number of switches and inductors due to the non-sharing of components. A DISO topology for street-lighting applications, based on a combination of a two-input boost converter and an impedance network, is introduced in (Abbasi Soltani et al., 2021).

In (Wai et al., 2011), a DISO boost converter has been presented for low-voltage and high-current applications. In order to achieve the ZVS capability of all input switches, an auxiliary circuit, including a diode, inductor, and capacitor is used. The input sources can provide the energy required by the load individually or simultaneously; in the case of two inputs, the sources are connected in series. The presented converter has a unidirectional power flow. The structure of a DISO bidirectional converter has been presented in (Faraji et al., 2021a) and is shown in Fig. 13. Coupled inductors are used to achieve soft switching in all switches. The input sources can deliver the required energy to the load either individually or simultaneously. The authors of (Faraji et al., 2019) have presented a MISO structure based on a boost converter with a small number of components. An (n) input type of this structure is shown in Fig. 14. The presented converter is made up of a coupled inductor, $(n + 1)$ switches, and $(n + 1)$ diodes. The voltage gain is considerable due to the usage of the coupled inductor, even though the voltage stress on the main switch is less than half the output voltage. A power flow path is provided in this circuit to charge the ESSs. Moreover, a simple resonant circuit, including a L_a inductor and a C_a capacitor is used to achieve the ZVS conditions for the main switch in the charge path and to provide ZCS conditions on the discharge path. The main disadvantage of the presented structure is that all switches do not operate under soft-switching conditions, and one switch operates under hard-switching conditions. Moreover, in ESS mode, the charge path switch should be switched at a high frequency, which increases losses.

In (Faraji et al., 2020), a boost converter-based DISO structure has been described for PV-battery applications. A voltage multiplier cell based on coupled inductors is utilized to achieve high voltage gain; however, the voltage stress on the switch is half the output voltage. In this topology, the switch in the ESS path is also connected to the main switch, and ZVS conditions are provided for all switches via a simple active clamp circuit. In this MPDC, soft switching performance depends significantly on the load, such that when the load is low, and energy flows from the PV source to the ESS, the active clamp circuit is turned off, and hard switching performance is achieved. Furthermore, the converter losses are substantial due to the clamp diode circuit and series switches. The structure of a DISO boost converter has been presented in (Zhou et al., 2022) for integrating RESs and ESSs with a small number of elements and the low voltage stress of the switches. A coupled inductor is used to obtain high voltage gain. The active clamp circuit is used for ZVS conditions of the switches and ZCS conditions of the diodes in this structure to reduce switch losses and increase efficiency. The shortcoming of this structure is the discontinuous current flow of resources (bidirectional port and port connected to ESS), which can have a detrimental impact on the performance of the RES as well as battery life and efficiency. In addition, soft switching conditions are not met in the charging mode of the ESS source of the renewable source. Authors of (Pourjafar et al., 2021) proposed a DISO topology for HES applications. As is shown in Fig. 15, the converter is comprised of a coupled inductor and super voltage lift circuit (SLVC) to increase voltage gain. Bidirectional power flow, low ripple, and continuous nature of the input current, ZVS, and ZCS operation of diodes are advantages of this MPDC.

A step-up/down MISO structure based on the SEPIC converter has been presented in (Haghighian et al., 2017). This structure has a bidirectional port (for connecting to an ESS) and (n) unidirectional inputs. The switches and diodes in this converter are not under soft switching. Moreover, ESS alone operation mode is not possible, which makes this topology improper for standalone PV/battery applications. The DISO structure is shown in Fig. 16. Another SEPIC-based three-port topology for PV-battery application is reported in (Cheraghi et al., 2021), and is depicted in Fig. 17. To increase voltage gain, a voltage doubler cell is used. The proposed MPDC has several advantages, including soft switching, low number of switches, and low current ripple.

In (Akar, 2016), a high-efficiency bidirectional MPDC has been developed by integrating the two topologies provided in (Haghighian et al., 2017; Jiang et al., 2013). The topology is shown in Fig. 18. Two auxiliary switches, S_{a1} and S_{a2}, two auxiliary diodes, D_{a1} and D_{a2}, an L_0

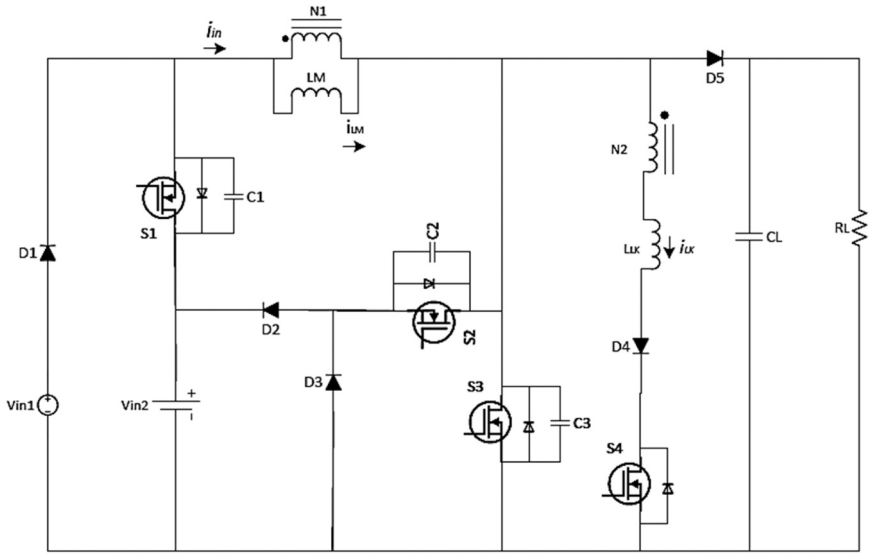

Fig. 13. DISO bidirectional converter (Faraji et al., 2021a).

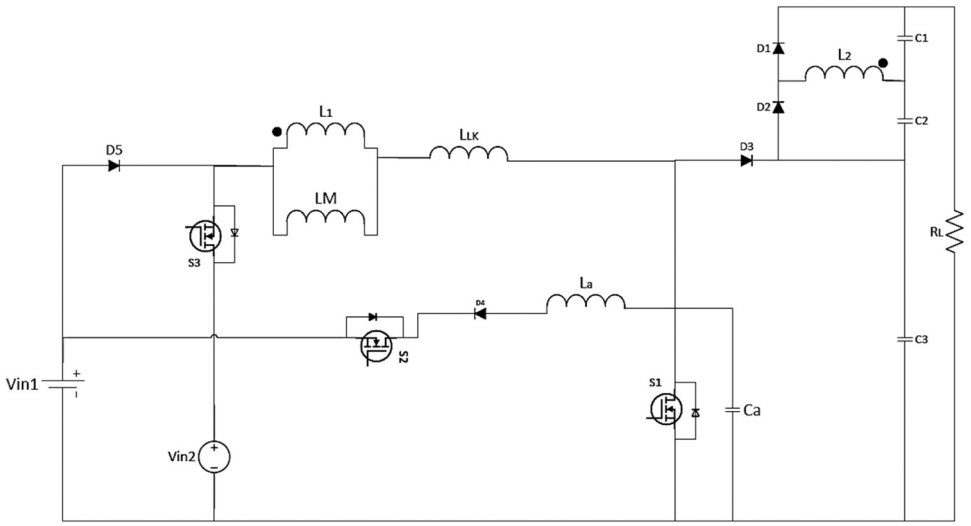

Fig. 14. Expandable DISO structure based on a boost converter (Faraji et al., 2019).

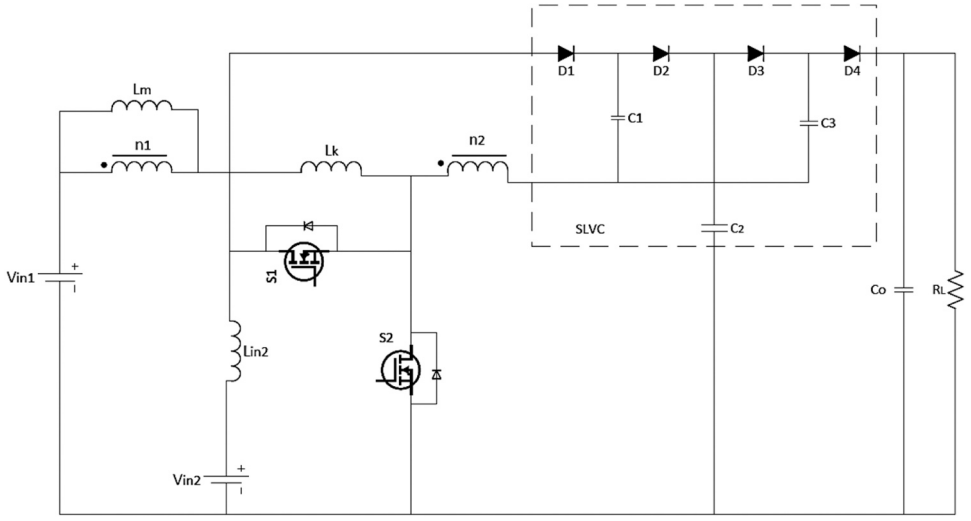

Fig. 15. DISO converter for HES (Pourjafar et al., 2021).

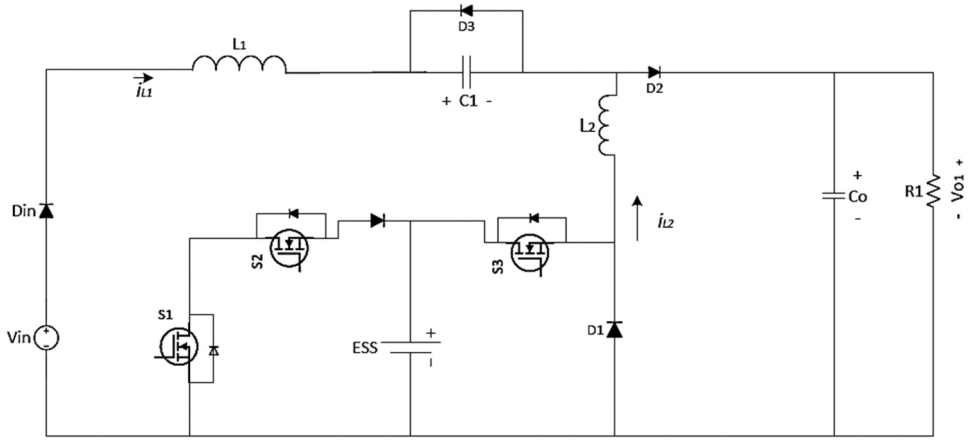

Fig. 16. SEPIC-based MISO converter (Haghighian et al., 2017).

inductor, and a coupled inductor are used in the proposed converter. In this topology, there will be no need to expand the capacity of the magnetic core by replacing the non-coupled inductor with the coupled inductor. The T_0 and Q_0 switches in this converter are switched under ZVS, improving the converter's performance at higher frequencies and reducing the switches' voltage and current stress. This converter has two

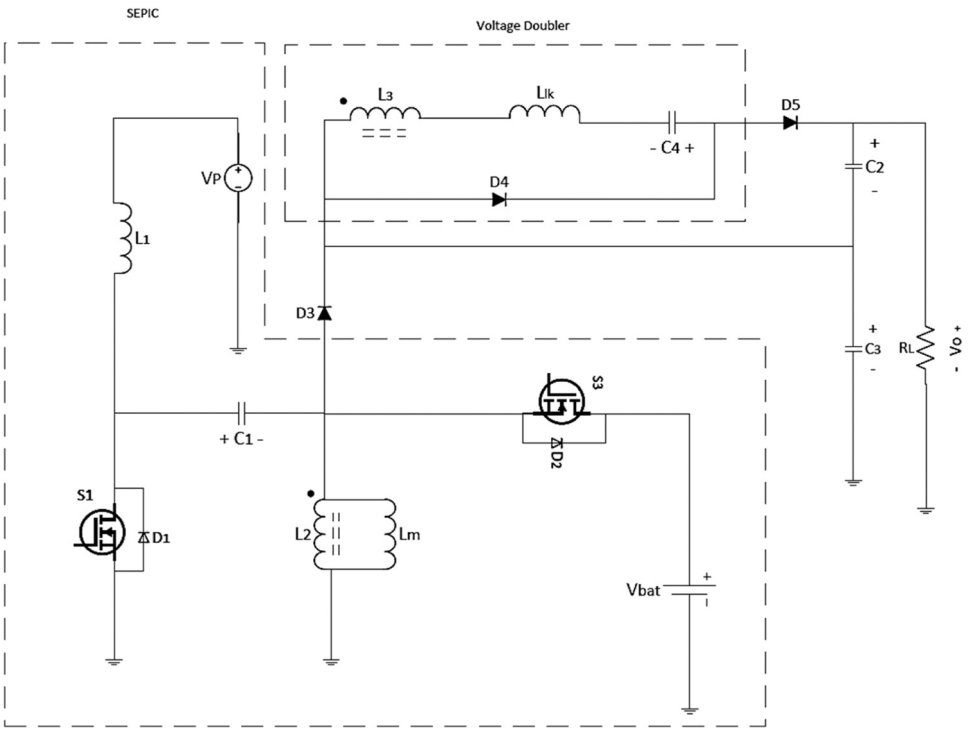

Fig. 17. High step-up three-port ZVS converter (Cheraghi et al., 2021).

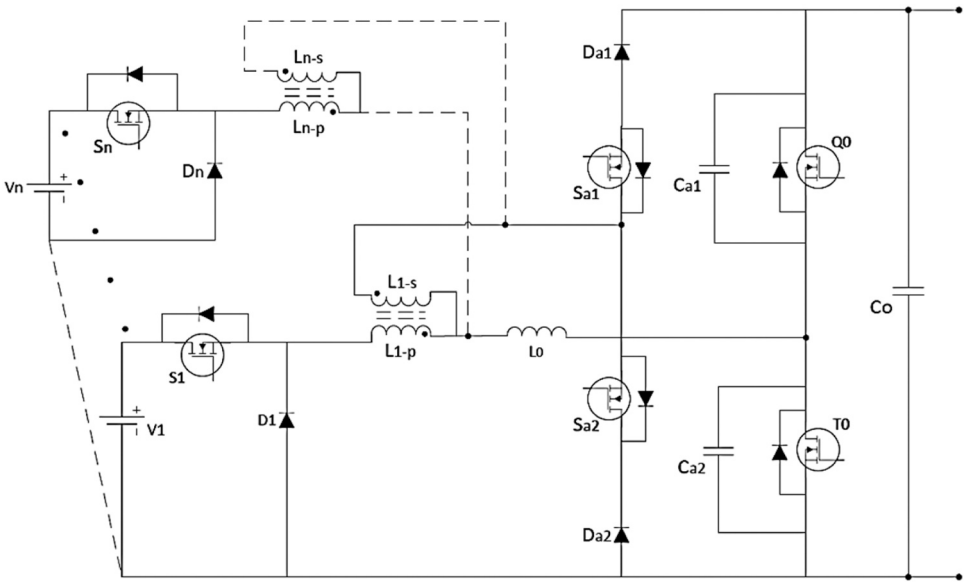

Fig. 18. Converter proposed in (Akar, 2016).

operation modes: charging mode in which the S_{a1} is ON and the S_{a2} is OFF, and discharge mode in which the S_{a2} is ON and the S_{a1} is OFF. As a result, auxiliary switches do not result in any further switch losses, which is one of the primary benefits of this topology. Furthermore, the current flowing through the inductor L_0 is bidirectional, providing the energy required for soft switching.

In (Faraji and Farzanehfard, 2021), a soft-switched high step-up converter has been proposed. In this topology, ESS can be charged from RES and load, making the structure proper for HRS and microgrid applications. Based on three switches leg, a family of MPDCs has been suggested in (Azizi et al., 2016). However, as the number of input ports increases, the complexity of the control system and the number of switches/inductors increases. A high voltage gain bidirectional Z-source-based DISO converter is presented in (Rostami et al., 2021). However, the number of components is high, and the converter does not have common ground. A soft-switched quasi-Z-source topology for a hybrid energy system has been proposed (Torki Harchegani et al., 2021), that can combine the energy of multiple input sources with varying voltage-current characteristics and use it to supply the load. Also, the power of the input sources can be transferred to load simultaneously or individually. In (Chandrasekar et al., 2020), a topology with positive high voltage gain, integrating a buck-boost converter with a bi-directional boost converter, with two unidirectional and one bi-directional port for PV-battery applications, has been proposed. A

DISO coupled-inductor reconfigurable converter with medium voltage gain is proposed in (Al-Soeidat et al., 2020) for PV-battery applications. The converter is able to operate as a boost converter, buck-boost converter, or forward converter in different modes of operation. Three control loops, namely IVR, OVR, and BVR, are utilized to control the converter. The OVR loop is a PI-based control loop employed to maintain the desired output voltage. The input PV port voltage, on the other hand, is managed along with a P&O algorithm through an IVR loop to maximize the input PV power. Additionally, the BVR loop is implemented to prevent overcharging of the battery. A bidirectional DISO converter with soft switching capability is proposed in (Faraji et al., 2021b). A MISO configuration is proposed in (Ravada et al., 2021) for the interface of PV, wind, and battery-supercapacitor-based hybrid energy storage in DC microgrid applications. In this topology, DC-link voltage is the sum of PV and battery voltages. In (Zhu et al., 2020b), a bidirectional DISO with high step-up voltage gain is proposed. However, the number of components is high. A bidirectional DISO for FC hybrid systems is suggested in (Ma et al., 2021), which employs a switched-capacitor unit to achieve high voltage gain and low voltage stress. In (Dezhbord et al., 2022), a DISO topology is introduced, which consists of a bidirectional battery port and two unidirectional input and output ports. This proposed converter uses two coupled inductor-based voltage multipliers to enhance voltage gain. Furthermore, it utilizes the leakage inductance of the coupled inductors to achieve ZCS conditions for all switches. Additionally, it mitigates the reverse-recovery power losses of the multiplier diodes by controlling the rate at which their current decreases.

A soft-switched DISO topology for HRS applications is proposed in (Faraji et al., 2021c). The converter is bidirectional, and the control system for the proposed converter is designed to ensure both system stability and the regulation of load voltage while also addressing MPPT and battery charging control. An expandable MISO converter with the capability of multiple RES integration is proposed in (N. Jayaram et al., 2023). Simple structure, high voltage gain, continuous input current, and low input current ripple are advantages of the topology. By replacing diodes with switches, bidirectional power flow can be achieved. A TISO topology appropriate for hybrid energy applications such as fast-charging EVs is introduced in (Aravind et al., 2023), which has high output voltage gain, low voltage stress, and high efficiency. The proposed converter is able to produce high voltage gain through an Actively Switched Inductor Capacitor (ALC) network. A MISO converter is designed in (Amaleswari and Prabhakar, 2021), utilizing voltage multiplier cells and implementing a current-sharing mechanism to enhance voltage gain. However, the proposed converter incorporates a higher number of components, impacting the overall cost and size of the converter. A DISO converter with seven operating modes was developed by combining bidirectional buck-boost configurations. Nonetheless, the voltage gain in this design is relatively low (Aljarajreh et al., 2021). In (Dhananjaya et al., 2023), an expandable MISO topology with source fault tolerant is discussed. A DISO converter with IoT wireless sensors is presented in (Lavanya et al., 2021). An DISO converter with a ZVT auxiliary circuit, designed for PV applications, is discussed in (Zhu et al., 2019). However, it's important to note that this topology is unidirectional. Additionally, the design involves a relatively high number of components.

2.2. Non-isolated SIMO converter

A unidirectional SIDO topology with only one inductor has been presented in (Wibowo et al., 2009). The suggested converter can function in both boost and buck-boost modes. A positive or negative output voltage can also be achieved. The voltage regulation of the two outputs is obtained independently of one another. Because just one inductor is used, only one current sensor can determine the source current. A SIMO unidirectional topology with an inductor has been presented in (Patra et al., 2012). The proposed MPDC can generate buck, boost, and inverted outputs simultaneously. A control mechanism based on the inductor current ripple is also discussed. Because just one inductor is used, only one current sensor can determine the source current. Based on the switched-capacitor, a series of SIMO topologies have been suggested in (Ye and Eric Cheng, 2015), with only one active switch and one inductor. However, they suffer from cross-regulation of the output voltages. Authors of (Wang et al., 2016) have suggested a model predictive voltage control approach to overcome the crossed regulation problem and enhance dynamic response for a SIMO buck-based converter.

As is shown in Fig. 19, a boost SIMO topology using an inductor has been proposed in (Nami et al., 2010). The output load voltages are adjusted in series in this converter. DC output voltages that have been adjusted can be employed in several high and low-power applications. The MPDC has three operating modes in dual output topology, as follows.

- First, when the S_0 switch is turned ON, the energy from the input source is stored in the inductor. As a result, the inductor current begins to rise. Because the output capacitors' required power is frequently supplied in this operating mode, both output capacitors are discharged, and the voltage across their terminals is decreased.
- In the second operating mode, the S_0 switch is turned OFF, and the S_1 switch begins to conduct, charging the output capacitor C_1 and increasing the voltage across it. The inductor current reduces in this operating mode. The voltage of the second capacitor, on the other hand, drops due to the power supply of the second output capacitor, C_2.
- When all the switches are turned OFF, and diode D_3 is turned ON in the third operating mode, the source and inductor energy are transmitted to both the output load and their corresponding capacitors. When the capacitors are charged, the voltage across them rises.

Using only one inductor, a reduced number of switches, and the ability to adjust the voltage of the output loads in series are the most important advantages of the proposed converter. The inability of this converter to provide bidirectional power flow, on the other hand, is its most significant disadvantage. Moreover, this structure requires (n + 1) switches and (n) diodes for n-output.

Another SIMO topology depicted in Fig. 20 has been presented in (Ray et al., 2013). This MPDC can operate in both buck and boost modes. This arrangement was achieved by substituting an HB converter for the switch in a standard boost converter. The HB converter's midpoint also serves as a load point. As a result, the proposed converter can supply two output ports. The buck and boost processes are supported in this converter by L_1 and L_2 inductors, respectively. Three functioning modes for this converter can be envisaged based on whether the Q_1 and Q_2 bidirectional switches are turned ON or OFF, as follows:

- Both the Q_1 and Q_2 switches are active in the first operating mode. As a result of these switches, the source energy is stored in the L_1 inductor. The L_2 inductor current is also in Freewheeling mode, as controlled by the Q_2 switch. Diode D is turned off in this mode.
- The Q_1 switch is turned ON, and the Q_2 switch is turned OFF in the second operating mode. In this scenario, the current flowing through the inductor L_1 is split into two parts: one part goes through the diode D, and the other part goes through the inductor L_2. A portion of the input source energy and energy stored in inductor L_1 is delivered to the load, while the remainder is stored in inductor L_2.
- Both the Q_1 and Q_2 switches are turned OFF in the third operating mode. As a result, the current of L_2 is in Freewheeling mode via the Q_2's reverse parallel diode. Through diode D, the current of L_1 is also transmitted to the corresponding output. As a result, the energy stored in both inductors is transmitted to the respective outputs.

The proposed converter can operate in both step-up and step-down

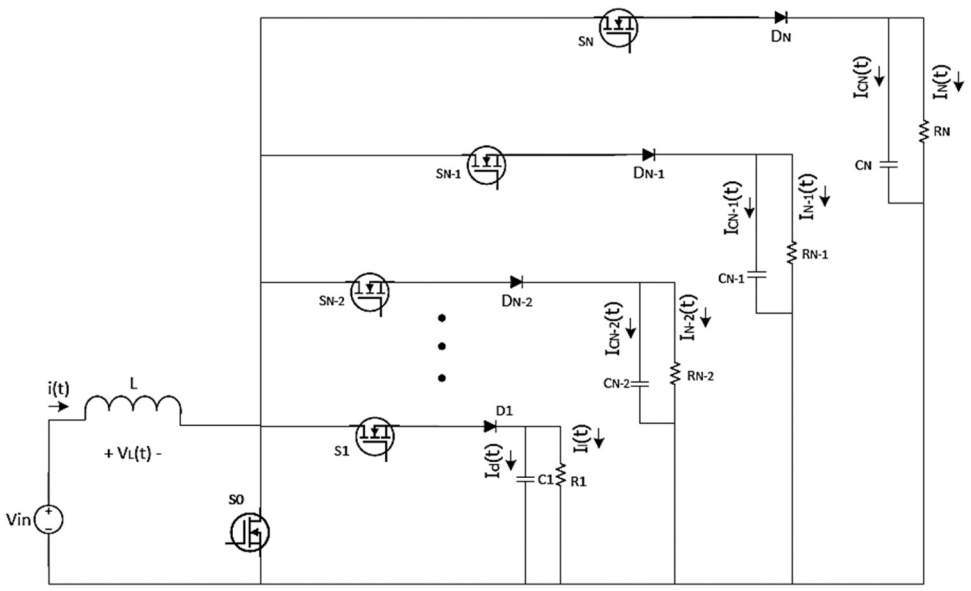

Fig. 19. Diode-clamped based SIMO converter (Nami et al., 2010).

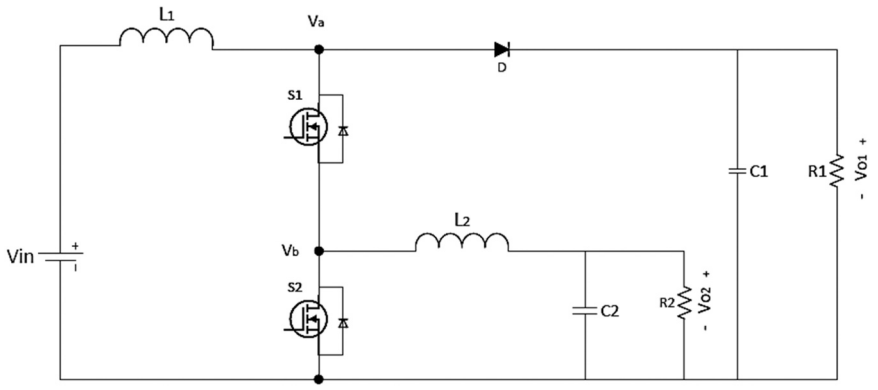

Fig. 20. SIMO converter with simultaneous buck/boost operation (Ray et al., 2013).

modes. The voltage range that can be created is also significantly greater than that of conventional independent converters. This converter may create any value from zero to the magnitude of the input voltage source at its output in the step-down mode. Still, traditional step-down converters cannot produce very small voltage values or a unit voltage conversion ratio at their output. This structure contains fewer devices than the standard independent step-up and step-down converters, making it less expensive and more efficient. The suggested converter can

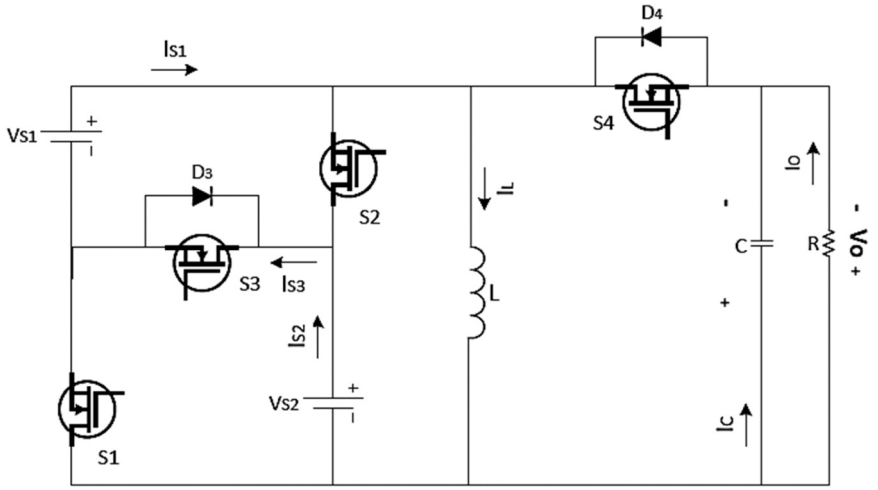

Fig. 21. DISO bridge type topology (Athikkal et al., 2019).

be controlled by two independent control variables, making it simple to control.

The authors of (Athikkal et al., 2019) have described a DISO bridge-type topology that can combine the energy input sources with distinct voltage-current characteristics and use it to supply the load. The structure is shown in Fig. 21. In this converter, the input sources can deliver power to the load either simultaneously or individually. An expandable SITO high voltage gain converter has been proposed in (Saadatizadeh et al., 2019). In this structure, the voltage gain can be increased by increasing the inductor-diode-capacitor cells on the first and second output sides and increasing the diode-capacitor cells on the third output side. Low ripple and continuous nature of the input current and low voltage stresses on the switches are advantages of this converter. By the combination of three-level buck and boost converters, as is shown in Fig. 22, a SIDO topology with low-voltage stress on the switches is presented in (Ganjavi et al., 2018). A coupled-inductor-based high step-up and high step-down three-Port topology with zero input current ripple is presented in (Saadatizadeh et al., 2021a). In the suggested converter, three different SIDO operation modes can be obtained by changing the place of the input source between each of the three ports. The converter is recommended for RES, DC motors drive, UPS, and greenhouse applications. However, this MPDC is composed of five switches and, two coupled inductors, and six capacitors, which increase the size and cost and reduce the power density. A similar idea is discussed in (Saadatizadeh et al., 2021b) by the same authors. In (ANON et al., 2020), a SIDO converter was developed by integrating buck and super-lift Luo converters. This configuration is suitable for both step-up and step-down modes.

2.3. Non-isolated MIMO converter

The single-stage MIMO modular structure has been proposed in (Behjati and Davoudi, 2011, 2013a, 2013b). As a result, the power of the desired number of input sources can be combined to produce the power of the desired number of loads at the output. The current of all input sources and output loads, on the other hand, can be calculated at any time due to the use of only one inductor jointly between input sources and loads, with only one current sensor and monitoring of critical command signals. This converter can function in both buck and boost modes. However, in this MPDC, the energy from both input sources cannot be transferred simultaneously; Only one input source can transfer energy to the inductor at any given moment. Moreover, this structure is unidirectional, output ports are not common grounded, and the input current is discontinuous with high ripple. An MPDC similar to that provided in (Behjati and Davoudi, 2011, 2013a) is proposed in (Behjati and Davoudi, 2012), except that its various output loads are connected in series. All of the converter's features specified in (Faraji et al., 2021c; N. Jayaram et al., 2023) are also established for this structure. It is suggested that the DC outputs of this converter be used as input voltage sources for multilevel inverters.

A TIDO is discussed for DC microgrid application in (S. et al., 2018). As is shown in Fig. 23, a DIDO structure with low voltage stress on switches/diodes has been presented in (Jalilzadeh et al., 2020a). The power flow in the given converter is bidirectional, and the input current of resources (bidirectional port and port connected to ESS) is continuous. Input sources can offer the load's required energy either individually or simultaneously. Switches S_2 and S_4 are turned OFF in the battery discharge mode, and the output voltages and discharge of the battery are regulated by controlling the duty cycle of S_1 and S_3 switches. Switch S_3 is turned OFF in battery charging mode, and the output voltages and battery charge are controlled by controlling the duty cycle of S_2, S_1, and S_4. A DIDO converter with low voltage stress on the switches is proposed in (Jalilzadeh et al., 2020b). The drawback of the converter is the high number of inductors and complex control algorithm. An expandable high-voltage gain converter based on diode-capacitor cells is proposed in (Shoaei et al., 2023) for PV applications. Although the converter is able to transfer the energy of input sources to output simultaneously, the converter is unidirectional.

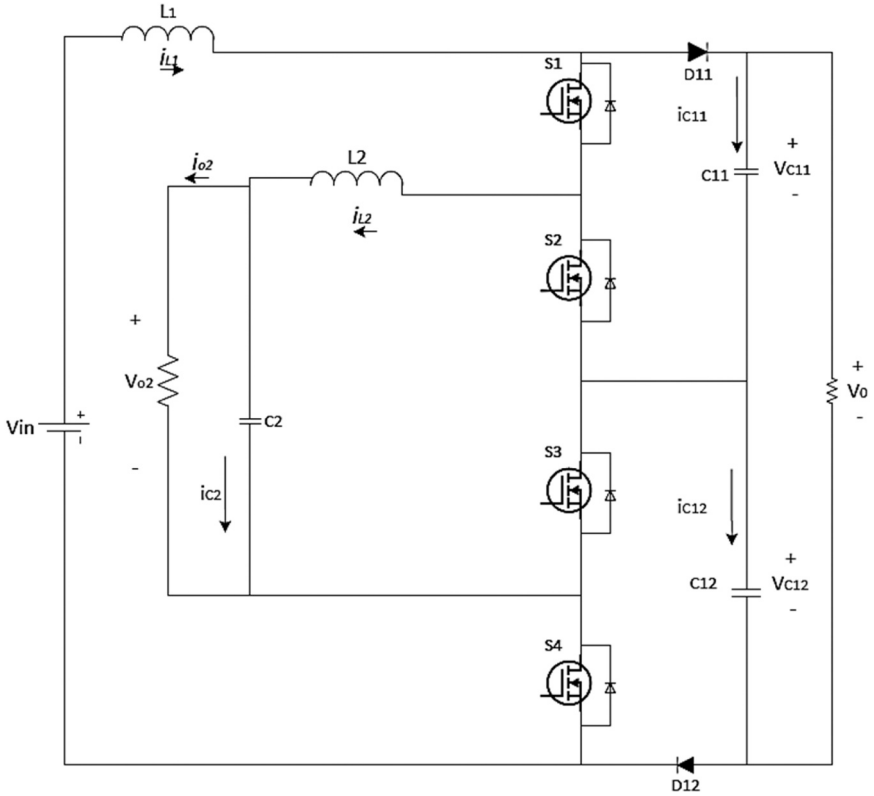

Fig. 22. SIDO three-level converter (Ganjavi et al., 2018).

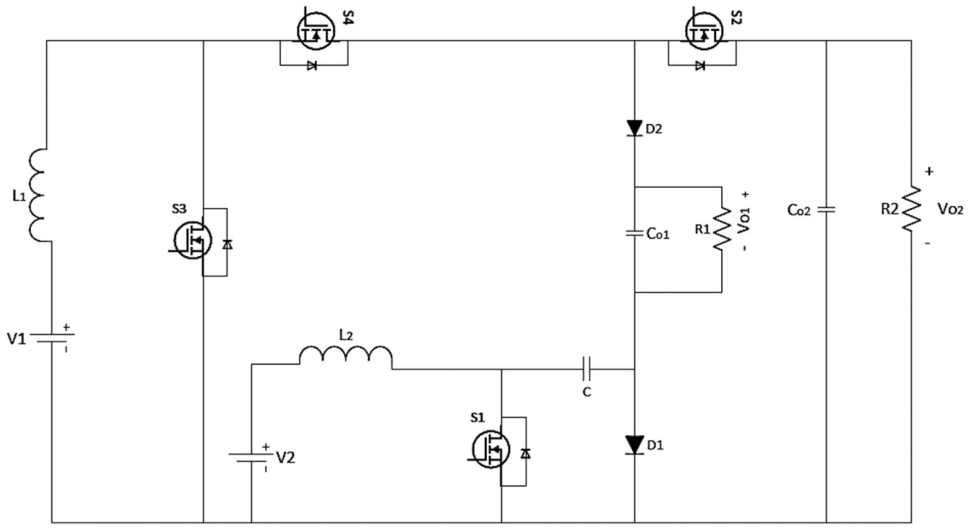

Fig. 23. DIDO converter in (Jalilzadeh et al., 2020a).

In (Nahavandi et al., 2015), a MIMO converter suitable for use in hybrid/electric vehicles has been presented. This converter uses only one common inductor for all input sources. Each input source is connected to the inductor via power diodes. To enable the ESS to be charged from the input sources, the inductor output provides a separate path. Using a current sensor, the flow of all input sources can be determined at all times. The unidirectional power flow, especially for use in the proposed hybrid/electric vehicles, is one of the drawbacks of this converter because, in such a case, it is not possible to use the return energy of the wheels during braking. Another shortcoming of this structure is that only one input source can transmit energy at any moment. Other downsides of this arrangement are the high current ripple and discontinuity of resources. General approaches for manufacturing MPDCs are provided in (Zhang et al., 2014; Wu et al., 2015). MPDCs are constructed by connecting several pulsed voltage source cells. These approaches can build MPDCs that are multi-input, multi-output, unidirectional, or bidirectional. For EV applications, in (Kumaravel et al., 2019), a bidirectional DIDO converter for integrating PV/battery/ultra-capacitor has been proposed. However, the voltage stress on the switches is high in the boost mode.

A MIMO bidirectional buck topology has been described in (Babaei and Abbasi, 2017). A DIDO structure is depicted in Fig. 24. In addition to generating separate voltage levels with bidirectional current path, this converter can integrate energy sources with different voltage-current characteristics. However, the large number of switches and inductors increases the proposed structure's size and weight. Other downsides of this converter are the high current ripples and discontinuity of resources current. The excessive number of active switches in the conduction path increases losses and reduces converter efficiency. In (Zhaikhan et al., 2017), a DIDO switched-capacitor converter is presented. However, in this topology, the number of switches is high. A DISO switched diode-capacitor-based topology with high gain and low voltage stress is discussed in (Hou et al., 2016). A MIMO boost converter based on switched-capacitors, proper to use in PV/FC applications, has been presented in (Babaei and Abbasi, 2016). This topology has several advantages, including operation at the high switching frequency, high voltage gain, continuous input source current, low voltage stress on switches, and the capability of using input sources with different voltage-current characteristics. The downsides of this structure include the inability of bidirectional power flow, the impossibility of power management between input sources, and a large number of employed components.

In (Mohseni et al., 2019), a MIMO structure based on the diode-capacitor voltage multiplier stage is discussed. In this converter, if one of the sources is disconnected, other sources can still feed their corresponding output. The ability to utilize different sources with various voltage/power levels and continuous input currents is another advantage of this converter. In (An and Lu, 2015), a single switch topology is developed for a stand-alone PV battery-powered pump system from the combination of a buck converter with a buck-boost converter. Variable-frequency control and PWM are utilized to achieve MPPT and output voltage regulation. However, due to the first quadrant operation of the buck-boost stage, variable speed is not achievable. By integrating of single stage boost and FB converter, a structure has been presented for stand-alone PV-battery-DC motor application in (An et al., 2019). In (Sato et al., 2017), a converter is proposed in which inputs can be controlled individually by integrating a PWM buck topology and a phase shift dual-active HF.

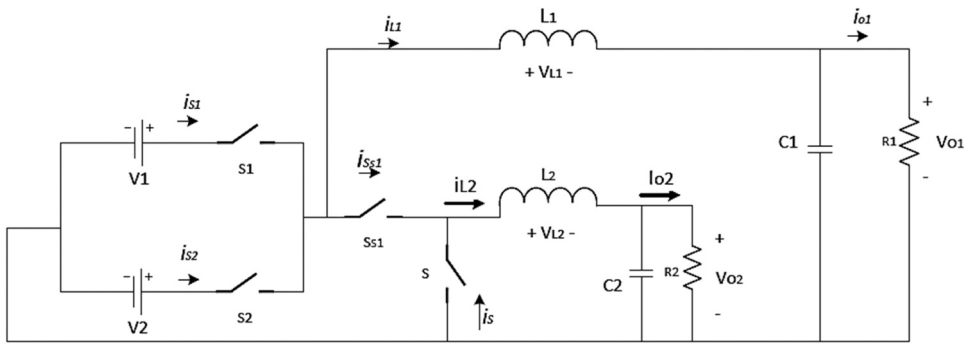

Fig. 24. MIMO bidirectional buck converter (Babaei and Abbasi, 2017).

For a bipolar DC microgrid application, a DIDO converter is introduced in (Aghdam et al., 2022). This proposed converter is capable of extracting the maximum power from the PV, charging or discharging the battery, and symmetrically delivering power to the output load. However, the converter suffers from hard-switching. A single inductor, unidirectional, DIDO bipolar converter for Interfacing PV–FC with low-voltage bipolar DC microgrids is described in (Prabhakaran and Agarwal, 2020; Prajof and Agarwal, 2015). However, it is worth noting that this configuration lacks the capability to boost voltage to maintain volt-second balance across its inductor. To integrate PV-battery into the bipolar DC microgrid, Ref (Tian et al., 2020) proposed a DIDO converter that combines a unipolar output SEPIC three-port converter and a unipolar output Cuk three-port converter. A limitation of this configuration is that the battery voltage must be higher than the PV voltage. In (Saafan et al., 2021, 2023), a TIDO configuration for DC microgrid applications is described, connecting three different PV-FC-Battery and two different loads. The proposed converter exhibits bidirectional buck-boost capability, allowing for the connection of various loads and sources with different voltage and power levels. In (Suresh et al., 2021), a DIDO converter for EV application is proposed. Nevertheless, the converter encounters certain challenges, including high voltage stress on specific output diodes, substantial current spikes in certain power switches, and constraints on power level scalability. Another bidirectional MIMO topology for EV applications based on the diode-capacitor cells is presented in (Maalandish et al., 2023). High voltage gain, low current ripple of sources, continuous nature of input sources' current, and ability to utilize the input sources simultaneously are advantages of the proposed topology. In (Saadatizadeh et al., 2022), an expandable MIMO topology comprised of the voltage multiplier cell with high voltage gain is proposed. However, the charging path is not provided for the ESS from other input ports. The MIMO topologies are synthesized in accordance with network theory in (Zhang et al., 2022), while optimizing the components. Nonetheless, there are limitations related to port voltage, duty ratio, and expandability of topologies.

A comparison of various non-isolated MPDCs is illustrated in Table A.

3. Partially isolated MPDCs

In (Sun et al., 2014), a high-efficiency three-port converter has been suggested by integrating dual buck-boost and DAB for the PV-battery hybrid system. The converter is depicted in Fig. 25. Bidirectionality, the source current's minimal ripple due to the input's interleaved structure, and ZVS operation are advantages of this converter. Moreover, by PWM and PS control, bidirectional power flow between each port can be obtained. Derived from the HB topology, in (Zhu et al., 2014), a three-port converter has been developed for PV-battery application. Load port and bidirectional non-isolated ESS port are realized on the secondary side of the transformer, while RES is connected to the primary isolated port. Low current ripple, continuous nature of the input current, and ZCS for switches and diodes are advantages of this converter. As is shown in Fig. 26, by integrating a boost stage into the phase-shift full-bridge, a three-port bidirectional converter for communication and hybrid RES applications has been suggested (Al-Atrash and Batarseh, 2007). In this topology, power flow in the boost stage is controlled by adjusting the duty cycle of switches, while PSM is used to regulate the load. Among the disadvantages of the proposed structure are hard switching of the rectifier stage, reverse recovery losses, and high voltage stress.

For satellite application, the authors of (Qian et al., 2009a, 2010a) proposed a three-port bidirectional structure shown in Fig. 27. A comprehensive approach is employed in (Qian et al., 2010a), and the state-space averaging method is utilized to derive the converter model under different modes of operation. Subsequently, a decoupling network is introduced to facilitate separate controller designs. Control strategy and power management for the suggested topology are further investigated in (Qian et al., 2009b, 2010b, 2011). For the topology in (Qian et al., 2010a), the authors of (Rios et al., 2021) proposed a robust LMI-based gain-scheduling controller that is not based on decoupling techniques. Moreover, input source disturbance rejection is enhanced by employing H∞ norm and D-stability pole placement constraints. Although the proposed controller considered the uncertainties of RES and ESS ports, the converter parameters' uncertainties were not considered. For a similar topology, authors of (Damasceno et al., 2021) discussed LQG/LTRI robust controller for PV-battery application. A three-port, bidirectional converter, proper to use in stand-alone renewable applications, has been presented in (Wu et al., 2011a, 2011b). The topology is composed of HB, forward–flyback, and buck structures. PWM and feedback control strategy are also studied for control and modulation of the proposed control. The suggested topology has several advantages, including simple and compact structure and control, reduced number of components, and ZVS for all switches. However, the converter suffers from high input current ripple.

A single-stage, three-port converter, proper to use in a stand-alone PV application, has been analyzed in (Hu et al., 2014). This topology, shown in Fig. 28, is derived from integrating two Buck-boost and an FB; the transformer of the conventional FB is split into two transformers, and the magnetizing inductances are employed as filter inductors. Moreover, the PWM technique is employed to realize power balance between RES and ESS, while the PSM of switching legs is utilized to regulate the load voltage. Another three-port converter for a stand-alone hybrid energy system is provided in (Sun et al., 2014). The topology, shown in Fig. 29, is made up of an interleaved bidirectional Buck-Boost and a FB LLC resonant converter. A similar topology is suggested in (Chen, 2014; Qin et al., 2014), in which two of rectifier diodes are replaced with active switches. In addition, to decouple control variables and achieve ZVS for all switches, a PWM plus secondary side PS control scheme is proposed. However, the topology is unidirectional from the battery to the load. A similar topology is suggested in (wu et al., 2015) for hybrid RESs, which combine an interleaved boost-FB and a bridgeless boost rectifier. The

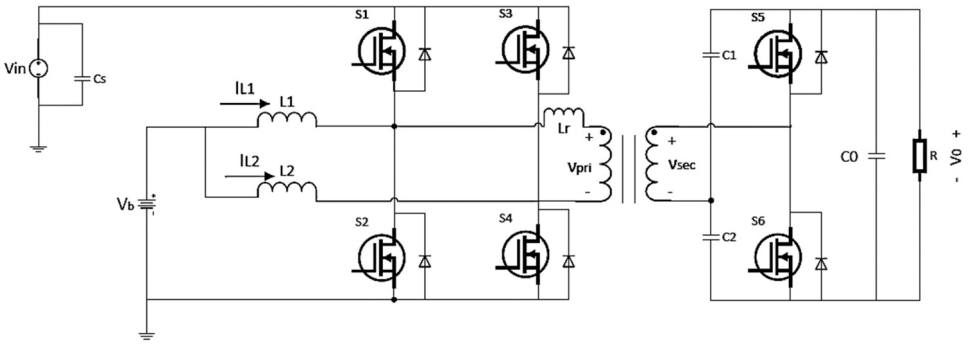

Fig. 25. Dual buck/boost integrated three-port bidirectional converter (Sun et al., 2014).

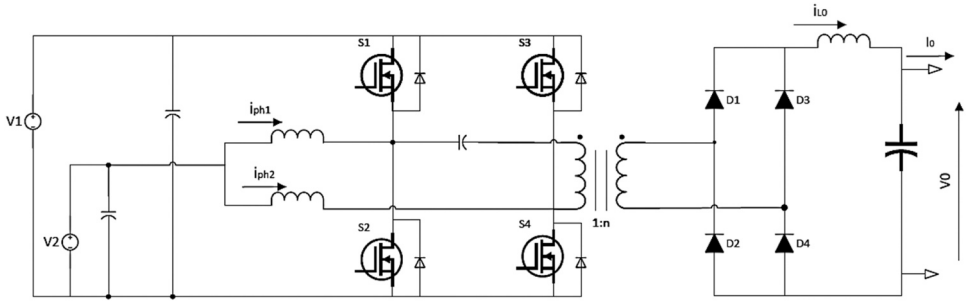

Fig. 26. Boost stage integrated phase-shift full-bridge converter (Al-Atrash and Batarseh, 2007).

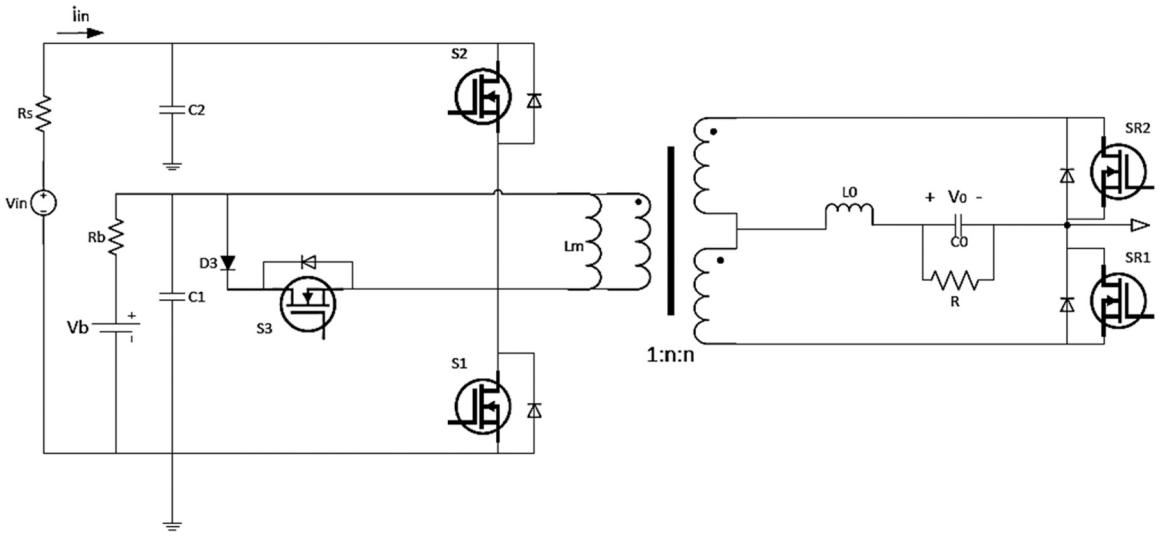

Fig. 27. Three-port modified HB converter topology (Qian et al., 2010a).

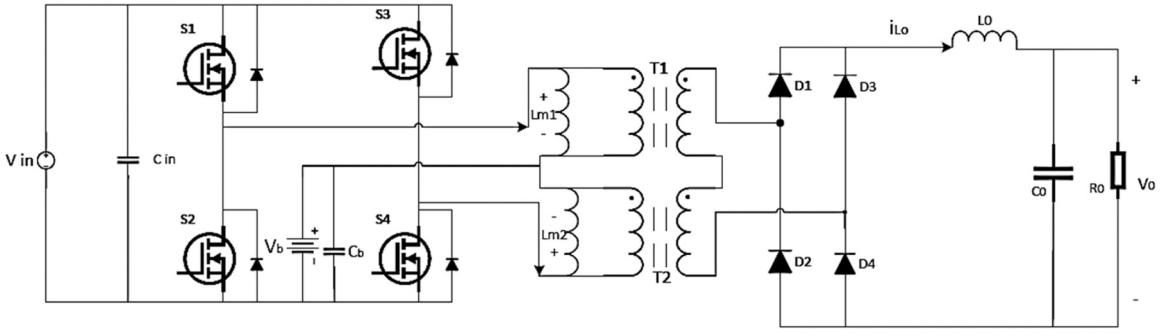

Fig. 28. The converter proposed in (Hu et al., 2014).

converter is depicted in Fig. 30. Relatively high efficiency, low current ripple, and bidirectional capability are the main advantages of this topology. However, body diodes of active switches on the secondary side operate under hard switching conditions, generating reverse recovery losses (Qin et al., 2014; wu et al., 2015). proposes a soft-switched DISO topology for integrating two low-voltage DC sources. In this configuration, two switch-inductor cells are integrated by utilizing the primary windings of the high-frequency transformer. Power is subsequently conveyed to the DC load via a FB circuit connected to the secondary winding of the high-frequency transformer. Also, the primary inductors are designed to operate in DCM. As a result, the issue of magnetizing inductance saturation in the high-frequency transformer is resolved.

In (Hu et al., 2015), an improved Flyback-Forward converter-based structure has been described for stand-alone PV-battery applications in which to transfer power to the output port, the leakage inductance of coupled inductors is used. The topology is shown in Fig. 31. By PWM and PS control schemes, power flow between each port can be controlled. This converter's operation consists of three operating modes. In the first operating mode, switches S_1 and S_2 are operated with 180° phase displacement, and energy is transferred from RES to ESS/load while the switches S_3 and S_4 are in a synchronous rectification state. In the second operating mode, ESS alone supplies the load, and the converter operates as the Flyback-Forward structure. S_3 and S_4 are the main switches, and S_1 and S_2 form an active clamp circuit. In the third operating mode, the load is disconnected, and RES charges ESS; The converter is the same as two paralleled Buck-Boost converters. However, this topology suffers from power delivery limitations from the battery to load. The authors of (Chen et al., 2015) have presented a three-port structure based on a

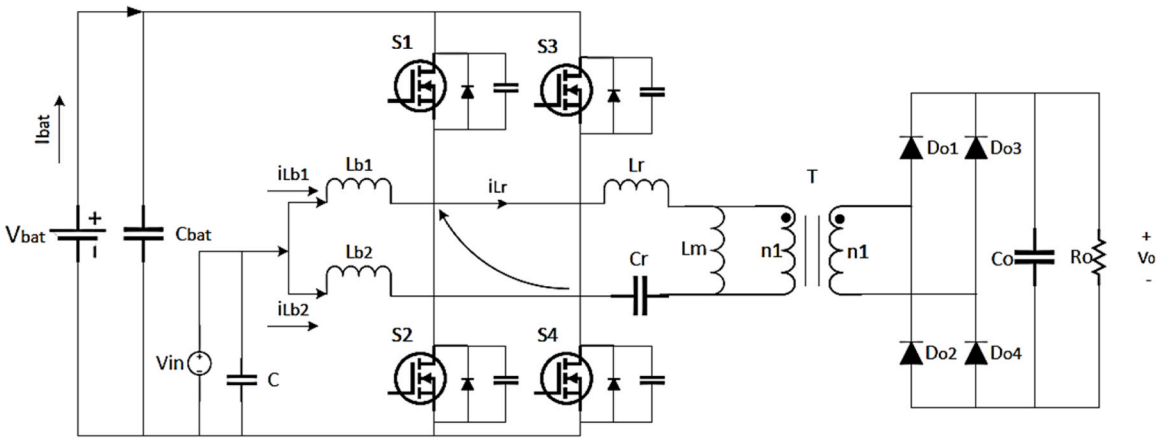

Fig. 29. LLC integrated three-port converter (Sun et al., 2014).

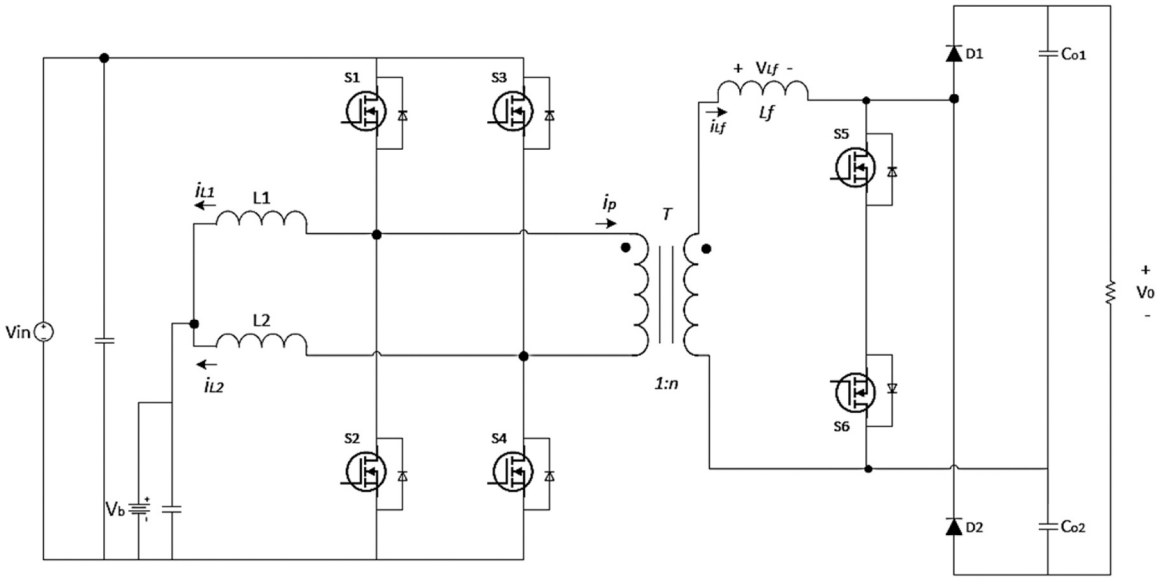

Fig. 30. The converter proposed in (wu et al., 2015).

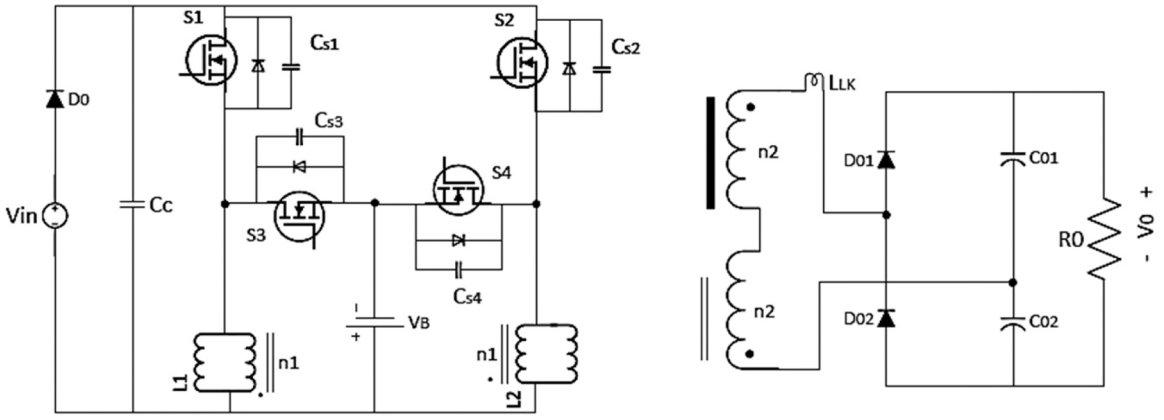

Fig. 31. Three port Flyback-Forward based converter (Hu et al., 2015).

Flyback converter. To eliminate low-frequency current ripple, an auxiliary circuit is employed. For simultaneous power management of multiple RESs, (Zeng et al., 2014) suggested a MISO structure. However, each input port requires one inductor, making the topology bulky. Moreover, with increases of load efficiency gradually decreases.

A PWM and PFM hybrid modulated converter, proper to use in a stand-alone PV application, has been analyzed in (Sun et al., 2015). The proposed structure is derived from integrating a two-phase interleaved

boost converter and an FB LLC resonant converter. The proposed topology has several advantages, including high voltage gain, small input current ripple, ZVS operating of all primary switches, and ZCS of all secondary diodes. In (Zeng et al., 2013), a three-port converter has been described for PV-battery applications. An LCL-resonant circuit is provided on the primary side of the converter to achieve the ZCS conditions for the main switches. However, power flow from load to ESS is impossible, making this topology suitable for stand-alone PV applications. A step-down three-port structure for HRS has been presented in (Vahid et al., 2021). In (Dobakhshari et al., 2020a), a high-gain converter for hybrid energy applications is presented. As is shown in Fig. 32, two transformers and two combined voltage-double rectifiers are utilized to achieve high voltage gain. Moreover, the number of semiconductors is reduced while all operate under ZVS conditions. Despite high voltage gain, the converter suffers from high voltage stress on its semiconductor elements. A similar idea to provide a high voltage gain DISO partially isolated converter is discussed in (Dobakhshari et al., 2020b).

For the PV/ battery hybrid system, in (Bayat and Baghramian, 2020), a quasi-Z source converter is proposed. As is shown in Fig. 33, to improve voltage gain, the switched capacitors and coupled inductor techniques are utilized. The converter's advantages are the continuity of the input current, the minimal ripple of the source current, bidirectional power flow, and low voltage stress on switches. In (Uno et al., 2018), a structure for a stand-alone PV system has been presented: a combination of a bidirectional PWM topology and a series-resonant converter. As is shown in Fig. 34, to realize a single-magnetic structure, the magnetizing inductance of the transformer is used as a filter for the PWM converter, whereas the leakage inductance accounts for the resonant tank of the series resonant converter. By integrating an FB structure and an NPC topology, the authors of (Kolahian et al., 2019) proposed an MPDC multiple RES into a bipolar MVDC microgrid. A three-phase interleaved DISO current-fed triple active bridge (TAB) bidirectional structure is suggested in (Wang and Li, 2013). The topology was further analyzed and developed in (de Oliveira et al., 2017, 2019). In (Lee and Jung, 2022), a SIDO DAB converter is introduced to facilitate the balancing of bipolar DC bus voltage levels without the need for supplementary voltage balancers. The input post consists of an FB converter, while output ports are comprised of an HB structure. The output ports are cascaded in series to produce bipolar DC voltage levels. The proposed converter divides a high-frequency transformer into two separate units to achieve the decoupling of bipolar power flows. This approach eliminates the requirement for complex decoupling algorithms, enabling independent control of the bipolar power flows to balance the bipolar voltage levels. An unidirectional expandable topology with bipolar symmetric output for bipolar DC microgrids is introduced in (Jiya et al., 2022, 2023), by combining a DAB or a PS-FB converter with a two-winding transformer. To facilitate the regulation of the output voltage and the integration of inputs with varying voltage levels, this topology employs multiple inputs through pulsating voltage sources and a time-multiplexed inductor charging technique. A compact size, bidirectional DISO topology utilizing a planar transformer is proposed in (Saadatizadeh et al., 2024) for high-frequency operation. However, voltage gain is not high.

A comparison of various partly isolated MPDCs is illustrated in Table B.

4. Isolated MPDCs

A magnetically coupled three-port configuration comprised of three HF converters is introduced in (Tao et al., 2006a). However, when the input port operating voltage varies widely in this topology, the soft-switching range will be reduced. In this converter, the three HB converters can also be replaced with three FB converters. The authors of (Tao et al., 2006b, 2008) have described a bidirectional three-port HB-based configuration comprising a high-frequency three-winding transformer with FC and supercapacitor. Two HBs are used to couple the FC and the load, and the supercapacitor is connected to a boost HB to compensate the slow transient response of the FC and realize a current-fed port. By the PS control of HBs, power flow between each port can be controlled, while voltage variations on the supercapacitor can be handled by PWM control. Besides galvanic isolation, ZVS operation under the entire phase-shift region, low current ripples, and less number of switches and gate-drive components are the advantages of the proposed structure. As is depicted in Fig. 35, in order to reduce input current ripples, in (Wang et al., 2012; Liu and Li, 2006) an inductor is added between input ports and HB structure. Also, a control method with PS and duty cycle regulation is applied to the converter. The proposed converter in (Liu and Li, 2006) is recommended for use in RES and FC hybrid EVs. This topology implements soft switching naturally by snubber capacitors and transformer leakage inductance. From a combination of a multiport DAB and buck-boost converter, a topology is proposed in (Aghajani et al., 2023) for bi-polar DC microgrid application. The phase shift PWM control strategy is utilized to regulate the output voltage and control the power flow between each port. A topology based on the series resonance converter, DAB, and SiC switches for EV fast and slow charging applications is discussed in (Dao et al., 2020).

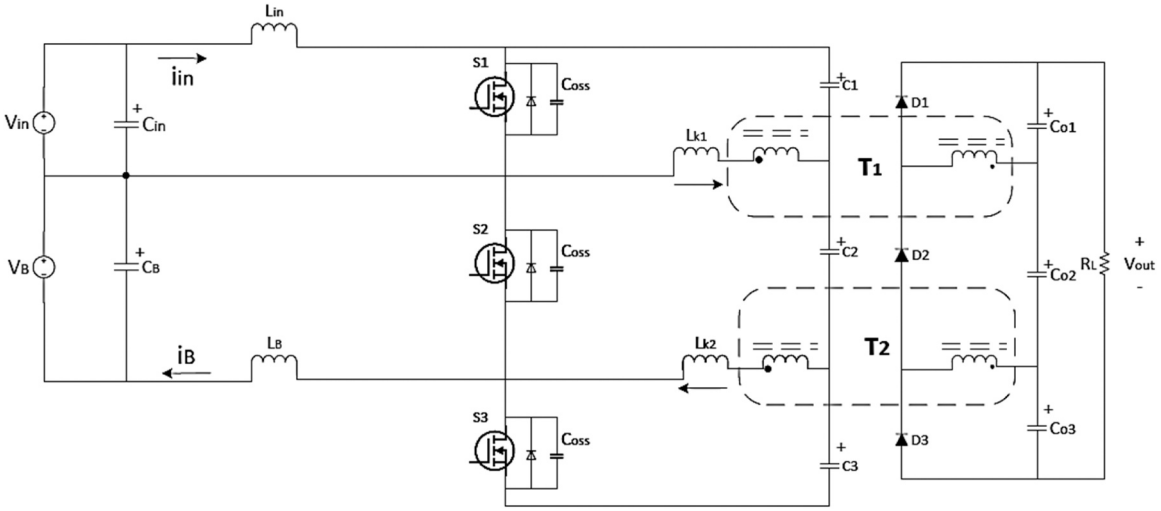

Fig. 32. The converter proposed in (Dobakhshari et al., 2020a).

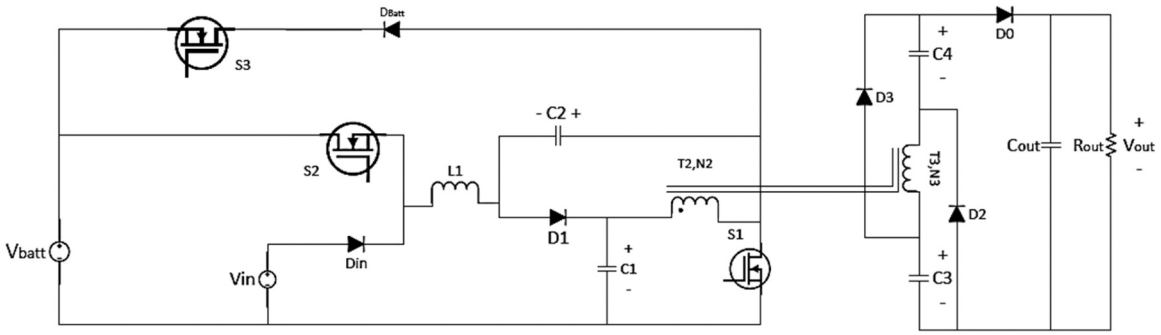

Fig. 33. The converter proposed in (Bayat and Baghramian, 2020).

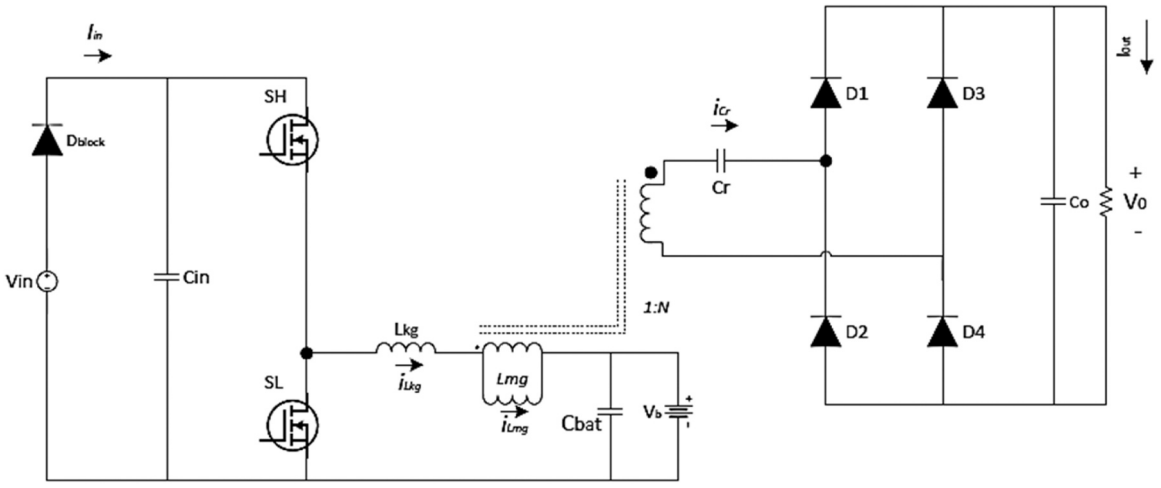

Fig. 34. Topology based on the integration of series-resonant and bidirectional PWM converter (Uno et al., 2018).

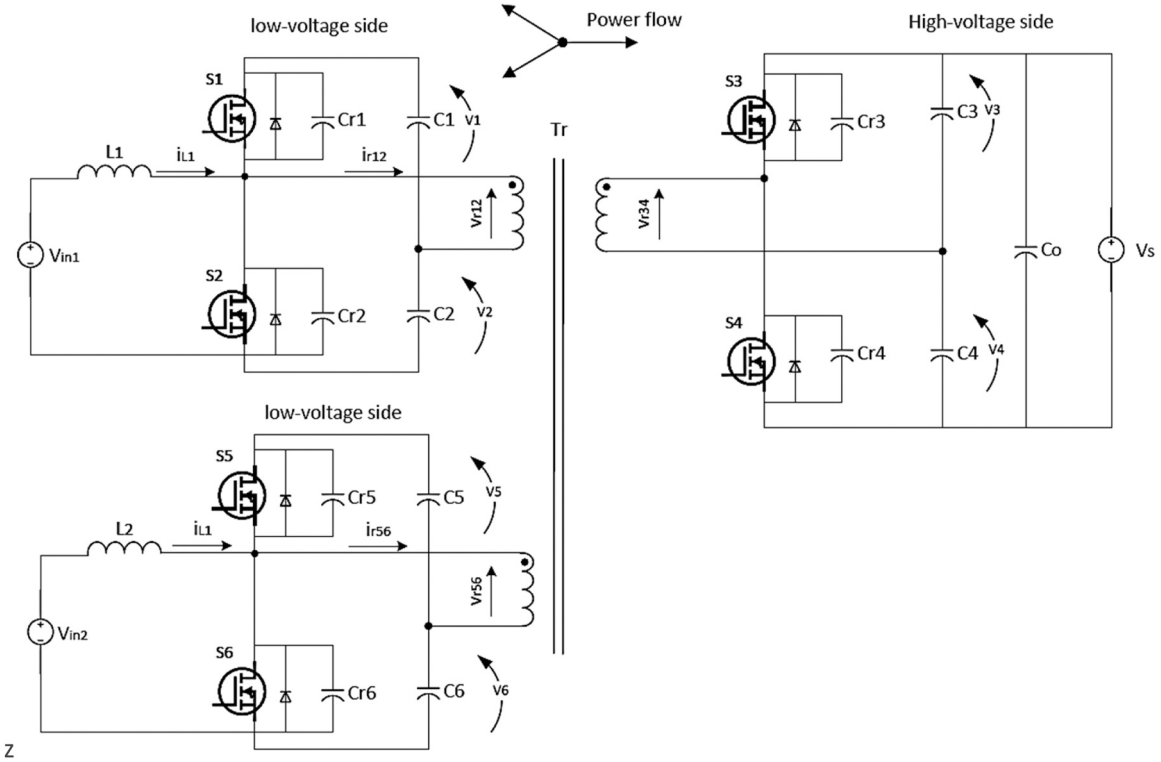

Fig. 35. HB-based three port-converter (Liu and Li, 2006).

In (Jun et al., 2010), a three-port bidirectional topology with two FB converters, and an HF circuit, has been studied. As is shown in Fig. 36, a two-input current-fed FB with output rectifier stage topology based on the flux deviation principle in the transformer has been suggested in (Chen et al., 2002; Chen et al., n.d.). The phase shift PWM control strategy is utilized to regulate the output voltage and control the power flow between each port. However, due to the rectifier stage, the power flow in this configuration is unidirectional from the input sources to the load, which makes the structure improper for grid-connected applications. The idea of a three-port bidirectional converter composed of three FB cells and a high-frequency transformer is investigated in (Zhao et al., 2008). An optimized DISO FB topology is discussed in (Li et al., 2011). The topology is depicted in Fig. 37. In this topology, power transfers from input to load either individually or simultaneously. A three-port bidirectional series resonant converter with PS control is investigated in (Krishnaswami and Mohan, 2009). In (Duarte et al., 2007; Michon et al., 2004), a three-port FB-based topology for hybrid FC/battery is proposed. Each FB converter operates at a fixed switching frequency and a fixed 50% duty cycle. However, the converter cannot handle wide voltage variations while maintaining soft switching. The decoupling control method for (Michon et al., 2004) is discussed in (Tao et al., 2005). A flatness-based control for a three-port bidirectional FB converter is discussed in (Phattanasak et al., 2011a, 2011b) to regulate the output voltage and power flow balancing between ports. Based on the topology and control method discussed in (Phattanasak et al., 2011a, 2011b), the authors of (Phattanasak et al., 2015) proposed a modular scheme for an FC and two storage devices.

From a combination of an FB LLC converter and a bidirectional LLC converter through a three-winding transformer, a SIDO converter for low voltage applications is presented in (Lin et al., 2022). A control system with two degrees of freedom, incorporating both PS and frequency variation, is employed for the converter, and the converter achieves ZVS of all switches ZCS of rectifying diodes through resonance. Nevertheless, the inclusion of two extra LCC and LC resonant tanks increases the component count and overall volume of the converter. Based on the DAB converter, a single-stage topology is proposed in (Lee and Jung, 2021), which is able to transfer bidirectional power between two bipolar DC buses, and without necessitating a supplementary voltage balancer, it can control the bipolar voltage levels under unbalanced load conditions. A DISO bidirectional current-fed series-resonant topology proper for ESS applications is discussed in (Wang et al., 2022). The structure is comprised of a three-winding transformer and three H-bridge converters. Each ESS input port is connected through two split inductors to the middle points of the H-bridge converter to form an interleaved parallel buck/boost converter. Two series resonance tanks are utilized to transfer energy from ESS to output, and a resonance tank on the output side is used to achieve power decoupling. Additionally, an optimization study comparing SPS-PWM and PWM with dual-phase-shift (DFS) modulation strategies is conducted to ensure that the converter operates with the minimum RMS value of the resonant current and achieves unity power factor. A DISO structure comprised of two active HBs in input, a three-leg FB in output, and two high-frequency transformers is discussed in (Kalpana, 2022). For PV-battery applications, a DISO structure is proposed in (Marei et al., 2022), where two HB converters and a rectifier are connected through a three-winding high-frequency transformer. In this configuration, the PV source is linked to an HB converter, with the addition of a diode to block circulating current from the battery port. Meanwhile, the battery is connected to another HB converter, with the addition of a bidirectional switch to prevent circulating current and manage the charging and discharging operations.

In (Messi Bene Eloundou et al., 2009), an expandable structure consisting of two FB converters connected to the primary side of a high-frequency three-winding transformer, and one FB rectifier comprised of diodes in series with transistors which are connected to the secondary side of the transformer is discussed. The topology is known as

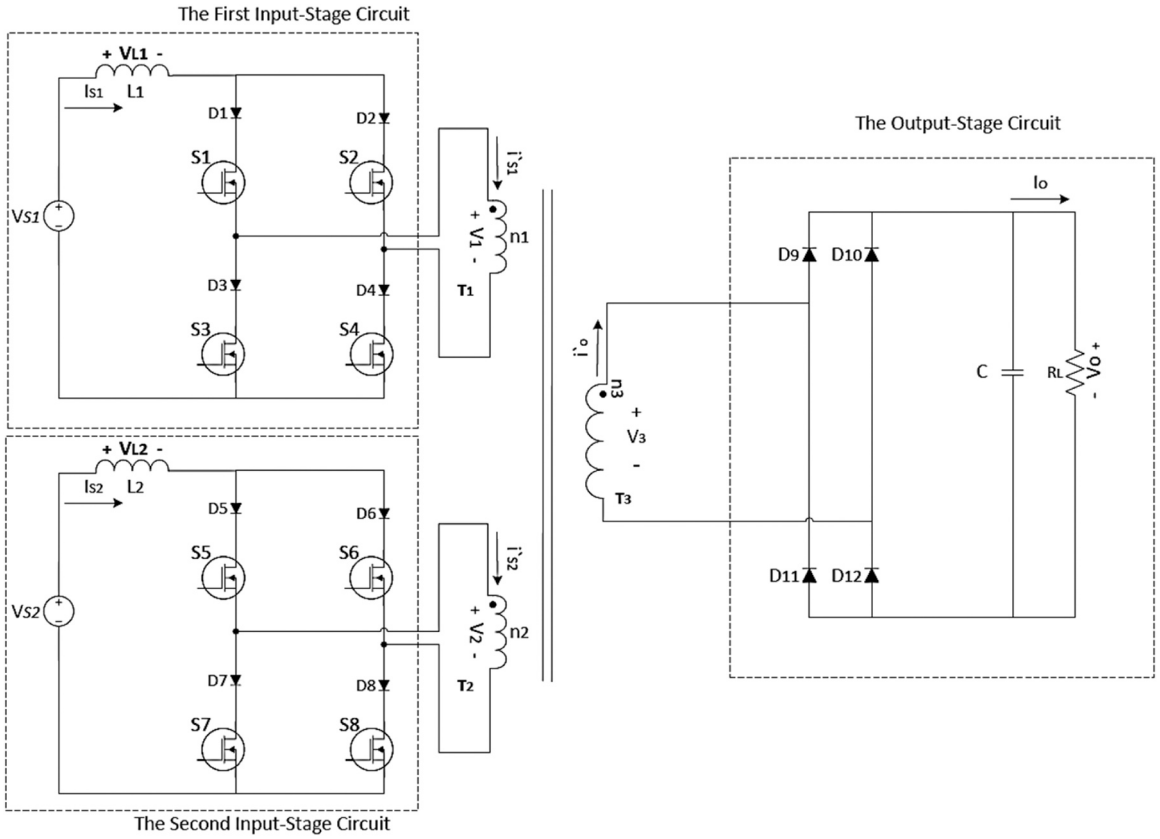

Fig. 36. The converter proposed in (Chen et al., 2002).

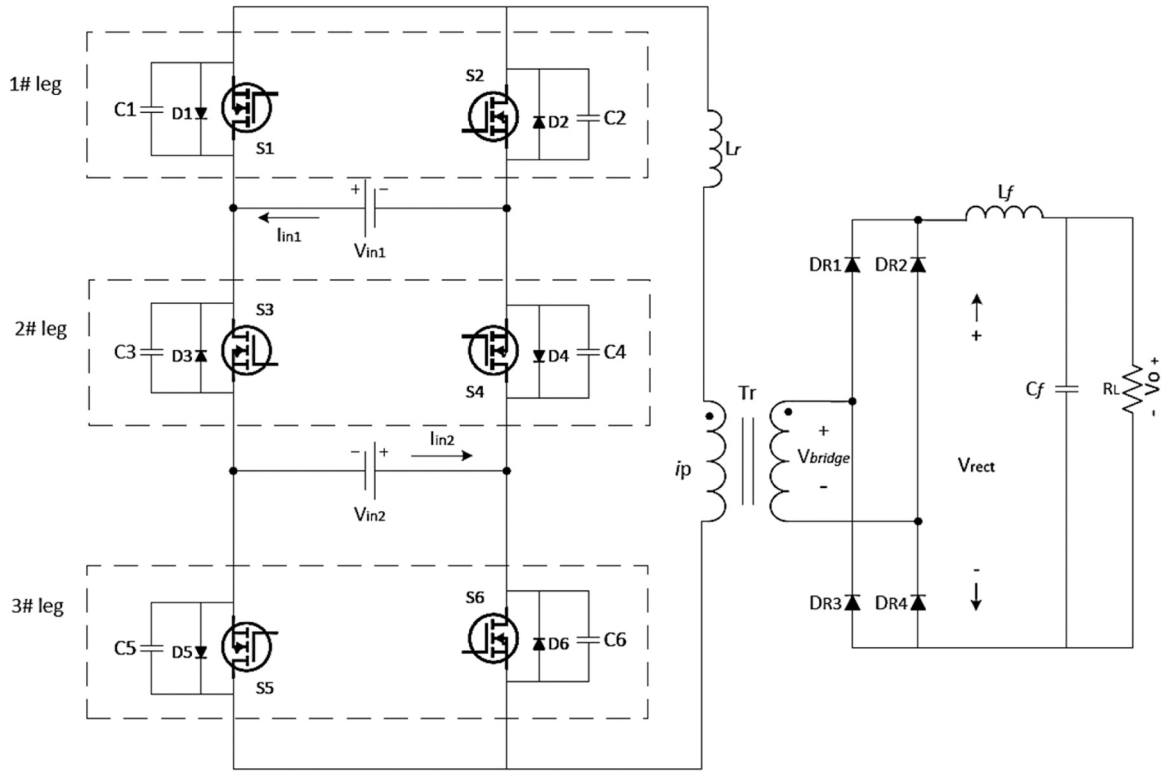

Fig. 37. Modified dual input FB converter (Li et al., 2011).

the triple active bridge (TAB) and is depicted in Fig. 38. In this converter, input switches operate under ZVS, and the output rectifier operates under ZCS. Moreover, the power of the input sources can be transferred simultaneously, individually, and bi-directionally. The shortcoming of this structure is the large number of switches and diodes and the lack of battery recharge control. To achieve full range ZVS, PSM is applied to voltage-fed TAB converter in (Jiang and Costinett, 2016), but input voltage variations are not taken into account. H∞ mixed sensitivity control for an FB three-port converter is studied in (You et al., 2019). A comparison study between variable duty ratio and variable frequency modulation for a TAB converter is presented in (Chattopadhyay et al., 2018). A detailed analysis of the current-fed TAB from modeling and control perspectives is presented in (Biswas et al., 2019, 2021). Authors of (Zou et al., 2020) introduced a generalized harmonic

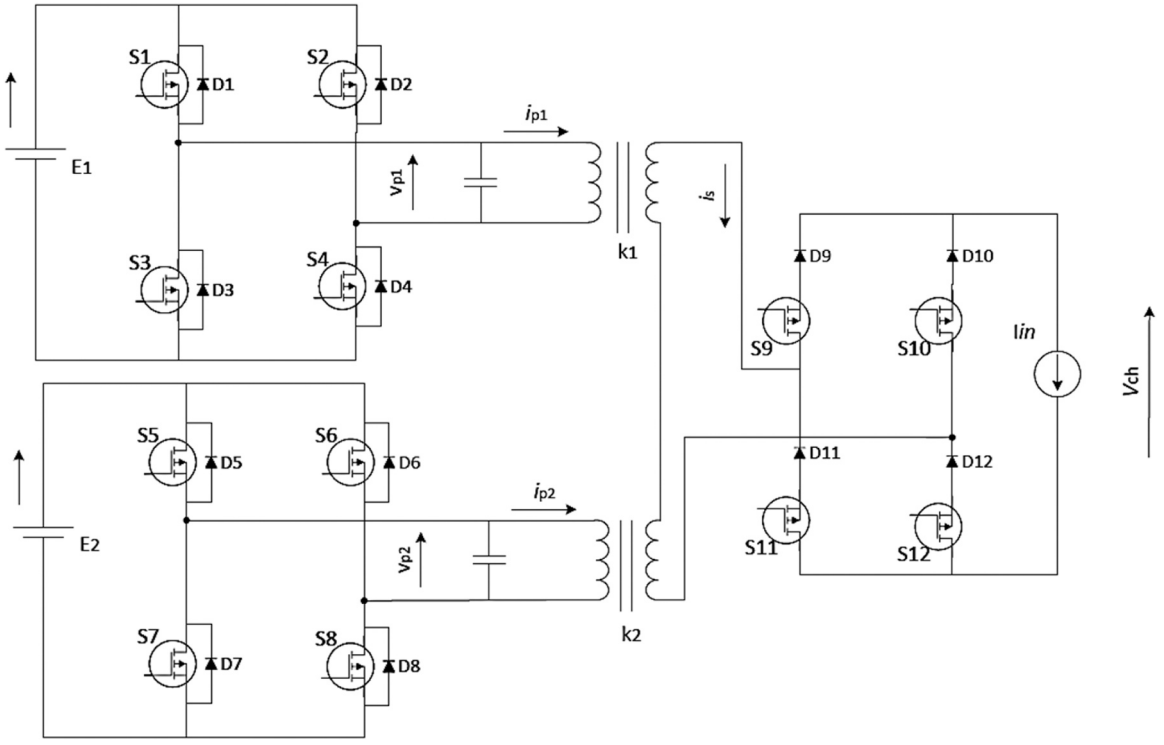

Fig. 38. The converter proposed in (Messi Bene Eloundou et al., 2009).

approximation model for the TAB converter. Subsequently, they developed an optimized control system to minimize the RMS current, ensure operation for switches, and address the effective management of power flows. Ref (Purgat et al., 2021). analyzed the ZVS regions of the TAB converter. The solution for the ZVS criteria incorporates various parameters, including the switches' parasitic capacitance, the transformer's leakage inductance, switching frequency, port voltage, and PS inside and between the FBs. Ref (Dey and Mallik, 2022)., investigated an optimized PWM scheme aimed at enhancing the efficiency of the TAB structure through the minimization of conduction losses. In (Ibrahim et al., 2021), an optimized penta PSM for the TAB converter is proposed for conduction loss reduction. This approach involves identifying favorable modulation patterns through numerical analysis to maximize efficiency. Subsequently, analytical optimization of the RMS current is performed. However, the implementation becomes intensive due to the large number of operation modes and the requirement for time-domain analysis. In (Ibrahim et al., 2024), the ANN approach was employed to estimate the optimal modulation parameters of the TAB. The objective is to achieve converter operation with the minimum total RMS currents. In (Kougioulis et al., 2022), a strategy for minimizing conduction losses has been devised through a detailed analysis of the TAB converter. This strategy aims to reduce the current stress on semiconductor devices and enhance overall efficiency. In (Liao et al., 2023), a feedforward neural network is developed for the MAB converter. AAN-based decoupling control is proposed in (Buticchi et al., 2022) for an MAB. The authors of (Qi et al., 2023; Zhao et al., 2022) investigated a decentralized adaptive control approach that dynamically adjusts each bridge's switching frequency and phase shift in a TAB converter to regulate power.

In (Jakka et al., 2017), as is shown in Fig. 39, a structure consisting of two FB converters, a three-leg converter, and two high-frequency transformers is discussed. This topology can achieve a wide range of outputs with fewer losses. However, the converter's size and cost have increased due to the large number of components. In (Pavlovic et al., 2013), based on the series resonant converter, a SIDO converter is proposed. Another multi-port resonant topology, based on a multi-winding medium frequency transformer, distributed resonant tank, and HB stages, has been suggested in (Tran et al., 2015). Ref (Tran and Dujic, 2016)., extended the work of (Tran et al., 2015) and suggested a structure composed of a three-winding medium frequency transformer, a multi-port LLC resonant circuit equipped with two additional buck/boost stages. The topology is shown in Fig. 40. A three-port bidirectional topology has been discussed in (Wang et al., 2018), which consists of three FB converters, a high-frequency three--winding transformer, and two resonant tanks made up of a series connection of an inductor and a capacitor, as well as a parallel connection of an inductor and a capacitor. The topology is shown in Fig. 41. The converter operates at a fixed switching frequency, and PSM is used for power flow balancing among ports. The idea of hardware decoupling against software decoupling for a series resonance three-port topology comprised of an HB converter, two FBs, and a three-winding high-frequency transformer is studied in (Wang et al., 2019). Time-sharing control is studied for an MAB in (Chen et al., 2019). In this control strategy, at any instance, only two ports are active, and other ports are deactivated as diode rectifiers. Accordingly, the MAB functions as SISO DAB. In addition, a hybrid time-sharing and PS control approach is developed in (Chen et al., 2019) to regulate voltage and power flow control. A three-port ZVS-PWM three-phase current-fed push-pull is studied in (Andersen and Barbi, 2013; Oliveira Albuquerque et al., 2019).

A current-fed three-port converter with FC/ESS inputs used in telecommunication applications is described in (Krishnaswami and Mohan, 2007). The topology is comprised of three FB converters and three separate transformers in which high-frequency capacitors are connected in parallel to the secondary side. The advantages of this topology are low current ripples due to input inductors, and bidirectional power flow capability. Based on the distributed transformer, in (Nielsen et al., 2012; Zhang et al., 2011), a DISO current-fed structure for the HRS has been discussed. As is shown in Fig. 42, there are four transformer windings with equal turn ratios. The converter is comprised of two boost inductors and two FB inverters on the primary side of the transformer, and two FB

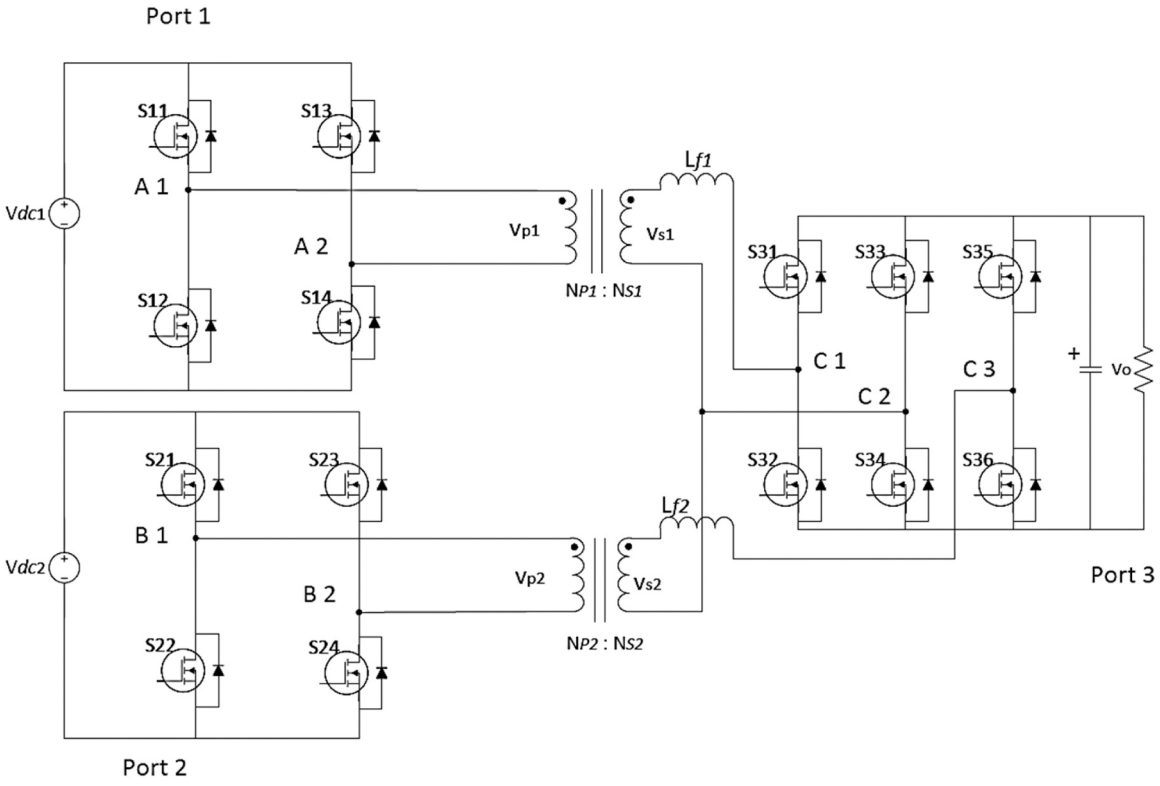

Fig. 39. Dual-transformer based asymmetrical TAB converter (Jakka et al., 2017).

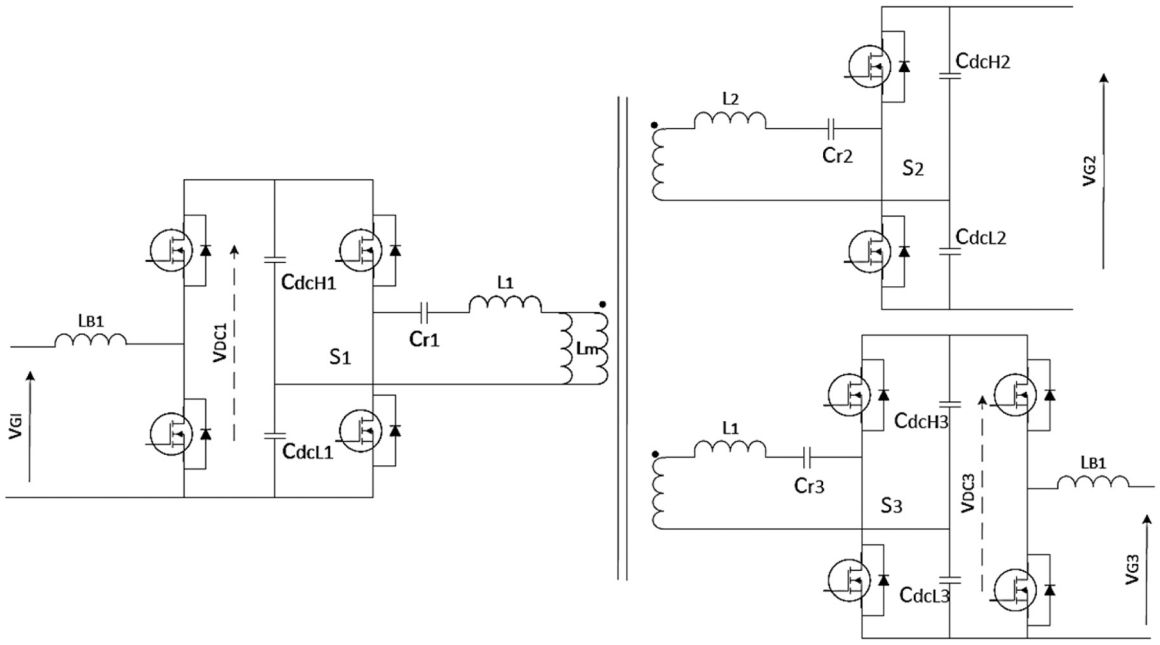

Fig. 40. Three port LLC resonant converter (Tran and Dujic, 2016).

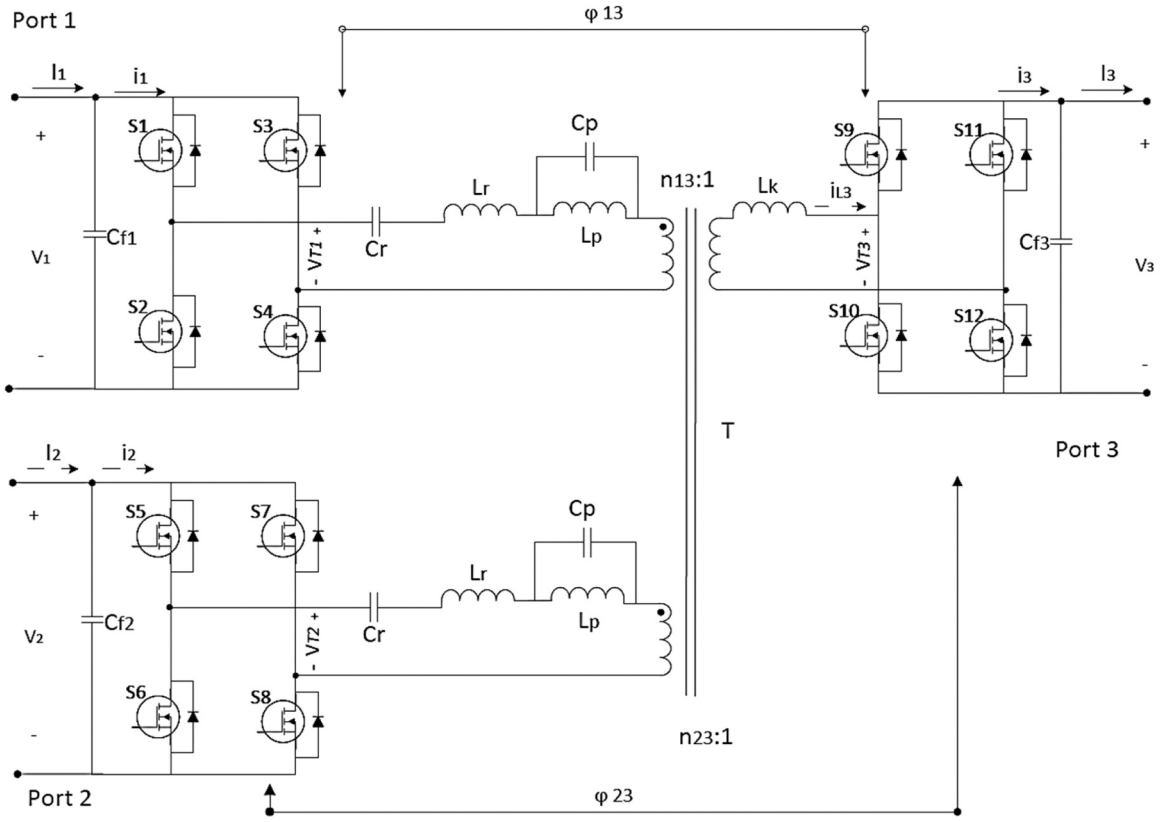

Fig. 41. Three-port resonant converter (Wang et al., 2018).

rectifiers on the secondary side. The converter's advantages include utilizing input energy simultaneously or individually, as well as low current ripples. The main disadvantage of this structure is the high number of components, resulting in low efficiency and production complexity. Moreover, All Inputs are not able to supply output power simultaneously. Ref (Bandyopadhyay et al., 2021). proposed a linear active disturbance rejection control approach to overcome coupling between the power flow of a quad-active bridge converter. Authors of (Gong et al., 2022) proposed a decoupling control approach based on sliding mode control for a quad-active bridge converter.

A comparison of various isolated MPDCs is illustrated in Table C.

5. Discussion and future research trends

This literature review analyzed and investigated the current state-of-the-art MPDCs from different standpoints and identified their

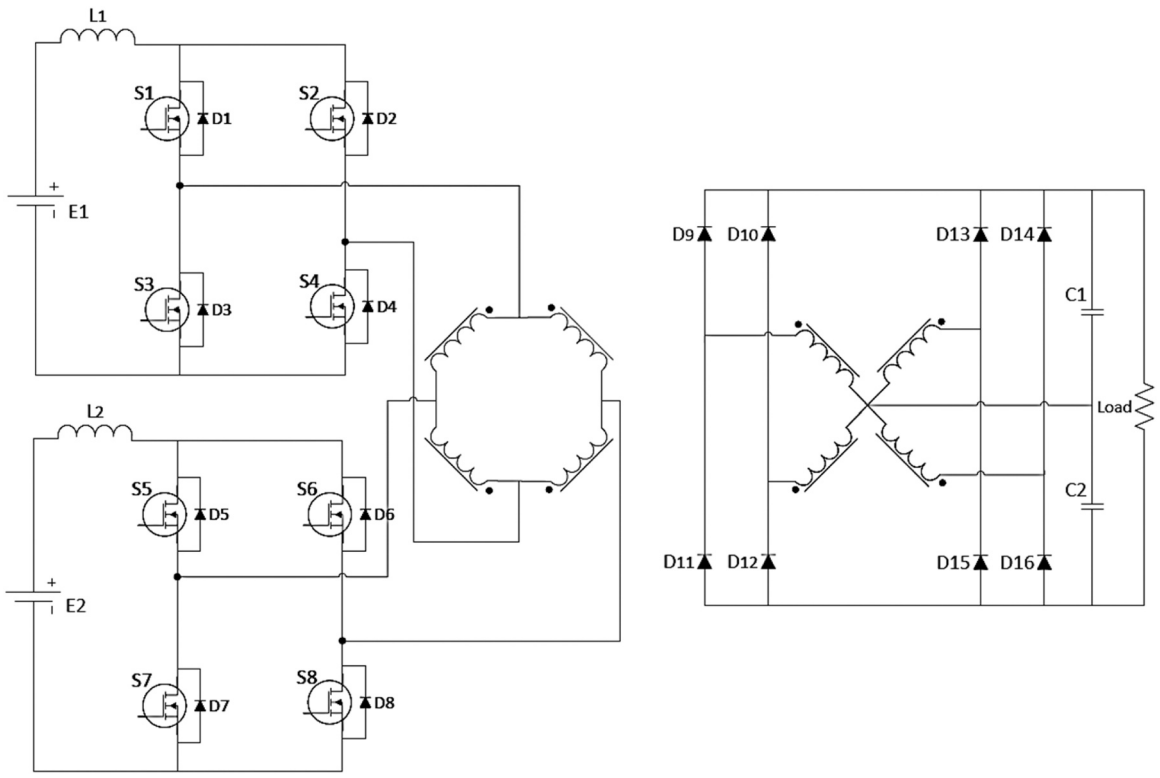

Fig. 42. The converter proposed in (Nielsen et al., 2012).

limitations. As a potential solution for future stable, reliable, and resilient smart grids and microgrids, the next-generation MPDC development has been moving towards higher efficiency, higher power density, and lower costs.

From the analysis of the MPDCs topology, isolated configurations are typically extensions of the SISO DAB structure and preferred in applications where high voltage gain and galvanic isolation between high and low voltages are required. Individual transformer windings for each port facilitate convenient voltage reduction or increase. However, designing a multi-winding high-frequency transformer introduces higher complexity compared to conventional two-winding transformers. Formulating a simple and accurate equivalent circuit model with measurable parameters also presents another challenge associated with multi-winding high-frequency transformers. The HB converters can be implemented on each side of a two-winding high-frequency transformer or multi-winding high-frequency transformer to reduce the overall number of switches and minimize associated switching losses. Table C provides a comparison of the isolated topologies. The partially isolated MPDCs with multiple input ports provide isolation between the input and output but lack isolation among all input ports. However, they exhibit compact sizes, have fewer power switches, and have the capability to achieve high power densities. Table B provides a comparison of the partially isolated topologies.

In contrast, non-isolated topologies are commonly derived from fundamental converters where switches and storage elements are shared within each switching cycle. These configurations are often favored for their cost-effectiveness and efficiency; however, they can not provide the galvanic isolation required in many RE applications, and voltage gain is relatively low. For non-isolated MPDCs, techniques such as switched capacitors, coupled inductors, and voltage multipliers are suggested to boost the voltage gain. While switched capacitor MPDCs generally show a fast dynamic response, they are prone to high-current transients that can affect both power density and efficiency. One common solution is the incorporation of inductors in the converter. In non-isolated MPDCs, the utilization of coupled inductors can efficiently increase the voltage. However, challenges such as reverse recovery problems, large voltage spikes, and increased bulkiness are associated with the use of coupled inductors. Voltage multiplier circuits (cells) are widely utilized for high-voltage applications due to their simplicity in implementation. Certain cells within this category are solely comprised of diodes and capacitors and, therefore, are referred to as switched/diode capacitor voltage multipliers. On the other hand, other voltage multipliers incorporate additional components, such as auxiliary switches, and some utilize inductors to enhance the voltage-boosting ratio. Voltage multipliers are straightforward to implement and can achieve high voltage levels. Nevertheless, they often result in high voltage stress on components, and multiple cells may be needed to reach the desired high voltage. In recent developments, non-isolated MPDCs with variable structures have been introduced. However, this advancement comes at the expense of an increased number of switches and higher costs. Table A provides a comparison of the non-isolated topologies.

The growing emphasis on energy efficiency and the development of RESs has led to increased research on MPDCs for a wide range of power conversion applications. Given that RESs typically generate low and variable output voltages, MPDCs are essential to meet the voltage requirements. RES and DGs play a crucial role in maintaining DC voltages within microgrids. Microgrids can operate in either grid-connected mode or islanding mode. In both modes of operation, reliability and fast dynamic response of MPDCs are vital. In terms of output voltage, DC microgrids can be classified into unipolar and bipolar ones. Bipolar configurations are able to improve the reliability and flexibility of DC microgrids. However, implementing such systems necessitates using advanced MPDCs and sophisticated control algorithms. In addition, MPDCs can form the backbone of MVDC and HVDC power grids and energy islands. Such a system will have many technical challenges requiring novel topologies and control algorithms. In this case, modular MPDC architecture with standard submodules can enhance the reliability and flexibility of the power conversion system and reduce cost. MPDCs also find applications in other fields, such as transportation

(automotive and railway technology), telecommunications, data centers, high/low-voltage technology, lighting, and aerospace applications. Table D provides an overview of the recommended applications of the aforementioned MPDCs.

MPDCs can be categorized into voltage-fed and current-fed converters based on their input. Current-fed MPDCs, in particular, are widely favored for low-voltage RE applications like PVs and FCs. The continuous input current provided by their input inductors results in low ripple, mitigating the adverse effects of high current ripple on low-voltage high-current sources.

Soft switching techniques are recommended to operate the converter at high frequencies with lower switching loss. Hard-switching MPDCs can face challenges such as high EMI due to high dv/dt and di/dt rates during switch transitions. As switching losses rise with increasing switching frequency, there is typically a constraint on the maximum achievable frequency. However, pursuing higher power density in MPDCs necessitates operating at higher frequencies and small component sizes. While most isolated configurations have soft-switching capability, many non-isolated topologies lack this feature.

In order for energy storage devices such as batteries, supercapacitors, and ultracapacitors to be integrated into MPDCs, the converter must feature at least one bidirectional port. As stated earlier, due to the intermittent nature of REs and the unpredictability of load demand, connecting an ESS to a bidirectional port is essential for optimizing the performance of the RES. In EVs and electric trains, reverse energy flow during deceleration and regenerative braking can be stored in the battery or ultracapacitor. Moreover, certain systems allow for energy transfer between EVs and the electric grid bidirectionally. While bidirectional energy transfer can be accomplished using unidirectional converters, one common approach for many configurations involves replacing unidirectional semiconductor components with bidirectional switches. Although the bidirectional port is essential for RESs and EVs, standalone RES or streetlighting applications do not require a bidirectional power flow capability between ESS and load ports. Hence, the design or selection of MPDCs should be based on the specific requirements of the applications. Simultaneous or independent transmission of energy from input sources and the continuity or discontinuity of input current are additional factors in the design or selection process of MPDCs.

The development of wide bandgap devices, especially SiC and GaN power switches, provides the opportunity for higher voltage gains with less count of switches. Compared to conventional switches, SiC devices offer fast switching speeds and low switching losses, enabling compact and efficient designs and higher power density.

MPDCs are highly non-linear MIMO systems with many control variables. The main challenge in modeling, designing, and controlling MPDCs is the inherent cross-coupling between control variables and power flows among the input-output ports. Accurate modeling of this intricate complexity is imperative for the formulation of effective controllers. Another key challenge in converter's design and control is uncertainties of the model parameters, such as component values and device characteristics, which can affect MPDC's dynamic and steady-state performance. Parasitic elements, such as parasitic capacitances and resistances, can further affect the performance of MPDCs. Including these elements in the model enhances accuracy but complicates the analysis and design of the controller. Parameter identification techniques help in obtaining reliable parameter values for the model. Utilizing robust control techniques such as H2/H∞ and LMI can ensure the robustness of the controller against structured and unstructured uncertainties. Furthermore, nonlinear control methodologies such as sliding mode, back-stepping, and singular perturbation provide a degree of robustness for the controller. MPDCs must operate reliably even in the presence of faults, making the design of control strategies for fault detection and mitigation an ongoing challenge. Despite such complexity, advanced control and switching techniques have not been comprehensively studied. Most of the works on MPDC control design have employed a decoupling control approach. However, the decoupling network design could become complicated as the number of inputs increases. To simplify decoupling control complexities, recent trends have favored hardware-level decoupling strategies. While these strategies facilitate control, these advancements come at the expense of more components.

Despite the significant advancements in intelligent control strategies and soft computing, enabling high-performance control of high-power converters, there has been limited research on applying these techniques to MPDCs. While SISO DC/DC converters have benefited from these developments, a notable gap exists in exploring intelligent control strategies and soft computing in MPDCs.

Although various control and modulation techniques have been developed for SISO power DC/DC converters in literature, PWM and PSM incorporated with PI controllers have been widely applied to MPDCs. PSM is a commonly used technique to control power flow in the isolated MAB configuration. By adjusting the magnitude and the sign of phase shifts, power flow magnitude and direction can be regulated. While PSM is simple and effective at moderate to high load conditions, it may face challenges at light-load conditions or with significant voltage mismatches among transformer terminals. This can lead to increased transformer RMS currents, posing a risk of losing ZVS and subsequently increasing switching and conduction losses. To address these challenges, utilizing not only the phase shifts but also the duty cycles has been suggested. However, the increased number of modulation variables significantly raises complexity. Controlling several modulation parameters results in hundreds of possible switching patterns. Examining each switching pattern separately to identify the optimal operation modes, especially concerning specific objectives, can be analytically complex and time-consuming. Generalized harmonic analysis or soft computing approaches can alleviate these complexities.

Based on the comparison of various MPDC characteristics outlined in Tables A, B, and C, future research in isolated topology design should focus on converters with reduced component counts. On the other hand, non-isolated converter design efforts should be directed toward topologies featuring higher voltage gain, bidirectional power flow, and soft-switching operation. Moreover, It is well known that controllers' effectiveness depends on specific operating points and precise converter parameters. Therefore, developing and implementing more sophisticated modulation and control techniques should be a significant research interest. It is important to emphasize that rejecting any converter or control techniques outright is not appropriate. The topologies and control algorithms, once perceived as complex and inefficient, have evolved into essential solutions for a wide range of applications.

CRediT authorship contribution statement

Soltani Mohsen: Supervision, Writing – review & editing. **Farajdadian Shahriar:** Writing – original draft, Writing – review & editing. **Hajizadeh Amin:** Supervision, Writing – review & editing.

Declaration of Competing Interest

The authors declare that they have no known competing financial interests or personal relationships that could have appeared to influence the work reported in this paper.

Data Availability

No data was used for the research described in the article.

Acknowledgements

Authors acknowledge the support of MARGIN project funded by Danida Fellowship Center and Ministry of Foreign Affairs of Denmark to research in growth and transition countries under the grant no. 21-M06-AAU.

Appendix A

Table A
Summary of non-isolated MPDCs.

MPDCs	Output voltage	S	D	L	C	SS	BPF
(Wai et al., 2011)	$Vo = \frac{1-d_1}{1+d_{cm1}-d_1}va$ $Va = \frac{v_1}{1-d_1}$	3	1	3	1	✓	×
(Haghighian et al., 2017)	$Vo = \frac{d_1 v_{in}}{1-d_1} + (d_1 + d_3)v_{ESS}$	3	3	2	2	×	✓
(Jalilzadeh et al., 2020a)	$v_{o1} = \frac{v_2}{1-d_1} + \frac{v_1}{1-d_3}$ $v_{o2} = \frac{v_1}{1-d_3}$	4	2	2	3	✓	✓
(Zhou et al., 2022)	-	4	3	2	3	×	✓
(Faraji et al., 2020)	$v_o = \frac{1+n}{1-d_2}[(1+d_1-d_2)v_1 + (d_2-d_1)v_2]$	4	4	2	2	✓	✓
(Chandrasekar et al., 2020)	-	4	4	3	2		✓
(Shoaei et al., 2023)	$v_o = \frac{m}{1-d_{n+1}} + \sum_{i=1}^{n} d_i v_i$	$n+1$	$n+2m-1$	1	$2m-1$	×	×
(Al-Soeidat et al., 2020)	-	3	1	1CI	3	×	✓
(Faraji et al., 2021c)	-	6	4	1		✓	✓
(Varesi et al., 2017)	$v_o = \frac{v_1}{(1-d_1)^2} + \sum_{i=2}^{n} \frac{v_i}{1-d_i}$	$n+1$	$n+1$	$n+1$	$n+1$	×	×
(Deihimi et al., 2017)	$v_o = \sum_{i=1}^{n} \frac{v_i}{1-d_i}$	n	$2n-1$	n	$2n$	×	×
(Zhou et al., 2012)	$v_o = \sum_{i=1}^{n} \frac{v_i}{1-d_i}$	n	n	n	n	×	×
(Banaei et al., 2014)	$v_o = \frac{1}{1-d_n}[d_n \left(\frac{d_1 v_1 + \ldots + d_{n-1}(1-d_1)(1-d_2)\ldots(1-d_{n-2})v_{n-1}}{(1-d_1)(1-d_2)\ldots(1-d_{n-1})}\right) + v_n]$	n	n	n	n	×	×
(Babaei and Abbasi, 2016)	$v_o = \frac{m}{1-d_{n+1}}[d_1 v_1 + \sum_{j=2}^{n}(d_j - d_{j-1})v_j]$	$n+1$	-	1	-	×	×
(Prabhala et al., 2016)	$v_o = \left(\frac{n+1}{2}\right)\left(\frac{v_1}{1-d_1}\right) + \left(\frac{n+1}{2}\right)\left(\frac{v_2}{1-d_2}\right)$ n is odd $v_o = \left(\frac{n+2}{2}\right)\left(\frac{v_1}{1-d_1}\right) + \left(\frac{n}{2}\right)\left(\frac{v_2}{1-d_2}\right)$ n is even	2	$n+1$	2	$n+1$	×	×
(Ahrabi et al., 2017)	$v_o = \frac{(V_{FC} + d_1 V_{batt} - r_2 i_{L2})}{(1-d_3)} + \frac{(V_{PV} + d_1 V_{batt} - r_1 i_{L1})}{(d_3 - d_2)}$	4	4	2	2	×	×
(Nahavandi et al., 2015)	-	4	2	1	2	×	×
(Behjati and Davoudi, 2011)	-	$n+m+1$	-	1	n	×	×
(Nami et al., 2010)	$v_n = \frac{R_n(1-\sum d_{n-1})V_{in}}{\sum R_n(1-\sum d_{n-1})^2}$	$n+1$	n	1	n	×	×
(Akar et al., 2016)	$v_o = V_1\frac{v_{s1}}{1-d_{To}} = V_2\frac{v_{s2}}{1-d_{To}}$	4	6	2	1	×	×
(Nejabatkhah et al., 2012)	-	4	4	2	1	×	✓
(Hintz et al., 2015)	-	6	6	2	1	×	✓
(Saafan et al., 2023)	$v_o = V_{FC}\frac{1}{1-d_4} + (V_{PV+}V_{bat})\frac{1-d_1-2d_4}{1-d_4}$	4	0	2	5	×	
(Chen et al., 2006)	$v_o = V_{HI}\frac{d_{HI}}{1-d_{Lo}} + V_{LO}\frac{d_{LO}}{1-d_{Lo}}$	2	2	1	1	×	×
(Yalamanchili et al., 2006)	$v_o = d_1 V_1 + d_2 V_2$	2	2	1	1	-	×
(Kumar and Jain, 2013a)	-	$n+2$	2	1	1	-	✓
(Akar, 2016)	-	5	5	2CI	2	✓	✓
(Athikkal et al., 2019)	-	4	2	1	1	×	
(Varesi et al., 2019)	$v_o = V_1\frac{2-d_1}{(1-d_1)^2} + V_2\frac{1}{(1-d_2)^2}$	$3n$	n	$2n$	$2n$	×	✓
(Varesi et al., 2018)	$v_o = V_1\frac{2-d_1}{(1-d_1)^2} + V_2\frac{1}{1-d_2}$	$n+3$	$n-1$	$n+1$	$n+1$	×	✓
(Kumaravel et al., 2019)	-	6	5	2	2	×	✓
(Saadatizadeh et al., 2021a)	-	6	-	2CI	5	×	×
(Shayeghi et al., 2021)	$Vo = \frac{2v_{in}}{1-d}$	3	-	2	3	×	✓
(Farakhor et al., 2019)	$v_o = V_{in}\frac{1}{(1-d)^2}$	3	4	2	2	-	✓
(Zahedi Saadabad et al., 2020)	$v_o = \frac{v_{in}(n+n')}{(n-1)(1-D)}$	2	2	3CI	1	✓	×
(Rostami et al., 2020)	$v_o = V_{in}\frac{1}{(1-d)^2}$	3	5	2	2	×	✓
(Rostami et al., 2021)	$Vo = \frac{(2-d)v_{in}}{1-2d}$	4	6	2	4		✓

(continued on next page)

Table A (*continued*)

MPDCs	Output voltage	S	D	L	C	SS	BPF
(Aravind et al., 2023)		4	4	2	2	×	
(Xu et al., 2021)	-	6	5	3	10	-	✓
(N. Jayaram et al., 2023)	$v_o = V_1\frac{d_1 - 2d_2 + d_1d_2}{(1-d_1)^2(d_1-d_2)} + V_2\frac{d_2(1-d_1)}{d_1(d_1-d_2)}$	5	1	4	4	×	✓
(Hou et al., 2016)	$Vo = \frac{3v_{in}}{1-d}$	2	4	2	5	×	×
(Kardan et al., 2017)	$Vo = \frac{v_1 + d_1\frac{v_2d_2 + v_bd_3}{1-d_2} + v_bd_3}{1-d_1}$	4	3	2	2	×	✓
(Colalongo et al., 2017)	$Vo = \frac{v_1}{1-d} + \frac{v_2}{d}$	4	4	4	4	×	×
(Dhananjaya et al., 2023)		5	5	2	2		
(ANON et al., 2020)		2	3	2	3	×	×
(Faraji et al., 2021b)	$v_o = \frac{V_1 - V_2d_2}{1-d_2-d_3}$	6	3	1CI	2	✓	✓
(Aghdam et al., 2022)		6	2	3	3	×	×
(Dezhbord et al., 2022)	$Vo = \frac{d(1+2n)v_{in}}{1-d}$	3	5	1CI	4	✓	✓
(Zhu et al., 2019)	$Vo = \frac{v_1}{1-d_1} + \frac{v_2}{1-d_2}$	2	10	2	7	×	×
(Sato et al., 2017)	-	4	1	2	4	-	✓

S: switch, D: diode, L: inductor, C: capacitor, CI: coupled inductor, SS: soft switching, BPF: bidirectional power flow

Appendix B

Table B
Summary of partially isolated MPDCs.

MPDCs	Control/Modulation strategy	S	D	L	Transformer	C	SS	BPF
(Sun et al., 2014)	PWM-PSM	6	-	2	1 * 2 winding	3	✓	✓
(Zhu et al., 2014)	PWM	3	3	2	1 * 4 winding	5	✓	✓
(Al-Atrash and Batarseh, 2007)	PWM-PSM	4	4	2	1	4	×	✓
(Rios et al., 2021; Qian et al., 2010a)	PWM	5	1	1	1 * 3 winding	3	✓	✓
(Wu et al., 2011a, 2011b	PWM	4	1	1	1 *3 winding	3	✓	✓
(Hu et al., 2014)	PWM-PSM	4	4	1	2 two winding	3	ZVS for switches	
(Bayat and Baghramian, 2020)	PWM	3	6	1	1 coupled inductor, two winding	4	✓	✓
(Zeng et al., 2013)		3	4	3	1 * 2 winding	5	ZVS and ZCS for the main switches	×
(Hu et al., 2015)	PWM-PSM	4	3	-	2 * 2 winding	3	-	-
(Uno et al., 2018)	PWM-PFM	2	4	0	1	4	-	✓
(Dobakhshari et al., 2020a, 2020b		3	3	2	2	8	✓	-
(Sun et al., 2015)	PWM-PFM	4	4	3	1 * 2 winding	4	✓	×
(Chen, 2014; Qin et al., 2014)	PWM-SSPSM	6	2	3	1 * 2 winding	3	✓	✓
(Lee and Jung, 2022)	PWM-PSM	8	0	3	1 * 2 winding	2	✓	
	PWM	4	0	2	1 * 2 winding	5	✓	✓
(Zeng et al., 2014)	-	3	7	4		5		

S: switch, D: diode, L: inductor, C: capacitor, SS: soft switching, BPF: bidirectional power flow

Appendix C

Table C
Summary of isolated MPDCs.

MPDCs	Output voltage	S	D	L	Transformer	C	SS	BPF
(Tao et al., 2006b, 2008	-	6	-	-	1 *3 winding	7	✓	✓
(Liu and Li, 2006)	-	6	-	2	1 * 3 winding	7	✓	✓
(Messi Bene Eloundou et al., 2009)	-	12	12	-	1 * 3 winding	2	✓	✓
(Tran et al., 2015)	-	6	6	3	1 * 3 winding	9	✓	✓
(Tran and Dujic, 2016)	-	12	12	2	1 * 3 winding	9	✓	✓
(Nielsen et al., 2012; Zhang et al., 2011)	$v_o = \frac{nv_1}{2(1-d_1)}$ $v_o = \frac{nv_2}{2(1-d_2)}$	8	8	2	4	2	×	×
(Wang et al., 2018)	-	12	0	4	1 * 3 winding	7	✓	✓
(Jakka et al., 2017)	$v_o = \frac{NR_l}{2f_s}[\frac{d_{13}(1-d_{13})v_1}{l_{f1}} + \frac{d_{23}(1-d_{23})v_2}{l_{f2}}]$	14	14	2	2 * 2 winding	1	✓	✓
(Chen et al. (2002); Chen et al., n.d.)	$v_o = \frac{N_3}{N_1}V_1 + \frac{N_2}{N_1}V_2$	8	12	2	1 * 3 winding	1	✓	
(Phattanasak et al., 2011a, 2011b	-	12	1	1	1 *3 winding	3	×	✓
(Krishnaswami and Mohan, 2009)	-	12	0	2	1 * 3 winding	5	✓	✓
(Li et al., 2011)	$v_o = \frac{D_1}{K}V_1 + \frac{D_2}{K}V_2$	8	10	2	1 * 2 winding	7	✓	
(Tao et al., 2006a)	$v_o = \frac{N_3}{N_1}V_1 + \frac{N_2}{N_1}V_2$	6	0	0	1 * 3 winding	7	✓	✓

S: switch, D: diode, L: inductor, C: capacitor, SS: soft switching, BPF: bidirectional power flow

Appendix D

Table D
Application of MPDCs.

MPDCs	Recommended Applications	MPDCs	Recommended Applications
(Chen et al., 2006)	PV-wind-water pump	(Tao et al., 2006a)	PV/FC/Battery
(Fan et al., 2010)	Thermoelectric-PV system in hybrid electric vehicles	(Phattanasak et al., 2015)	FC-supercapacitor
(Zahedi Saadabad et al., 2020)	PV-battery	(Tran et al., 2015)	HRS/DC microgrids
(Kardan et al., 2017)	PV/FC/Battery	(Wang et al., 2018)	Wind/PV/ESS
(Rostami et al., 2020)	PV-battery	(Nielsen et al., 2012)	Wind/PV/FC
(Chen et al., 2013)	Stand-alone PV-battery	(Wu et al., 2011b)	PV-battery
(Akar et al., 2016)	HEV	(Al-Atrash and Batarseh, 2007)	PV-battery-FC-Telecommunication
(Dobbs and Chapman, 2003)	FC-Ultracapacitor	(Wai et al., 2011)	FC/Battery-EV
(Khaligh et al., 2009)	Wind/PV/ESS	(Sun et al., 2015)	Stand-alone PV-battery
(Yuan-mao and Cheng, 2013)	Low-power DC application	(Zeng et al., 2013)	PV-battery
(Nejabatkhah et al., 2012)	PV/FC/Battery	(Jakka et al., 2017)	HRS/DC microgrids
(Shayeghi et al., 2021)	EV	(Zeng et al., 2014)	Wind/PV
(Xu et al., 2021)	PV-battery	(Zhu et al., 2014)	Stand-alone PV-battery
(Prabhala et al., 2016)	PV farms	(Athikkal et al., 2019)	Supercapacitor-Battery- EV
(Zhou et al., 2012)	Grid-connected PV systems	(Zhang et al., 2014)	HRS/DC microgrids
(Faraji et al., 2020)	PV-battery	(An and Lu, 2015)	PV-Battery-water pump
(Haghighian et al., 2017)	Wind/PV/ESS	(An et al., 2019)	Stand-alone PV-battery-DC motor
(Kumaravel et al., 2019)	PV/battery/ultra-capacitor -EV	(Sun et al., 2014)	PV-Battery
(Liu and Li, 2006)	RES-FC hybrid EV	(Hu et al., 2014)	Stand-alone PV-battery
(Hintz et al., 2015)	HEV/FCV	(Hu et al., 2015)	Stand-alone PV-battery
(Messi Bene Eloundou et al., 2009)	HEV/EV	(Babaei and Abbasi, 2016)	PV/FC
(Cheraghi et al., 2021)	PV-battery	(Mohseni et al., 2019)	PV/FC
(Hou et al., 2016)	PV-FC	(Vahid et al., 2021)	HRS-ESS
(Chen et al., 2002)	PV/Wind/FC	(Bayat and Baghramian, 2020)	PV-battery
(Khadem Haghighian and Hosseini, 2015)	Grid-connected hybrid PV/FC/battery	(Uno et al., 2018)	Stand-alone PV-battery
(Sun et al., 2014)	Stand-alone PV-battery	(Wang and Li, 2013)	PV-battery
(Chen, 2014)	PV-battery	(Qin et al., 2014)	PV-battery- Aerospace systems
(Krishnaswami and Mohan, 2007)	FC/ESS- Telecommunication	(Nahavandi et al., 2015)	PV/FC/Battery/ Supercapacitor
(Chandrasekar et al., 2020)	PV-battery	(Faraji et al., 2021c)	PV-battery
(Ravada et al., 2021)	HRS//battery/supercapacitor-DC microgrids applications	(Aravind et al., 2023)	PV-battery-EV
(Prabhakaran and Agarwal, 2020; Prajof and Agarwal, 2015)	PV/FC-bipolar DC microgrids	(Saafan et al., 2021, 2023	PV/FC/battery-DC microgrid
(Suresh et al., 2021)	EV	(Abbasi Soltani et al., 2021)	Street lighting
(Aghajani et al., 2023)	PV/FC-bipolar DC microgrids	(Khasim et al., 2023)	EV
(Marei et al., 2022)	PV-battery	(Saadatizadeh et al., 2024)	PV-battery
(Fares et al., 2022)	Aerial vehicles		

References

Abbasi Soltani, B., Sabahi, M., Babaei, E., Pouladi, J., 2021. Two-input boost converter for street-lighting applications. Comput. Electr. Eng. 92, 107126 https://doi.org/10.1016/j.compeleceng.2021.107126.

Abraham, C., Jose, B.R., Mathew, J., Evzelman, M., 2017. Modelling, simulation and experimental investigation of a new two input, series-parallel switched capacitor converter. IET Power Electron 10, 368–376. https://doi.org/10.1049/iet-pel.2015.1000.

Affam, A., Buswig, Y.M., Othman, A.-K.B.H., Julai, N.Bin, Qays, O., 2021. A review of multiple input DC-DC converter topologies linked with hybrid electric vehicles and renewable energy systems. Renew. Sustain. Energy Rev. 135, 110186 https://doi.org/10.1016/j.rser.2020.110186.

Aghajani, A.A., Eldoromi, M., Nakhaei, B., Birjandi, A.A.M., 2023. Multi-port dual-active-bridge DC-DC converter for Bi-polar DC microgrid application using buck-boost voltage balancer. In: 14th Power Electron. Drive Syst. Technol. Conf., 2023. IEEE, pp. 1–5. https://doi.org/10.1109/PEDSTC57673.2023.10087139

Aghdam, B.A., Nia, P.H., Nazarpour, D., 2022. A new multi-port DC/DC converter for PV/battery/DC gird energy systems. In: 9th Iran. Conf. Renew. Energy Distrib. Gener., 2022. IEEE, pp. 1–8. https://doi.org/10.1109/ICREDG54199.2022.9804540.

Agrawal, N., Kumar, L., Ghosh, S., 2016. Power management in double-input DC/DC converter. In: IEEE 1st Int. Conf. Power Electron. Intell. Control Energy Syst., 2016. IEEE, pp. 1–6. https://doi.org/10.1109/ICPEICES.2016.7853195.

Ahmadi, R., Ferdowsi, M., 2012. Double-input converters based on H-bridge cells: derivation, small-signal modeling, and power sharing analysis. IEEE Trans. Circuits Syst. I Regul. Pap. 59, 875–888. https://doi.org/10.1109/TCSI.2011.2169910.

Ahrabi, R.R., Ardi, H., Elmi, M., Ajami, A., 2017. A novel step-up multiinput DC–DC converter for hybrid electric vehicles application. IEEE Trans. Power Electron. 32, 3549–3561. https://doi.org/10.1109/TPEL.2016.2585044.

Akar, F., 2016. A high-efficiency bidirectional non-isolated multi-input converter. In: 19th Int. Symp. Electr. Appar. Technol., 2016. IEEE, pp. 1–4. https://doi.org/10.1109/SIELA.2016.7542969.

Akar, F., Tavlasoglu, Y., Ugur, E., Vural, B., Aksoy, I., 2016. A bidirectional nonisolated multi-input DC–DC converter for hybrid energy storage systems in electric vehicles. IEEE Trans. Veh. Technol. 65, 7944–7955. https://doi.org/10.1109/TVT.2015.2500683.

Akar, F., Tavlasoglu, Y., Vural, B., 2017. An energy management strategy for a concept battery/ultracapacitor electric vehicle with improved battery life. IEEE Trans. Transp. Electrif. 3, 191–200. https://doi.org/10.1109/TTE.2016.2638640.

Al-Atrash, H., Batarseh, I., 2007. Boost-Integrated Phase-Shift Full-Bridge Converter for Three-Port Interface. In: IEEE Power Electron. Spec. Conf., 2007. IEEE, pp. 2313–2321. https://doi.org/10.1109/PESC.2007.4342371.

Alhatlani, A., Batarseh, I., 2019. Review of partially isolated three-port converters for PV-battery systems that interface a PV, bidirectional battery, and load. In: IEEE Conf. Power Electron. Renew. Energy, 2019. IEEE, pp. 465–472. https://doi.org/10.1109/CPERE45374.2019.8980006.

Aljarajreh, H., Lu, D.D.-C., Siwakoti, Y.P., Aguilera, R.P., Tse, C.K., 2021. A method of seamless transitions between different operating modes for three-port DC-DC converters. IEEE Access 9, 59184–59195. https://doi.org/10.1109/ACCESS.2021.3073948.

Al-Soeidat, M.R., Aljarajreh, H., Khawaldeh, H.A., Lu, D.D.-C., Zhu, J., 2020. A reconfigurable three-port DC–DC converter for integrated PV-battery system. IEEE J. Emerg. Sel. Top. Power Electron. 8, 3423–3433. https://doi.org/10.1109/JESTPE.2019.2941595.

Amaleswari, R., Prabhakar, M., 2021. Non-isolated multi-input DC-DC converter with current sharing mechanism. Int. J. Electron. 108, 237–263. https://doi.org/10.1080/00207217.2020.1789760.

An, L., Lu, D.D.-C., 2015. Design of a single-switch DC/DC converter For a PV-battery-powered pump system with PFM+PWM control. IEEE Trans. Ind. Electron. 62, 910–921. https://doi.org/10.1109/TIE.2014.2359414.

An, L., Cheng, T., Lu, D.D.-C., 2019. Single-stage boost-integrated full-bridge converter with simultaneous MPPT, wide DC motor speed range, and current ripple reduction. IEEE Trans. Ind. Electron. 66, 6968–6978. https://doi.org/10.1109/TIE.2018.2878112.

Andersen, R.L., Barbi, I., 2013. A ZVS-PWM three-phase current-fed push–pull DC–DC converter. IEEE Trans. Ind. Electron. 60, 838–847. https://doi.org/10.1109/TIE.2012.2189539.

2020 ANON, 2020. Developing a super-lift luo-converter with integration of buck converters for electric vehicle applications. CSEE J. Power Energy Syst. https://doi.org/10.17775/CSEEJPES.2020.01880.

Aravind, R., Chokkalingam, B., Mihet-Popa, L., 2023. A transformerless non-isolated multi-port DC–DC converter for hybrid energy applications. IEEE Access 11, 52050–52065. https://doi.org/10.1109/ACCESS.2023.3280195.

Athikkal, S., Guru Kumar, G., Sundaramoorthy, K., Sankar, A., 2019. A non-isolated bridge-type DC–DC converter for hybrid energy source integration. IEEE Trans. Ind. Appl. 55, 4033–4043. https://doi.org/10.1109/TIA.2019.2914624.

Azizi, M., Mohamadian, M., Beiranvand, R., 2016. A new family of multi-input converters based on three switches leg. IEEE Trans. Ind. Electron. 63, 6812–6822. https://doi.org/10.1109/TIE.2016.2581765.

Babaei, E., Abbasi, O., 2016. Structure for multi-input multi-output dc–dc boost converter. IET Power Electron 9, 9–19. https://doi.org/10.1049/iet-pel.2014.0985.

Babaei, E., Abbasi, O., 2017. A new topology for bidirectional multi-input multi-output buck direct current-direct current converter. Int. Trans. Electr. Energy Syst. 27, e2254 https://doi.org/10.1002/etep.2254.

Bairabathina, S., Balamurugan, S., 2020. Review on non-isolated multi-input step-up converters for grid-independent hybrid electric vehicles. Int. J. Hydrog. Energy 45, 21687–21713. https://doi.org/10.1016/j.ijhydene.2020.05.277.

Banaei, M.R., Ardi, H., Alizadeh, R., Farakhor, A., 2014. Non-isolated multi-input–single-output DC/DC converter for photovoltaic power generation systems. IET Power Electron 7, 2806–2816. https://doi.org/10.1049/iet-pel.2013.0977.

Bandyopadhyay, S., Qin, Z., Bauer, P., 2021. Decoupling control of multiactive bridge converters using linear active disturbance rejection. IEEE Trans. Ind. Electron. 68, 10688–10698. https://doi.org/10.1109/TIE.2020.3031531.

Bayat, P., Baghramian, A., 2020. Partly isolated three-port DC–DC converter based on impedance network. IET Power Electron 13, 2175–2193. https://doi.org/10.1049/iet-pel.2019.1348.

Behjati, H., Davoudi, A., 2011. A multi-port dc-dc converter with independent outputs for vehicular applications. In: IEEE Veh. Power Propuls. Conf., 2011. IEEE, pp. 1–5. https://doi.org/10.1109/VPPC.2011.6042983.

Behjati, H., Davoudi, A., 2012. A MIMO topology with series outputs: an interface between diversified energy sources and diode-clamped multilevel inverter. In: Twenty-Seventh Annu. IEEE Appl. Power Electron. Conf. Expo., 2012. IEEE, pp. 1–6. https://doi.org/10.1109/APEC.2012.6165790.

Behjati, H., Davoudi, A., 2013a. Single-stage multi-port DC–DC converter topology. IET Power Electron 6, 392–403. https://doi.org/10.1049/iet-pel.2012.0339.

Behjati, H., Davoudi, A., 2013b. A multiple-input multiple-output DC–DC converter. IEEE Trans. Ind. Appl. 49, 1464–1479. https://doi.org/10.1109/TIA.2013.2253440.

Bhattacharjee, A.K., Kutkut, N., Batarseh, I., 2019. Review of multiport converters for solar and energy storage integration. IEEE Trans. Power Electron. 34, 1431–1445. https://doi.org/10.1109/TPEL.2018.2830788.

Biswas, I., Kastha, D., Bajpai, P., 2019. TAB based multiport converter with optimized transformer RMS current and improved ZVS range for DC microgrid applications. IECON 2019 - 45th Annu. Conf. IEEE Ind. Electron. Soc. IEEE, pp. 2050–2055. https://doi.org/10.1109/IECON.2019.8926843.

Biswas, I., Kastha, D., Bajpai, P., 2021. Small signal modeling and decoupled controller design for a triple active bridge multiport DC–DC converter. IEEE Trans. Power Electron. 36, 1856–1869. https://doi.org/10.1109/TPEL.2020.3006782.

Buticchi, G., Farjudian, A., Oh, J., Tarisciotti, L., 2022. An ANN-assisted control for the power decoupling of a multiple active bridge DC-DC converter. IECON 2022 – 48th Annu. Conf. IEEE Ind. Electron. Soc. IEEE, pp. 1–6. https://doi.org/10.1109/IECON49645.2022.9968534.

Chandrasekar, B., Nallaperumal, C., Padmanaban, S., Bhaskar, M.S., Holm-Nielsen, J.B., Leonowicz, Z., Masebinu, S.O., 2020. Non-isolated high-gain triple port DC–DC buck-boost converter with positive output voltage for photovoltaic applications. IEEE Access 8, 113649–113666. https://doi.org/10.1109/ACCESS.2020.3003192.

Chattopadhyay, R., Gohil, G., Acharya, S., Nair, V., Bhattacharya, S., 2018. Efficiency improvement of three port high frequency transformer isolated triple active bridge converter. In: IEEE Appl. Power Electron. Conf. Expo., 2018. IEEE, pp. 1807–1814. https://doi.org/10.1109/APEC.2018.8341262.

Chen, Y., Wang, P., Li, H., Chen, M., 2019. Power flow control in multi-active-bridge converters: theories and applications. In: IEEE Appl. Power Electron. Conf. Expo., 2019. IEEE, pp. 1500–1507. https://doi.org/10.1109/APEC.2019.8722122.

Y.-M. Chen, Y.-C. Liu, F.-Y. Wu, T.-F. Wu, Multi-input DC/DC converter based on the flux additivity, in: Conf. Rec. 2001 IEEE Ind. Appl. Conf. 36th IAS Annu. Meet. (Cat. No.01CH37248), IEEE, n.d.: pp. 1866–1873. https://doi.org/10.1109/IAS.2001.955785.

Chen, Y.-M., Liu, Y.-C., Lin, S.-H., 2006. Double-Input PWM DC/DC converter for high-/low-voltage sources. IEEE Trans. Ind. Electron. 53, 1538–1545. https://doi.org/10.1109/TIE.2006.882001.

Chen, Y.-M., Huang, A.Q., Yu, X., 2013. A high step-up three-port DC–DC converter for stand-alone PV/battery power systems. IEEE Trans. Power Electron 28, 5049–5062. https://doi.org/10.1109/TPEL.2013.2242491.

Chen, Yaow-Ming, Liu, Yuan-Chuan, Wu, Feng-Yu, 2002. Multi-input DC/DC converter based on the multiwinding transformer for renewable energy applications. IEEE Trans. Ind. Appl. 38, 1096–1104. https://doi.org/10.1109/TIA.2002.800776.

Chen, Z., 2014. Three-port ZVS converter with PWM plus secondary-side phase-shifted for photovoltaic-storage hybrid systems. In: IEEE Appl. Power Electron. Conf. Expo. - APEC 2014, 2014. IEEE, pp. 3066–3071. https://doi.org/10.1109/APEC.2014.6803742.

Chen, Z., Wu, Q., Li, M., Xu, Y., Wang, Q., 2015. A three-port DC-DC converter with low frequency current ripple reduction technique. In: IEEE Appl. Power Electron. Conf. Expo., 2015. IEEE, pp. 2069–2074. https://doi.org/10.1109/APEC.2015.7104634.

Cheraghi, R., Adib, E., Golsorkhi, M.S., 2021. A nonisolated high step-up three-port soft-switched converter with minimum switches. IEEE Trans. Ind. Electron. 68, 9358–9365. https://doi.org/10.1109/TIE.2020.3026306.

Colalongo, L., Dotti, D., Richelli, A., Kovács-Vajna, Z.M., 2017. Non-isolated multiple-input boost converter for energy harvesting. Electron. Lett. 53, 1132–1134. https://doi.org/10.1049/el.2017.1590.

Damasceno, D.P., Rios, C.S. do N., Gadelha Barbosa, S., Barreto, L.H.S.C., Bezerra Correia, W., Gonzalez Nogueira, F., Oliveira, D. de S., 2021. Three-port isolated DC-DC converter with LQG/LTRI robust control applied to photovoltaic systems with energy storage. In: Brazilian Power Electron. Conf., 2021. IEEE, pp. 1–6. https://doi.org/10.1109/COBEP53665.2021.9684068.

Dao, N.D., Lee, D.-C., Phan, Q.D., 2020. High-efficiency SiC-based isolated three-port DC/DC converters for hybrid charging stations. IEEE Trans. Power Electron. 35, 10455–10465. https://doi.org/10.1109/TPEL.2020.2975124.

Deihimi, A., Seyed Mahmoodieh, M.E., Iravani, R., 2017. A new multi-input step-up DC–DC converter for hybrid energy systems. Electr. Power Syst. Res. 149, 111–124. https://doi.org/10.1016/j.epsr.2017.04.017.

Dey, S., Mallik, A., 2022. Multivariable-modulation-based conduction loss minimization in a triple-active-bridge converter. IEEE Trans. Power Electron. 37, 6599–6612. https://doi.org/10.1109/TPEL.2022.3141334.

Dezhbord, M., Mohseni, P., Hosseini, S.H., Mirabbasi, D., Islam, M.R., 2022. A high step-up three-port DC–DC converter with reduced voltage stress for hybrid energy systems. IEEE J. Emerg. Sel. Top. Ind. Electron. 3, 998–1009. https://doi.org/10.1109/JESTIE.2022.3146056.

Dhananjaya, M., Chaitanya, B.K., Babu, T.S., Potnuru, D., Aljafari, B., Kannan, R., Lohani, T.K., 2023. Design of multi-input single output DC–DC converter with preserved output voltage under source-fault. IET Power Electron 16, 1732–1742. https://doi.org/10.1049/pel2.12488.

A. Di Napoli, F. Crescimbini, L. Solero, F. Caricchi, F.G. Capponi, Multiple-input DC-DC power converter for power-flow management in hybrid vehicles, in: Conf. Rec. 2002 IEEE Ind. Appl. Conf. 37th IAS Annu. Meet. (Cat. No.02CH37344), IEEE, n.d.: pp. 1578–1585. https://doi.org/10.1109/IAS.2002.1043745.

Dobakhshari, S.S., Fathi, S.H., Milimonfared, J., 2020a. A new soft-switched three-port DC/DC converter with high voltage gain and reduced number of semiconductors for hybrid energy applications. IEEE Trans. Power Electron. 35, 3590–3600. https://doi.org/10.1109/TPEL.2019.2933182.

Dobakhshari, S.S., Fathi, S.H., Milimonfared, J., 2020b. High step-up double input converter with soft switching and reduced number of semiconductors. IET Power Electron 13, 1995–2007. https://doi.org/10.1049/iet-pel.2019.1394.

Dobbs, B.G., Chapman, P.L., 2003. A multiple-input DC-DC converter topology. IEEE Power Electron. Lett. 1, 6–9. https://doi.org/10.1109/LPEL.2003.813481.

Duarte, J.L., Hendrix, M., Simoes, M.G., 2007. Three-port bidirectional converter for hybrid fuel cell systems. IEEE Trans. Power Electron 22, 480–487. https://doi.org/10.1109/TPEL.2006.889928.

Fan, Ying, Ge, Luming, Hua, Wei, 2010. Multiple-input DC-DC converter for the thermoelectric-photovoltaic energy system in Hybrid Electric Vehicles. In: IEEE Veh. Power Propuls. Conf., 2010. IEEE, pp. 1–5. https://doi.org/10.1109/VPPC.2010.5729192.

Faraji, R., Farzanehfard, H., 2021. Fully soft-switched multiport DC–DC converter with high integration. IEEE Trans. Power Electron. 36, 1901–1908. https://doi.org/10.1109/TPEL.2020.3010412.

Faraji, R., Adib, E., Farzanehfard, H., 2019. Soft-switched non-isolated high step-up multi-port DC-DC converter for hybrid energy system with minimum number of switches. Int. J. Electr. Power Energy Syst. 106, 511–519. https://doi.org/10.1016/j.ijepes.2018.10.038.

Faraji, R., Farzanehfard, H., Kampitsis, G., Mattavelli, M., Matioli, E., Esteki, M., 2020. Fully soft-switched high step-up nonisolated three-port DC–DC converter using GaN HEMTs. IEEE Trans. Ind. Electron. 67, 8371–8380. https://doi.org/10.1109/TIE.2019.2944068.

Faraji, R., Ding, L., Rahimi, T., Kheshti, M., Islam, M.R., 2021a. Soft-switched three-port DC-DC converter with simple auxiliary circuit. IEEE Access 9, 66738–66750. https://doi.org/10.1109/ACCESS.2021.3076183.

Faraji, R., Ding, L., Rahimi, T., Farzanehfard, H., Hafezi, H., Maghsoudi, M., 2021b. Efficient multi-port bidirectional converter with soft-switching capability for electric vehicle applications. IEEE Access 9, 107079–107094. https://doi.org/10.1109/ACCESS.2021.3097750.

Faraji, R., Ding, L., Esteki, M., Mazloum, N., Khajehoddin, S.A., 2021c. Soft-switched single inductor single stage multiport bidirectional power converter for hybrid energy systems. IEEE Trans. Power Electron. 36, 11298–11315. https://doi.org/10.1109/TPEL.2021.3074378.

Farakhor, A., Abapour, M., Sabahi, M., 2019. Design, analysis, and implementation of a multiport DC–DC converter for renewable energy applications. IET Power Electron 12, 465–475. https://doi.org/10.1049/iet-pel.2018.5633.

Fares, A.M., Klumpner, C., Sumner, M., 2022. A novel multiport DC-DC converter for enhancing the design and performance of battery–supercapacitor hybrid energy storage systems for unmanned aerial vehicles. Appl. Sci. 12, 2767. https://doi.org/10.3390/app12062767.

Ferreira, A. de O., Brito, A.U., Galhardo, M.A.B., Ferreira, L., Macêdo, W.N., 2020. Modeling, control and simulation of a small photovoltaic-wind water pumping

system without battery bank. Comput. Electr. Eng. 84, 106619 https://doi.org/10.1016/j.compeleceng.2020.106619.
Ganjavi, A., Ghoreishy, H., Ahmad, A.A., 2018. A novel single-input dual-output three-level DC–DC converter. IEEE Trans. Ind. Electron. 65, 8101–8111. https://doi.org/10.1109/TIE.2018.2807384.
Gavris, M., Cornea, O., Muntean, N., 2011a. Multiple input DC-DC topologies in renewable energy systems - a general review. In: IEEE 3rd Int. Symp. Exploit. Renew. Energy Sources, 2011. IEEE, pp. 123–128. https://doi.org/10.1109/EXPRES.2011.5741805.
Gavris, M., Muntean, N., Cornea, O., 2011b. A new dual-input hybrid buck DC-DC converter. Int. Aegean Conf. Electr. Mach. Power Electron. Electromotion, Jt. Conf. IEEE, pp. 109–114. https://doi.org/10.1109/ACEMP.2011.6490578.
Gavris, M., Cornea, O., Muntean, N., 2012. Dual input hybrid buck LC converter. Int. Symp. Power Electron. Power Electron. Electr. Drives, Autom. Motion. IEEE,, pp. 309–314. https://doi.org/10.1109/SPEEDAM.2012.6264572.
Gong, S., Li, X., Han, J., Sun, Y., Xu, G., Jiang, Y., Huang, S., 2022. Sliding mode control-based decoupling scheme for quad-active bridge DC–DC converter. IEEE J. Emerg. Sel. Top. Power Electron. 10, 1153–1164. https://doi.org/10.1109/JESTPE.2021.3096228.
Haghighian, S.K., Tohidi, S., Feyzi, M.R., Sabahi, M., 2017. Design and analysis of a novel SEPIC-based multi-input DC/DC converter. IET Power Electron 10, 1393–1402. https://doi.org/10.1049/iet-pel.2016.0654.
Hema Rani, P., Navasree, S., George, S., Ashok, S., 2019. Fuzzy logic supervisory controller for multi-input non-isolated DC to DC converter connected to DC grid. Int. J. Electr. Power Energy Syst. 112, 49–60. https://doi.org/10.1016/j.ijepes.2019.04.018.
Hintz, A., Prasanna, U.R., Rajashekara, K., 2015. Novel modular multiple-input bidirectional DC–DC power converter (MIPC) for HEV/FCV application. IEEE Trans. Ind. Electron. 62, 3163–3172. https://doi.org/10.1109/TIE.2014.2371778.
Hou, S., Chen, J., Sun, T., Bi, X., 2016. Multi-input step-up converters based on the switched-diode-capacitor voltage accumulator. IEEE Trans. Power Electron. 31, 381–393. https://doi.org/10.1109/TPEL.2015.2399853.
Hu, W., Wu, H., Xing, Y., Sun, K., 2014. A full-bridge three-port converter for renewable energy application. In: IEEE Appl. Power Electron. Conf. Expo. - APEC 2014, 2014. IEEE, pp. 57–62. https://doi.org/10.1109/APEC.2014.6803289.
Hu, Y., Xiao, W., Cao, W., Ji, B., Morrow, D.J., 2015. Three-Port DC–DC converter for stand-alone photovoltaic systems. IEEE Trans. Power Electron 30, 3068–3076. https://doi.org/10.1109/TPEL.2014.2331343.
Ibrahim, A.A., Caldognetto, T., Mattavelli, P., 2021. Conduction loss reduction of isolated bidirectional DC-DC triple active bridge. In: IEEE Fourth Int. Conf. DC Microgrids, 2021. IEEE, pp. 1–8. https://doi.org/10.1109/ICDCM50975.2021.9504652.
Ibrahim, A.A., Zilio, A., Younis, T., Biadene, D., Caldognetto, T., Mattavelli, P., 2024. Optimal modulation of triple active bridge converters by an artificial-neural-network approach. IEEE Trans. Ind. Electron. 71, 2590–2600. https://doi.org/10.1109/TIE.2023.3270529.
Jakka, V.N.S.R., Shukla, A., Demetriades, G.D., 2017. Dual-transformer-based asymmetrical triple-port active bridge (DT-ATAB) isolated DC–DC converter. IEEE Trans. Ind. Electron. 64, 4549–4560. https://doi.org/10.1109/TIE.2017.2674586.
Jalilzadeh, T., Rostami, N., Babaei, E., Hosseini, S.H., 2020a. Bidirectional multi-port DC–DC converter with low voltage stress on switches and diodes. IET Power Electron 13, 1593–1604. https://doi.org/10.1049/iet-pel.2019.0525.
Jalilzadeh, T., Rostami, N., Babaei, E., Hosseini, S.H., 2020b. Multiport DC–DC converter with step-up capability and reduced voltage stress on switches/diodes. IEEE Trans. Power Electron. 35, 11902–11915. https://doi.org/10.1109/TPEL.2020.2982454.
Jiang, L., Costinett, D., 2016. A triple active bridge DC-DC converter capable of achieving full-range ZVS. In: IEEE Appl. Power Electron. Conf. Expo., 2016. IEEE, pp. 872–879. https://doi.org/10.1109/APEC.2016.7467974.
Jiang, L., Mi, C.C., Li, S., Zhang, M., Zhang, X., Yin, C., 2013. A novel soft-switching bidirectional DC–DC converter with coupled inductors. IEEE Trans. Ind. Appl. 49, 2730–2740. https://doi.org/10.1109/TIA.2013.2265874.
Jiya, I.N., Van Khang, H., Kishor, N., Ciric, R., 2022. Novel high gain multiport isolated DC-DC converter with bipolar symmetric outputs. IECON 2022 – 48th Annu. Conf. IEEE Ind. Electron. Soc. IEEE, pp. 1–6. https://doi.org/10.1109/IECON49645.2022.9968834.
Jiya, I.N., Van Khang, H., Gunawardena, P., Kishor, N., Li, Y.R., 2023. Novel isolated multiport DC converter with natural bipolar symmetry for renewable energy source integration to DC grids. IEEE Access 11, 117729–117740. https://doi.org/10.1109/ACCESS.2023.3326752.
Jun, X., Xing, Z., Chong-wei, Z., Sheng-yong, L., 2010. A novel three-port bi-directional DC-DC converter. 2nd Int. Symp. Power Electron. Distrib. Gener. Syst. IEEE,, pp. 717–720. https://doi.org/10.1109/PEDG.2010.5545784.
Kalpana, K.R., R., 2022. An isolated dual-input half-bridge DC–DC boost converter with reduced circulating power between input ports. IEEE Can. J. Electr. Comput. Eng. 45, 68–76. https://doi.org/10.1109/ICJECE.2021.3130723.
Kardan, F., Alizadeh, R., Banaei, M.R., 2017. A new three input DC/DC converter for hybrid PV/FC/battery applications. IEEE J. Emerg. Sel. Top. Power Electron. 5, 1771–1778. https://doi.org/10.1109/JESTPE.2017.2731816.
Khadem Haghighian, S., Hosseini, S.H., 2015. A novel multi-input DC/DC converter with a general power management strategy for grid connected hybrid PV/FC/battery system. 6th Power Electron. Drive Syst. Technol. Conf. IEEE, pp. 1–6. https://doi.org/10.1109/PEDSTC.2015.7093240.
Khaligh, A., 2008. A multiple-input DC-DC positive buck-boost converter topology. In: Twenty-Third Annu. IEEE Appl. Power Electron. Conf. Expo., 2008. IEEE, pp. 1522–1526. https://doi.org/10.1109/APEC.2008.4522926.
Khaligh, A., Cao, Jian, Lee, Young-Joo, 2009. A multiple-input DC–DC converter topology. IEEE Trans. Power Electron 24, 862–868. https://doi.org/10.1109/TPEL.2008.2009308.
Khasim, S.R., Dhanamjayulu, C., Muyeen, S.M., 2023. A single inductor multi-port power converter for electric vehicle applications. IEEE Access 11, 3367–3385. https://doi.org/10.1109/ACCESS.2023.3234105.
Khosrogorji, S., Ahmadian, M., Torkaman, H., Soori, S., 2016. Multi-input DC/DC converters in connection with distributed generation units – a review. Renew. Sustain. Energy Rev. 66, 360–379. https://doi.org/10.1016/j.rser.2016.07.023.
Kolahian, P., Tarzamni, H., Nikafrooz, A., Hamzeh, M., 2019. Multi-port DC–DC converter for bipolar medium voltage DC micro-grid applications. IET Power Electron 12, 1841–1849. https://doi.org/10.1049/iet-pel.2018.6031.
Kougioulis, I., Wheeler, P., Ahmed, M.R., 2022. An integrated on-board charger and auxiliary power module for electric vehicles. In: IEEE Appl. Power Electron. Conf. Expo., 2022. IEEE, pp. 1162–1169. https://doi.org/10.1109/APEC43599.2022.9773777.
Krishnaswami, H., Mohan, N., 2007. A current-fed three-port bi-directional DC-DC converter. INTELEC 07 - 29th Int. Telecommun. Energy Conf. IEEE,, pp. 523–526. https://doi.org/10.1109/INTLEC.2007.4448833.
Krishnaswami, H., Mohan, N., 2009. Three-port series-resonant DC–DC converter to interface renewable energy sources with bidirectional load and energy storage ports. IEEE Trans. Power Electron 24, 2289–2297. https://doi.org/10.1109/TPEL.2009.2022756.
Kumar, L., Jain, S., 2013a. Multiple-input DC/DC converter topology for hybrid energy system. IET Power Electron 6, 1483–1501. https://doi.org/10.1049/iet-pel.2012.0309.
Kumar, L., Jain, S., 2013b. A multiple source DC/DC converter topology. Int. J. Electr. Power Energy Syst. 51, 278–291. https://doi.org/10.1016/j.ijepes.2013.02.020.
Kumaravel, S., Achathuparambil Narayanankutty, R., Rao, V.S., Sankar, A., 2019. Dual input–dual output DC–DC converter for solar PV/battery/ultra-capacitor powered electric vehicle application. IET Power Electron 12, 3351–3358. https://doi.org/10.1049/iet-pel.2019.0123.
Lavanya, A., Jegatheesan, R., Vijayakumar, K., 2021. Design of novel dual input DC–DC converter for energy harvesting system in IoT sensor nodes. Wirel. Pers. Commun. 117, 2793–2808. https://doi.org/10.1007/s11277-020-07048-0.
Lee, J.-Y., Jung, J.-H., 2021. Multi-port DC-DC converter for interconnecting bipolar DC buses of bipolar DC distribution system. In: IEEE Energy Convers. Congr. Expo., 2021. IEEE, pp. 1191–1196. https://doi.org/10.1109/ECCE47101.2021.9595214.
Lee, J.-Y., Jung, J.-H., 2022. Modified three-port DAB converter employing voltage balancing capability for bipolar DC distribution system. IEEE Trans. Ind. Electron. 69, 6710–6721. https://doi.org/10.1109/TIE.2021.3102425.
Li, Y., Zhao, C., Chen, J.Y., Du, R., Zhang, Y., 2011. Optimizing design of soft-switching dual-input full-bridge DC/DC converter. In: IEEE Veh. Power Propuls. Conf., 2011. IEEE, pp. 1–6. https://doi.org/10.1109/VPPC.2011.6043011.
Li, Yan, Yang, Dongsheng, Ruan, Xinbo, 2008. Interleaved dual-edge modulation scheme for double-input converter to minimize inductor current ripple. In: IEEE Power Electron. Spec. Conf., 2008. IEEE, pp. 1783–1789. https://doi.org/10.1109/PESC.2008.4592202.
Liao, M., Li, H., Wang, P., Sen, T., Chen, Y., Chen, M., 2023. Machine learning methods for feedforward power flow control of multi-active-bridge converters. IEEE Trans. Power Electron. 38, 1692–1707. https://doi.org/10.1109/TPEL.2022.3215459.
Lin, Z., Pan, S., Wang, M., Lin, W., Gong, J., Yao, L., Jain, P., 2022. A three-port LCC resonant converter for the 380-V/48-V hybrid DC system. IEEE Trans. Power Electron. 37, 10864–10876. https://doi.org/10.1109/TPEL.2022.3167272.
Liu, D., Li, H., 2006. A ZVS Bi-directional DC–DC converter for multiple energy storage elements. IEEE Trans. Power Electron 21, 1513–1517. https://doi.org/10.1109/TPEL.2006.882450.
Liu, Y.-C., Chen, Y.-M., 2009. A systematic approach to synthesizing multi-Input DC–DC converters. IEEE Trans. Power Electron 24, 116–127. https://doi.org/10.1109/TPEL.2008.2009170.
Ma, Y., Huangfu, Y., Xu, L., Bai, H., Gao, F., 2021. A novel nonisolated multi-port bidirectional DC-DC converter with high voltage gain for fuel cell hybrid system. In: IEEE Transp. Electrif. Conf. Expo, 2021. IEEE, pp. 376–381. https://doi.org/10.1109/ITEC51675.2021.9490105.
Maalandish, M., Hosseini, S.H., Sabahi, M., Rostami, N., Khooban, M., 2023. B-MIMO high step-up DC/DC converter with high capability to control inputs. IET Power Electron 16, 1499–1513. https://doi.org/10.1049/pel2.12486.
Mahmoudi, M., Safari, A., 2019. LMI based robust control design for multi-input–single-output DC/DC converter. Int. J. Dyn. Control. 7, 379–387. https://doi.org/10.1007/s40435-018-0449-4.
Marei, M.I., Alajmi, B.N., Abdelsalam, I., Ahmed, N.A., 2022. An integrated topology of three-port DC-DC converter for PV-battery power systems. IEEE Open J. Ind. Electron. Soc. 3, 409–419. https://doi.org/10.1109/OJIES.2022.3182977.
Messi Bene Eloundou, N., Gustin, F., Berthon, A., 2009. Multi-source high frequency Link DC-DC converter for EV or HEV applications. In: IEEE 6th Int. Power Electron. Motion Control Conf., 2009. IEEE, pp. 1282–1287. https://doi.org/10.1109/IPEMC.2009.5157583.
Michon, M., Duarte, J.L., Hendrix, M., Simoes, M.G., 2004. A three-port bi-directional converter for hybrid fuel cell systems. IEEE 35th Annu. Power Electron. Spec. Conf. (IEEE Cat. No.04CH37551). IEEE,, pp. 4736–4742. https://doi.org/10.1109/PESC.2004.1354836 (n.d.).
Mohseni, P., Hosseini, S.H., Sabahi, M., Jalilzadeh, T., Maalandish, M., 2019. A new high step-up multi-input multi-output DC–DC converter. IEEE Trans. Ind. Electron. 66, 5197–5208. https://doi.org/10.1109/TIE.2018.2868281.

Mummadi, V., Bhimavarapu, A.R., 2020. Robust multi-variable controller design for two-input two-output fourth-order DC-DC converter. Electr. Power Compon. Syst. 48, 86–104. https://doi.org/10.1080/15325008.2020.1736213.
N. Jayaram, Gaurav, Halder, S., Panda, K.P., Pulavarthi, S.V.K., 2023. A novel design with condensed component of multi-input high gain nonisolated DC–DC converter for performance enhancement in carbon neutral energy application. IEEE J. Emerg. Sel. Top. Ind. Electron. 4, 37–49. https://doi.org/10.1109/JESTIE.2022.3211779.
Nahavandi, A., Hagh, M.T., Sharifian, M.B.B., Danyali, S., 2015. A nonisolated multiinput multioutput DC–DC boost converter for electric vehicle applications. IEEE Trans. Power Electron 30, 1818–1835. https://doi.org/10.1109/TPEL.2014.2325830.
Nami, A., Zare, F., Ghosh, A., Blaabjerg, F., 2010. Multi-output DC–DC converters based on diode-clamped converters configuration: topology and control strategy. IET Power Electron 3, 197. https://doi.org/10.1049/iet-pel.2008.0341.
Nejabatkhah, F., Danyali, S., Hosseini, S.H., Sabahi, M., Niapour, S.M., 2012. Modeling and control of a new three-input DC–DC boost converter for hybrid PV/FC/battery power system. IEEE Trans. Power Electron 27, 2309–2324. https://doi.org/10.1109/TPEL.2011.2172465.
Nielsen, H.R., Andersen, M.A.E., Zhang, Z., Thomsen, O.C., 2012. Dual-input isolated full-bridge boost dc–dc converter based on the distributed transformers. IET Power Electron 5, 1074–1083. https://doi.org/10.1049/iet-pel.2011.0181.
de Oliveira, R.N.M., Mazza, L.C.S., Oliveira, D.S., Oliveira Filho, H.M., 2017. A three-port three-phase isolated DC-DC converter feasible to PV connection on a DC distribution system. In: Brazilian Power Electron. Conf., 2017. IEEE, pp. 1–6. https://doi.org/10.1109/COBEP.2017.8257272.
de Oliveira, R.N.M., dos Santos Mazza, L.C., de Oliveira Filho, H.M., de, D., Oliveira, S., 2019. A three-port isolated three-phase current-fed DC–DC converter feasible to PV and storage energy system connection on a DC distribution grid. IEEE Trans. Ind. Appl. 55, 4910–4919. https://doi.org/10.1109/TIA.2019.2921519.
Oliveira Albuquerque, L.L., Victor Dantas de Sa, M., Lucena de Oliveira, F.A., Soares de Freitas, I., Andersen, R.L., 2019. Dynamic modeling and control of a three-port ZVS-PWM three-phase push pull DC-DC converter. In: IEEE 15th Brazilian Power Electron. Conf. 5th IEEE South. Power Electron. Conf., 2019. IEEE, pp. 1–6. https://doi.org/10.1109/COBEP/SPEC44138.2019.9065501.
Onar, O.C., Shirazi, O.H.A., Khaligh, A., 2010. Grid interaction operation of a telecommunications power system with a novel topology for multiple-input buck-boost converter. IEEE Trans. Power Deliv. 25, 2633–2645. https://doi.org/10.1109/TPWRD.2009.2031490.
Onwuchekwa, C.N., Kwasinski, A., 2012. A modified-time-sharing switching technique for multiple-input DC–DC converters. IEEE Trans. Power Electron 27, 4492–4502. https://doi.org/10.1109/TPEL.2011.2180740.
Patra, P., Patra, A., Misra, N., 2012. A single-inductor multiple-output switcher with simultaneous buck, boost, and inverted outputs. IEEE Trans. Power Electron 27, 1936–1951. https://doi.org/10.1109/TPEL.2011.2169813.
Pavlovic, Z., Oliver, J.A., Alou, P., Garcia, O., Cobos, J.A., 2013. Bidirectional multiple port DC/DC transformer based on a series resonant converter. In: Twenty-Eighth Annu. IEEE Appl. Power Electron. Conf. Expo., 2013. IEEE, pp. 1075–1082. https://doi.org/10.1109/APEC.2013.6520433.
Phattanasak, M., Gavagsaz-Ghoachani, R., Martin, J.-P., Pierfederici, S., Davat, B., 2011a. Flatness based control of an isolated three-port bidirectional DC-DC converter for a fuel cell hybrid source. In: IEEE Energy Convers. Congr. Expo., 2011. IEEE, pp. 977–984. https://doi.org/10.1109/ECCE.2011.6063878.
Phattanasak, M., Gavagsaz-Ghoachani, R., Martin, J.-P., Nahid-Mobarakeh, B., Pierfederici, S., Davat, B., 2011b. Comparison of two nonlinear control strategies for a hybrid source system using an isolated three-port bidirectional DC-DC converter. In: IEEE Veh. Power Propuls. Conf., 2011. IEEE, pp. 1–6. https://doi.org/10.1109/VPPC.2011.6043161.
Phattanasak, M., Gavagsaz-Ghoachani, R., Martin, J.-P., Nahid-Mobarakeh, B., Pierfederici, S., Davat, B., 2015. Control of a hybrid energy source comprising a fuel cell and two storage devices using isolated three-port bidirectional DC–DC converters. IEEE Trans. Ind. Appl. 51, 491–497. https://doi.org/10.1109/TIA.2014.2336975.
Pourjafar, S., Shayeghi, H., Sedaghat, F., SeyedShenava, S., 2021. A dual-input DC-DC structure with high voltage gain suggested for hybrid energy systems. IET Power Electron 14, 1792–1805. https://doi.org/10.1049/pel2.12149.
Prabhakaran, P., Agarwal, V., 2020. Novel four-port DC–DC converter for interfacing solar PV–fuel cell hybrid sources with low-voltage bipolar DC microgrids. IEEE J. Emerg. Sel. Top. Power Electron. 8, 1330–1340. https://doi.org/10.1109/JESTPE.2018.2885613.
Prabhala, V.A.K., Fajri, P., Gouribhatla, V.S.P., Baddipadiga, B.P., Ferdowsi, M., 2016. A DC–DC converter with high voltage gain and two input boost stages. IEEE Trans. Power Electron 31, 4206–4215. https://doi.org/10.1109/TPEL.2015.2476377.
Prajof, P., Agarwal, V., 2015. Novel solar PV-fuel cell fed dual-input-dual-output dc-dc converter for dc microgrid applications. In: IEEE 42nd Photovolt. Spec. Conf., 2015. IEEE, pp. 1–6. https://doi.org/10.1109/PVSC.2015.7356273.
Purgat, P., Bandyopadhyay, S., Qin, Z., Bauer, P., 2021. Zero voltage switching criteria of triple active bridge converter. IEEE Trans. Power Electron. 36, 5425–5439. https://doi.org/10.1109/TPEL.2020.3027785.
Qi, Y., Liu, X., Li, W., Zhou, Z., Liu, W., Rajashekara, K., 2023. Decentralized control for a multiactive bridge converter. IEEE Trans. Ind. Electron. 70, 11412–11421. https://doi.org/10.1109/TIE.2022.3231282.
Qian, Z., Abdel-Rahman, O., Reese, J., Al-Atrash, H., Batarseh, I., 2009a. Dynamic analysis of three-port DC/DC converter for space applications. In: Twenty-Fourth Annu. IEEE Appl. Power Electron. Conf. Expo., 2009. IEEE, pp. 28–34. https://doi.org/10.1109/APEC.2009.4802628.
Qian, Z., Abdel-Rahman, O., Hu, H., Batarseh, I., 2010b. Multi-channel three-port DC/DC converters as maximum power tracker, battery charger and bus regulator. In: Twenty-Fifth Annu. IEEE Appl. Power Electron. Conf. Expo, 2010. IEEE, pp. 2073–2079. https://doi.org/10.1109/APEC.2010.5433521.
Qian, Z., Abdel-Rahman, O., Zhang, K., Hu, H., Shen, J., Batarseh, I., 2011. Design and analysis of three-port DC/DC converters for satellite platform power system. In: IEEE Energy Convers. Congr. Expo., 2011. IEEE, pp. 1454–1460. https://doi.org/10.1109/ECCE.2011.6063952.
Qian, Zhijun, Abdel-Rahman, O., Pepper, M., Batarseh, I., 2009b. Analysis and design for paralleled three-port DC/DC converters with democratic current sharing control. In: IEEE Energy Convers. Congr. Expo., 2009. IEEE, pp. 1375–1382. https://doi.org/10.1109/ECCE.2009.5316290.
Qian, Zhijun, Abdel-Rahman, O., Al-Atrash, H., Batarseh, I., 2010a. Modeling and control of three-port DC/DC converter interface for satellite applications. IEEE Trans. Power Electron 25, 637–649. https://doi.org/10.1109/TPEL.2009.2033926.
Qin, Xiaoqing, Wu, Hongfei, Zhang, Junjun, Xing, Yan, 2014. PWM+SSPS-controlled full-bridge three-port converter for aerospace power system. In: IEEE Conf. Expo Transp. Electrif. Asia-Pacific (ITEC Asia-Pacific), 2014. IEEE, pp. 1–6. https://doi.org/10.1109/ITEC-AP.2014.6940755.
Ravada, B.R., Tummuru, N.R., Ande, B.N.L., 2021. Photovoltaic-wind and hybrid energy storage integrated multi-source converter configuration for DC microgrid applications. IEEE Trans. Sustain. Energy 12, 83–91. https://doi.org/10.1109/TSTE.2020.2983985.
Ray, O., Prasad, J.A., Mishra, S., 2013. A multi-port DC-DC converter topology with simultaneous buck and boost outputs. In: IEEE Int. Symp. Ind. Electron., 2013. IEEE, pp. 1–6. https://doi.org/10.1109/ISIE.2013.6563802.
Reddy, B.A., Veerachary, M., 2016. Robust multivariable controller design using H-infinity Loop shaping for TIFOI DC-DC converter. In: IEEE Uttar Pradesh Sect. Int. Conf. Electr. Comput. Electron. Eng., 2016. IEEE, pp. 372–377. https://doi.org/10.1109/UPCON.2016.7894682.
Rehman, Z., Al-Bahadly, I., Mukhopadhyay, S., 2015. Multiinput DC–DC converters in renewable energy applications – an overview. Renew. Sustain. Energy Rev. 41, 521–539. https://doi.org/10.1016/j.rser.2014.08.033.
Rios, C.S., Nogueira, F.G., Torrico, B.C., Junior, W.B., 2021. Robust control of a DC-DC three-port isolated converter. Trans. Inst. Meas. Control. 43, 2658–2675. https://doi.org/10.1177/01423312211002928.
Rostami, S., Abbasi, V., Talebi, N., Kerekes, T., 2020. Three-port DC–DC converter based on quadratic boost converter for stand-alone PV/battery systems. IET Power Electron 13, 2106–2118. https://doi.org/10.1049/iet-pel.2019.1025.
Rostami, S., Abbasi, V., Parastesh, M., 2021. Design and implementation of a multiport converter using Z-source converter. IEEE Trans. Ind. Electron. 68, 9731–9741. https://doi.org/10.1109/TIE.2020.3022538.
S, K., Sarathi, A., Kumar, G.G., A, S., 2018. Three inputs and two outputs boost DC-DC converter for DC microgrid applications. In: 2nd IEEE Int. Conf. Power Electron. Intell. Control Energy Syst., 2018. IEEE, pp. 188–193. https://doi.org/10.1109/ICPEICES.2018.8897461.
Saadatizadeh, Z., Heris, P.C., Babaei, E., Sabahi, M., 2019. A new nonisolated single-input three-output high voltage gain converter with low voltage stresses on switches and diodes. IEEE Trans. Ind. Electron. 66, 4308–4318. https://doi.org/10.1109/TIE.2018.2864710.
Saadatizadeh, Z., Babaei, E., Blaabjerg, F., Cecati, C., 2021a. Three-port high step-up and high step-down DC-DC converter with zero input current ripple. IEEE Trans. Power Electron. 36, 1804–1813. https://doi.org/10.1109/TPEL.2020.3007959.
Saadatizadeh, Z., Chavoshipour Heris, P., Babaei, E., Blaabjerg, F., Cecati, C., 2021b. SIDO coupled inductor-based high voltage conversion ratio DC–DC converter with three operations. IET Power Electron 14, 1735–1752. https://doi.org/10.1049/pel2.12130.
Saadatizadeh, Z., Heris, P.C., Mantooth, H.A., 2022. Modular expandable multiinput multioutput (MIMO) high step-up transformerless DC–DC converter. IEEE Access 10, 53124–53142. https://doi.org/10.1109/ACCESS.2022.3175876.
Saadatizadeh, Z., Heris, P.C., Mantooth, A., 2024. High-frequency three-port DC–DC converter with zero-voltage switching operation. IEEE Trans. Ind. Electron. 71, 537–548. https://doi.org/10.1109/TIE.2023.3245209.
Saafan, A.A., Khadkikar, V., El Moursi, M.S., Zeineldin, H.H., 2021. A new multiport DC-DC converter for DC microgrid applications. In: IEEE Ind. Appl. Soc. Annu. Meet., 2021. IEEE, pp. 1–7. https://doi.org/10.1109/IAS48185.2021.9677403.
Saafan, A.A., Khadkikar, V., Moursi, M.S.El, Zeineldin, H.H., 2023. A new multiport DC-DC converter for DC microgrid applications. IEEE Trans. Ind. Appl. 59, 601–611. https://doi.org/10.1109/TIA.2022.3213235.
Sato, Y., Nagata, H., Uno, M., 2017. Non-isolated multi-port converter integrating PWM and phase-shift converters. TENCON 2017 - 2017 IEEE Reg. 10 Conf. IEEE,, pp. 1097–1102. https://doi.org/10.1109/TENCON.2017.8228021.
Shayeghi, H., Pourjafar, S., Hashemzadeh, S.M., 2021. A switching capacitor based multi-port bidirectional DC–DC converter. IET Power Electron 14, 1622–1636. https://doi.org/10.1049/pel2.12137.
Shoaei, A., Abbaszadeh, K., Allahyari, H., 2023. A single-inductor multi-input multilevel high step-up DC–DC converter based on switched-diode-capacitor cells for PV applications. IEEE J. Emerg. Sel. Top. Ind. Electron. 4, 18–27. https://doi.org/10.1109/JESTIE.2022.3173178.
Smith, N., McCann, R., 2012. Investigation of a multiple input converter for grid connected thermoelectric-photovoltaic hybrid system. In: IEEE Green Technol. Conf., 2012. IEEE, pp. 1–5. https://doi.org/10.1109/GREEN.2012.6200938.
Sun, X., Shen, Y., Li, W., Wu, H., 2015. A PWM and PFM hybrid modulated three-port converter for a standalone PV/battery power system. IEEE J. Emerg. Sel. Top. Power Electron. 3, 984–1000. https://doi.org/10.1109/JESTPE.2015.2424718.

Sun, Xiaofeng, Liu, F., Xiong, Liangliang, Wang, Baocheng, 2014a. Research on dual Buck/Boost integrated three-port bidirectional DC/DC converter. In: IEEE Conf. Expo Transp. Electrif. Asia-Pacific (ITEC Asia-Pacific), 2014. IEEE, pp. 1–6. https://doi.org/10.1109/ITEC-AP.2014.6941114.

Sun, Xiaofeng, Shen, Yanfeng, Li, Wuying, 2014b. A novel LLC integrated three-port DC-DC converter for stand-alone PV/battery system. In: IEEE Conf. Expo Transp. Electrif. Asia-Pacific (ITEC Asia-Pacific), 2014. IEEE, pp. 1–6. https://doi.org/10.1109/ITEC-AP.2014.6941090.

Suresh, K., Bharatiraja, C., Chellammal, N., Tariq, M., Chakrabortty, R.K., Ryan, M.J., Alamri, B., 2021. A multifunctional non-isolated dual input-dual output converter for electric vehicle applications. IEEE Access 9, 64445–64460. https://doi.org/10.1109/ACCESS.2021.3074581.

Tao, H., Kotsopoulos, A., Duarte, J.L., Hendrix, M.A.M., 2005. A soft-switched three-port bidirectional converter for fuel cell and supercapacitor applications. IEEE 36th Conf. Power Electron. Spec. IEEE, pp. 2487–2493. https://doi.org/10.1109/PESC.2005.1581982 (n.d.).

Tao, H., Kotsopoulos, A., Duarte, J.L., Hendrix, M.A.M., 2006a. Family of multiport bidirectional DC–DC converters. IEE Proc. - Electr. Power Appl. 153, 451. https://doi.org/10.1049/ip-epa:20050362.

Tao, H., Kotsopoulos, A., Duarte, J.L., Hendrix, M.A.M., 2006b. Triple-half-bridge bidirectional converter controlled by phase shift and PWM. Twenty-First Annu. IEEE Appl. Power Electron. Conf. Expo. APEC '06., IEEE, pp. 1256–1262. https://doi.org/10.1109/APEC.2006.1620700 (n.d.).

Tao, Haimin, Duarte, J.L., Hendrix, M.A.M., 2008. Three-port triple-half-bridge bidirectional converter with zero-voltage switching. IEEE Trans. Power Electron 23, 782–792. https://doi.org/10.1109/TPEL.2007.915023.

Thounthong, P., Pierfederici, S., Martin, J.-P., Hinaje, M., Davat, B., 2010. Modeling and control of fuel cell/supercapacitor hybrid source based on differential flatness control. IEEE Trans. Veh. Technol. 59, 2700–2710. https://doi.org/10.1109/TVT.2010.2046759.

Tian, Q., Zhou, G., Leng, M., Xu, G., Fan, X., 2020. A nonisolated symmetric bipolar output four-port converter interfacing PV-battery system. IEEE Trans. Power Electron. 35, 11731–11744. https://doi.org/10.1109/TPEL.2020.2983113.

Torki Harchegani, A., Asghari, A., Jazaeri, M., 2021. A new soft-switching multi-input quasi-Z-source converter for hybrid sources systems. IET Renew. Power Gener. 15, 1451–1468. https://doi.org/10.1049/rpg2.12124.

Tran, Y.-K., Dujic, D., 2016. A multiport isolated DC-DC converter. In: IEEE Appl. Power Electron. Conf. Expo., 2016. IEEE, pp. 156–162. https://doi.org/10.1109/APEC.2016.7467867.

Tran, Y.-K., Dujic, D., Barrade, P., 2015. Multiport resonant DC-DC converter. IECON 2015 - 41st Annu. Conf. IEEE Ind. Electron. Soc. IEEE,, pp. 003839–003844. https://doi.org/10.1109/IECON.2015.7392699.

Uno, M., Oyama, R., Sugiyama, K., 2018. Partially isolated single-magnetic multiport converter based on integration of series-resonant converter and bidirectional PWM converter. IEEE Trans. Power Electron. 33, 9575–9587. https://doi.org/10.1109/TPEL.2018.2794332.

Vahid, S., Zolfi, P., EL-Refaie, A., 2021. A novel step-down three-port power converter for semi-isolated renewable and hybrid energy storage system applications. IECON 2021 – 47th Annu. Conf. IEEE Ind. Electron. Soc. IEEE, pp. 1–7. https://doi.org/10.1109/IECON48115.2021.9589088.

Varesi, K., Ghandomi, A.A., Hosseini, S.H., Sabahi, M., Babaei, E., 2017. An improved structure for Multi-Input high step-up DC-DC converters. In: 8th Power Electron. Drive Syst. Technol. Conf., 2017. IEEE, pp. 241–246. https://doi.org/10.1109/PEDSTC.2017.7910330.

Varesi, K., Hosseini, S.H., Sabahi, M., Babaei, E., 2018. A high-voltage gain nonisolated noncoupled inductor based multi-input DC-DC topology with reduced number of components for renewable energy systems. Int. J. Circuit Theory Appl. 46, 505–518. https://doi.org/10.1002/cta.2428.

Varesi, K., Hossein Hosseini, S., Sabahi, M., Babaei, E., Saeidabadi, S., Vosoughi, N., 2019. Design and analysis of a developed multiport high step-Up DC–DC converter with reduced device count and normalized peak inverse voltage on the switches/diodes. IEEE Trans. Power Electron. 34, 5464–5475. https://doi.org/10.1109/TPEL.2018.2866492.

Veerachary, M., 2008. Multi-input integrated buck-boost converter for photovoltaic applications. In: IEEE Int. Conf. Sustain. Energy Technol., 2008. IEEE, pp. 546–551. https://doi.org/10.1109/ICSET.2008.4747068.

Veerachary, M., Mohan, M.M., Reddy, B.A., 2013. Centralized digital controller for two-input integrated DC-DC converter. In: IEEE 10th Int. Conf. Power Electron. Drive Syst., 2013. IEEE, pp. 244–249. https://doi.org/10.1109/PEDS.2013.6527022.

Wai, R.-J., Lin, C.-Y., Liaw, J.-J., Chang, Y.-R., 2011. Newly designed ZVS multi-input converter. IEEE Trans. Ind. Electron. 58, 555–566. https://doi.org/10.1109/TIE.2010.2047834.

Wang, B., Kanamarlapudi, V.R.K., Xian, L., Peng, X., Tan, K.T., So, P.L., 2016. Model predictive voltage control for single-inductor multiple-output DC–DC converter with reduced cross regulation. IEEE Trans. Ind. Electron. 63, 4187–4197. https://doi.org/10.1109/TIE.2016.2532846.

Wang, K., Liu, W., Wu, F., 2022. Topology-level power decoupling three-port isolated current-fed resonant DC-DC converter. IEEE Trans. Ind. Electron. 69, 4859–4868. https://doi.org/10.1109/TIE.2021.3082066.

Wang, L., Wang, Z., Li, H., 2012. Asymmetrical duty cycle control and decoupled power flow design of a three-port bidirectional DC-DC converter for fuel cell vehicle application. IEEE Trans. Power Electron 27, 891–904. https://doi.org/10.1109/TPEL.2011.2160405.

Wang, P., Lu, X., Wang, W., Xu, D., 2019. Hardware decoupling and autonomous control of series-resonance-based three-port converters in DC microgrids. IEEE Trans. Ind. Appl. 55, 3901–3914. https://doi.org/10.1109/TIA.2019.2906112.

Wang, Y., Han, F., Yang, L., Xu, R., Liu, R., 2018. A three-port bidirectional multi-element resonant converter with decoupled power flow management for hybrid energy storage systems. IEEE Access 6, 61331–61341. https://doi.org/10.1109/ACCESS.2018.2872683.

Wang, Z., Li, H., 2013. An integrated three-port bidirectional DC–DC converter for PV application on a DC distribution system. IEEE Trans. Power Electron 28, 4612–4624. https://doi.org/10.1109/TPEL.2012.2236580.

Wang, Z., Luo, Q., Wei, Y., Mou, D., Lu, X., Sun, P., 2020. Topology analysis and review of three-port DC–DC converters. IEEE Trans. Power Electron. 35, 11783–11800. https://doi.org/10.1109/TPEL.2020.2985287.

Wibowo, S., Mori, I., Tsushida, K., Miwa, S., Kobayashi, H., 2009. A single-inductor dual-output DCDC converter. IEICE 22nd Circuits Syst. Work. Karuizawa 367–371.

wu, Hongfei, Zhang, J., Qin, X., Mu, T., Xing, Y., 2015. Secondary-side-regulated soft-switching full-bridge three-port converter based on bridgeless boost rectifier and bidirectional converter for multiple energy interface, 1–1 IEEE Trans. Power Electron.. https://doi.org/10.1109/TPEL.2015.2473002.

Wu, H., Chen, R., Zhang, J., Xing, Y., Hu, H., Ge, H., 2011a. A family of three-port half-bridge converters for a stand-alone renewable power system. IEEE Trans. Power Electron 26, 2697–2706. https://doi.org/10.1109/TPEL.2011.2125991.

Wu, H., Xing, Y., Chen, R., Zhang, J., Sun, K., Ge, H., 2011b. A three-port half-bridge converter with synchronous rectification for renewable energy application. In: IEEE Energy Convers. Congr. Expo., 2011. IEEE, pp. 3343–3349. https://doi.org/10.1109/ECCE.2011.6064220.

Wu, H., Zhang, J., Xing, Y., 2015. A family of multiport buck–boost converters based on DC-link-inductors (DLIs). IEEE Trans. Power Electron 30, 735–746. https://doi.org/10.1109/TPEL.2014.2307883.

Xian, L., Wang, G., Wang, Y., 2012. Implementation and control of a double-input DC/DC converter for PEMFC/battery hybrid power supply. In: 7th IEEE Conf. Ind. Electron. Appl, 2012. IEEE,, pp. 285–290. https://doi.org/10.1109/ICIEA.2012.6360738.

Xu, P., Wen, H., Hao, W., Yang, Y., Ma, J., Wang, Y., Zhou, J., 2021. Nonisolated switching-capacitor-integrated three- port converters with seamless PWM/PFM modulation. Sol. Energy 224, 160–174. https://doi.org/10.1016/j.solener.2021.04.023.

Yalamanchili, K.P., Ferdowsi, M., Corzine, K., 2006. New double input DC-DC converters for automotive applications. In: IEEE Veh. Power Propuls. Conf., 2006. IEEE, pp. 1–6. https://doi.org/10.1109/VPPC.2006.364366.

Ye, Y., Eric Cheng, K.W., 2015. Single-switch single-inductor multi-output pulse width modulation converters based on optimised switched-capacitor. IET Power Electron 8, 2168–2175. https://doi.org/10.1049/iet-pel.2014.0743.

Yi, W., Ma, H., Peng, S., Liu, D., Ali, Z.M., Dampage, U., Hajjiah, A., 2022. Analysis and implementation of multi-port bidirectional converter for hybrid energy systems. Energy Rep. 8, 1538–1549. https://doi.org/10.1016/j.egyr.2021.12.068.

You, J., Liu, H., Fu, B., Xiong, X., 2019. H∞ Mixed sensitivity control for a three-port converter. Energies 12, 2231. https://doi.org/10.3390/en12122231.

Yuan-mao, Y., Cheng, K.W.E., 2013. Multi-input voltage-summation converter based on switched-capacitor. IET Power Electron 6, 1909–1916. https://doi.org/10.1049/iet-pel.2013.0015.

Zahedi Saadabad, N., Hossein Hosseini, S., Nasiri, A., Sabahi, M., 2020. New soft-switched high gain three-port DC–DC converter with coupled inductors. IET Power Electron 13, 4562–4571. https://doi.org/10.1049/iet-pel.2020.0452.

Zeng, J., Qiao, W., Qu, Liyan, 2013. An isolated three-port bidirectional DC-DC converter for photovoltaic systems with energy storage. In: IEEE Ind. Appl. Soc. Annu. Meet., 2013. IEEE, pp. 1–8. https://doi.org/10.1109/IAS.2013.6682520.

Zeng, J., Qiao, W., Qu, L., Jiao, Y., 2014. An isolated multiport DC–DC converter for simultaneous power management of multiple different renewable energy sources. IEEE J. Emerg. Sel. Top. Power Electron. 2, 70–78. https://doi.org/10.1109/JESTPE.2013.2293331.

Zhaikhan, A., Subburaj, V., Jena, D., Perumal, P., Ruderman, A., 2017. Design, modeling and analysis of a new dual input-output switched capacitor converter. TENCON 2017 - 2017 IEEE Reg. 10 Conf. IEEE,, pp. 673–677. https://doi.org/10.1109/TENCON.2017.8227946.

Zhang, H., Dong, D., Liu, W., Ren, H., Zheng, F., 2022. Systematic synthesis of multiple-input and multiple-output DC–DC converters for nonisolated applications. IEEE J. Emerg. Sel. Top. Power Electron. 10, 6470–6481. https://doi.org/10.1109/JESTPE.2021.3118797.

Zhang, Junjun, Wu, Hongfei, Huang, Jun, Xing, Yan, Ma, Xudong, 2014. A novel multi-port bidirectional converter for interfacing distributed DC micro-grid. In: IEEE 23rd Int. Symp. Ind. Electron., 2014. IEEE, pp. 2344–2348. https://doi.org/10.1109/ISIE.2014.6864985.

Zhang, N., Sutanto, D., Muttaqi, K.M., 2016. A review of topologies of three-port DC–DC converters for the integration of renewable energy and energy storage system. Renew. Sustain. Energy Rev. 56, 388–401. https://doi.org/10.1016/j.rser.2015.11.079.

Zhang, Z., Thomsen, O.C., Andersen, M.A.E., Nielsen, H.R., 2011. A novel dual-input isolated current-fed DC-DC converter for renewable energy system. In: Twenty-Sixth Annu. IEEE Appl. Power Electron. Conf. Expo., 2011. IEEE, pp. 1494–1501. https://doi.org/10.1109/APEC.2011.5744790.

Zhao, C., Round, S.D., Kolar, J.W., 2008. An isolated three-port bidirectional DC-DC converter with decoupled power flow management. IEEE Trans. Power Electron 23, 2443–2453. https://doi.org/10.1109/TPEL.2008.2002056.

Zhao, H., Qi, Y., Li, W., 2022. Decentralized power management for multi-active bridge converter. IECON 2022 – 48th Annu. Conf. IEEE Ind. Electron. Soc. IEEE,, pp. 1–6. https://doi.org/10.1109/IECON49645.2022.9968432.

Zhou, G., Tian, Q., Wang, L., 2022. Soft-switching high gain three-port converter based on coupled inductor for renewable energy system applications. IEEE Trans. Ind. Electron. 69, 1521–1536. https://doi.org/10.1109/TIE.2021.3060614.

Zhou, L.-W., Zhu, B.-X., Luo, Q.-M., 2012. High step-up converter with capacity of multiple input. IET Power Electron 5, 524. https://doi.org/10.1049/iet-pel.2011.0177.

Zhu, B., Zeng, Q., Vilathgamuwa, D.M., Li, Y., She, X., 2019. Non-isolated high-voltage gain dual-input DC/DC converter with a ZVT auxiliary circuit. IET Power Electron 12, 861–868. https://doi.org/10.1049/iet-pel.2018.5465.

Zhu, B., Hu, H., Wang, H., Li, Y., 2020a. A multi-input-port bidirectional DC/DC converter for DC microgrid energy storage system applications. Energies 13, 2810. https://doi.org/10.3390/en13112810.

Zhu, B., Huang, Y., Hu, S., Wang, H., 2020b. A multi-operating mode multi-port DC/DC converter with high step-up voltage gain. 2020 IEEE 9th Int. Power Electron. Motion Control Conf. (IPEMC2020-ECCE Asia). IEEE, pp. 2877–2881. https://doi.org/10.1109/IPEMC-ECCEAsia48364.2020.9367683.

Zhu, H., Zhang, D., Athab, H., Wu, B., Gu, Y., 2014. PV isolated three-port converter and energy balancing control method for PV-battery power supply applications, 1–1 IEEE Trans. Ind. Electron.. https://doi.org/10.1109/TIE.2014.2378752.

Zou, S., Lu, J., Khaligh, A., 2020. Modelling and control of a triple-active-bridge converter. IET Power Electron 13, 961–969. https://doi.org/10.1049/iet-pel.2019.0920.